AD NUMBER: AD0489874

LIMITATION CHANGES

TO:

Approved for public release; distribution is unlimited.

FROM:

Distribution authorized to US Government Agencies and their Contractors; Export Control; 27 Jun 1966. Other requests shall be referred to US Army Missile Command, Redstone Arsenal, AL, 35809.

AUTHORITY

Per USAMC ltr dtd 23 Aug 1971

AD

REPORT NO. RS-TR-66-6

METEOROLOGICAL ROCKET PROGRAM FISCAL YEAR REPORT

by
Glen D. Estes

June 1966

DISTRIBUTION LIMITED
SEE NOTICES PAGE

U.S. ARMY MISSILE COMMAND
Redstone Arsenal, Alabama

27 June 1966

Report No. RS-TR-66-6

METEOROLOGICAL ROCKET PROGRAM FISCAL YEAR REPORT

by
Glen D. Estes

DA Project No. 1S025001D125
AMC Management Structure Code No. 5027.12.46100

DISTRIBUTION LIMITED
SEE NOTICES PAGE

Missile Design Branch
Structures and Mechanics Laboratory
Research and Development Directorate
U. S. Army Missile Command
Redstone Arsenal, Alabama 35809

ABSTRACT

This report contains results of design, analysis, fabrication, and testing carried out by the Structures and Mechanics Laboratory to advance the design of the Meteorological Data Sounding System and Research Development Test and Evaluation rockets.

A description of each vehicle and results of component test carried out during this phase of the exploratory development program is included.

CONTENTS

ILLUSTRATIONS

BLANK PAGE

Section I. INTRODUCTION

1. Scope

This report presents the efforts of the Structures and Mechanics Laboratory for Fiscal Year 1966 on the rocket components for Meteorological Data Sounding System (MDSS) and meteorological rocket for Research Development Test and Evaluation (RDT&E).

2. Background

During Fiscal Year 1965, the Structures and Mechanics Laboratory carried out the second year of exploratory development for the rocket components for MDSS and meteorological rocket for RDT&E. The results of this exploratory development were presented in Report Nos. RS-TN-65-1 and RS-TN-65-2.

During August 1965, the Structures and Mechanics Laboratory received Scope of Work No. ME-01-66 from the Development Division requesting that this laboratory perform the task of furthering the design and development of the airframes and separation devices for the rocket components for MDSS and the meteorological rocket for RDT&E as follows:

1) Assist the Development Division in the preparation of technical requirements, technical evaluation of proposals, and the generation of scopes of work for pre-U.S.-Canadian development contract effort and the U.S.-Canadian development sharing program contract.
2) Conduct the necessary studies and investigations, i.e., aerodynamic, thermal, dynamic, stress, materials, etc., to ensure preliminary designs which have a high probability of fulfilling the required missions. Prepare a preliminary design package incorporating the details of the studies, investigations, and designs for use in the pre-U.S.-Canadian development contact.
3) Provide the necessary information, data, design, etc., to the contractor during pre-U.S.-Canadian development sharing to eliminate redundant effort.
4) Effect necessary technical supervision of the contractor during the pre-U.S.-Canadian development contract.
5) Continue separation device design and development.

6) Continue installation and packaging technique studies in the area of separation and deceleration device components.

7) Coordinate efforts with the other U.S. Army Missile Command (MICOM) laboratories and remain cognizant of developments at the U.S. Army Electronics Command to ensure timely resolution of interface problems in assigned mission areas.

Section II. LABORATORY EFFORTS, FISCAL YEAR 1966

The rocket components presented in Report Nos. RS-TN-65-1 and RS-TN-65-2 were a result of Fiscal Year 1965 exploratory development.

During Fiscal Year 1966, further exploratory development was carried out in the areas noted in the scope of work with the following results.

1. Design Studies

Further design studies were carried out for separation devices and airframes for both vehicles. These studies were directed toward enhancing reliability and handling of the rounds. The results of these studies are presented in Section III of this report.

2. Component Fabrication and Test

a. Launcher Test Vehicle

Fabrication of 20 vehicles for launcher test was carried over from Fiscal Year 1965. This vehicle (Figure 1), designed to test the shipping container-launcher concept for the MDSS vehicle, was made from a 2.75-inch Folding-Fin Aircraft Rocket (FFAR). The 2.75-inch FFAR was modified to simulate the MDSS profile and burntime within the launcher.

Modifications to the 2.75-inch FFAR consisted of the following:

1) Folding fins were removed and delta fins bonded to the motor bottle. These fins were necessary to simulate MDSS vehicle launch from the tube.
2) The 2.75-inch practice head was removed and a 50.27-inch tube and ogive was substituted to simulate the length of the vehicle for MDSS.

Ten of the 20 modified vehicles were flight fired, two were loaded with inert propellant for launcher vibration and drop test, two were set up for launcher design studies, and the disposition of the remaining six is undecided.

b. Drag Test Vehicle

The validity of the drag values being used by MICOM in parametric studies for MDSS and RDT&E vehicles has been questioned by other agencies doing meteorological rocket design. Consequently, the Development Division requested that the Structures and Mechanics Laboratory design an ogive and launch mechanism to be used on the Loki motor to prove out these drag values.

Using the MDSS and RDT&E drag routine, performance predictions for the modified Loki were made and then a total of five vehicles were flight fired to prove out these predictions.

Modifications to the existing LOKI motor consisted of removal of the dart detent and separation plunger and replacing these with an adapter and solid ogive weighing 11.5 pounds (Figure 2).

The launch mechanism for this rocket consisted of a front flyaway shoe that fitted into a "T" slot on an existing rail and a slotted tube rear shoe at the rear to accept the fins and nozzle burley of the motor aft end.

Instrumentation for these flights consisted of a velocimeter, radar, and cameras. The cameras covered launch only.

On the first two firings, the MICOM designed rear shoe was not used and the end result was misslaunch that caused fin failure and thus erratic flight.

The next three firings utilized the MICOM rear shoe, and based on camera coverage, launch of all three rockets was nearly perfect (launch QE = 80 degrees; azimuth = 355 degrees). However, radar and velocimeter failed to track these flights, therefore, no useful data were obtained. It should be noted that a HAWK radar unit picked up one flight during descent at approximately 13,000 feet altitude and 41,760 feet range at an azimuth of 354 degrees.

c. Separation Device

After functional tests were completed on the separation device described in Report No. RS-TN-65-2, further studies were carried out to substantiate separation force and energy calculations (July, Fiscal Year 1966). These studies consisted mainly of separation tests which were carried out using test hardware with pressure, force, and distance being recorded.

Test hardware used during these tests consisted of the following items (Figure 3):

1) A steel slug that simulated motor weight and attachment.
2) An aluminum pedestal section. (Aluminum was used so that a repeated test could be performed using the same hardware.)
3) The separation piston described in Report No. RS-TN-65-2, complete with mechanical timer and frangible valve.
4) An inner cylindrical tube attacked to the piston that served to transmit separation force to the shear joint (also housed decent vehicle-piston sleeve).

An Instron testing machine was used to record force and distance measurements. Piston pressurizations were accomplished using the special tank pressurizer fabricated for this purpose. Tank pressures and pressures applied to the motor slug during testing were measured with calibrated gages. To facilitate piston friction measurement, the motor slug was modified to provide a pressure inlet. This pressure inlet also served as a safety pressure release when the separation device was pressurized and assembled. A safety plug was fabricated to insert in this inlet to arm the system immediately prior to separation.

The test consisted of controlled expansion with the test hardware placed in the Instron machine (Figure 3) which recorded force as a function of piston travel. The rate of expansion was controlled by the machine cross-head speed which was set at 10 inches per minute. Expansion during each test was allowed to continue until the cross head separated from the test hardware. Leakage through the threaded joint connecting the motor to the pedestal substantially affected the test results; therefore, the final tests were run with the joint sealed with a nonhardening pipe joint sealer. Initial pressure within the separation piston was 200 pounds per square inch. Prior to each test, the piston O-ring and pedestal inner surface were lubricated throughly with Dow Corning pneumatic grease (silicone), Military Specification MIL-L-4343A.

Piston friction force was measured on the Instron machine by measuring expansion force at 10 inches per minute velocity and at successive increasing pressure levels up to 200 pounds per square inch.

Results of separation test and friction test are presented in Figures 4 through 6. Figure 4 presents piston friction force as a function of pressure acting on the piston, Figure 5 is a comparison of measured separation force with calculated isothermal and adiabatic expansion without correction for friction, and Figure 6 is a comparison of measured force and calculated adiabatic and isothermal expansion including corrections for friction.

One test of the complete assembly was run to check the separation sequence. This test will be discussed later in this section.

At the conclusion of these tests, it was decided that the overall design concept should be viewed from a standpoint of eliminating minor deficiencies noted during the test. These deficiencies included having to store the piston in a pressurized state for a long as five years, having to store the timer with the mainspring wound tight, and having to provide a safety device that would prevent rocket separation during transportation and handling. (Possible leak in joint between pedestal and motor was considered in airframe studies.)

The end result of this study was a separation device redesign which contained a self-sealing polyethylene piston to replace the gas container piston, a modification to the timer which incorporated a firing pin on the striker arm that would initiate a precussion actuated device, and a .25-caliber cartridge and primer filled with black powder to supply the required separation pressure.

A piston was fabricated and preliminary tests, using air pressure, were conducted to determine if it was self-sealing. At the same time, cartridges were loaded with black powder of various grain sizes and tested to determine if enough pressure could be generated to affect separation. Figure 7 shows the test results of a cartridge selected. The cartridge was loaded with 225 milligrams of A-5 and 246 milligrams of A-3 black powder.

A separation device incorporating the above components was fabricated and a series of five tests conducted using the pedestal, motor slug, and instrument slug left over from previous test (November, Fiscal Year 1966). The assembled device was fired in the vertical position with the motor slug resting on a concrete pad.

Results of these tests are as follows:

1) Test 1 - Action time occurred at 58 seconds. Results were a good, clean separation with an eight-pound instrument slug reaching an estimated height of seven feet from pedestal section.
2) Test 2 - Action time occurred at 58 seconds; however, cartridge did not detonate. Malfunction was due to annealing of springs on timer striker arm during first test.
3) Test 3 - Timer spring was replaced. Action time occurred at 63 seconds. Again, cartridge did not detonate. Malfunction was due to faulty primer.

4) Test 4 - Action time occurred at 63 seconds. Achieved clean separation.
5) Test 5 - Repeat of Test 4.

The results of these tests indicated that this design was more practical than the piston-gas container design mentioned earlier. These tests also showed that the addition of a check valve would allow insertion of the separation device through the forward end of the pedestal, thus eliminating the need for the threaded joint between pedestal and motor.

A piston including the check valve was fabricated and tested in a forward section similar to that described in Section III of this report. The results of these tests were very satisfactory. However, further study along the line of molding and tubing tolerance may show the check valve to be unnecessary.

d. Parachute Studies

Testing of the parachutes mentioned in Report No. RS-TN-65-2 was being conducted during writing of this report (July and August, Fiscal Year 1966). Inasmuch as reduced data from these tests were not available, it was noted that one parachute reportedly withstood loading of up to 200 percent of opening shock force.

(1) Parachute Design. Using Technical Report No. ASD-TR-61-579, "Performance of and Design Criteria for Deployable Aerodynamic Decelerators," as a reference, it was determined that a flat plate canopy would yield a coefficient drag of 0.75. Using the equation $\text{Drag} = C_D \frac{\text{Density}}{2} V^2 S$, where Drag = suspended weight, $C_D = 0.75$, V = terminal velocity at sea level, and S = canopy area, a curve was plotted that presented canopy diameter as a function of suspended load (Figure 8). This curve shows that a 72-inch diameter canopy would lower a 10-pound weight at 20 feet per second at sea level.

Considering an impact velocity of 20 feet per second, a canopy diameter of 72 inches, and a suspended load of 10 pounds, a curve was plotted with parachute velocity as a function of altitude from 100,000 feet to sea level (Figure 9).

This parachute design should present the following performance:

1) Canopy diameter - 72 inches.
2) Opening shock should be approximately twice the normal load.
3) Stability of parachute should not exceed a ± 30-degree angle of oscillation.

(2) Parachute Test. As noted in Report No. RS-TN-65-2, three parachute canopies were fabricated using one-half-mil polyester sheet. Shrouds for these parachutes were made of 144-pound-test nylon string for the 12 and 16 shroud line parachutes, and fiber glass tape for the eight shroud line parachute. Also, the 12 shroud line parachute canopy contained reinforced edges. These three parachutes were tested to determine if canopies could withstand opening shock loads anticipated.

Test hardware for these tests were as follows (Figure 10):

1) A tube installed on top of a 10-foot tower mounted in the bed of a half-ton truck. This tube was used to house the parachute and parachute cannister.
2) A split cannister to package the parachute and ballute.
3) A 24-inch diameter pilot parachute was used to pull the split cannister out of the tube.
4) A simulated ballute.
5) Lanyards connecting the pilot parachute to the ballute and connecting the test parachute to a load cell mounted on the tower just forward of the tube.
6) A wire actuated release pin, when pulled, permitted the split cannister and its contents to be pulled from the tube.

Instrumentation to record air speed, test parachute load, and release time was used. Camera coverage was provided for most tests.

Parachutes were first deployed at an air speed of 33 miles per hour, the calculated value that would simulate opening shock at 100,000 feet with a 415 feet per second velocity. All three test parachutes withstood this opening shock. However, it was noted that the pilot parachute oscillations caused binding of the split cannister within the tube, so it was replaced with a 100-foot line with a drag weight on it.

The next series of tests conducted consisted of deploying the parachutes at 33 miles per hour and increasing the speed until parachute failure occurred.

The eight shroud line parachute failed at 55 miles per hour with a 152-pound load. The 16 shroud line parachute failed at 31 miles per hour with a 55-pound load. This early failure was caused by a slight tear existing in the canopy edge near one of the lines. However, had the tear not existed, this parachute would have failed as the eight shroud line parachute did, because of the lack of reinforced edges.

A number of tests were performed on the 12 shroud line parachute up to 55 miles per hour without any deterioration to the canopy or lines. Figure 11 shows a typical deployment.

A plot of load as a function of air speed, for this parachute, is shown in Figure 12 along with calculated values.

Maximum elapse time for release of split cannister until parachute deployment was 12.5 seconds. For the majority of the tests, this elapse time was between five and eight seconds.

At the end of these tests, the following conclusions were made:

1) The one-half-mil polyester was strong and tough enough to be used for the parachute canopy.
2) Reinforcement or folding would be necessary for all cut edges of the one-half-mil polyester.
3) Desired performance and strength could be obtained with a parachute of the 12 shroud line design.

At the completion of these tests (end of July, Fiscal Year 1966), another 12 shroud line parachute was fabricated. The new parachute and the parachute remaining from the above tests were installed within the device shown in Figure 13. This device consists of the motor slug, pedestal, and separation piston, which were used in the first separation test, and a new ogive and instrument section. The old parachute was attached to the piston by inserting a pin through the piston and piston sleeve and through a ring on the parachute lanyard. The new parachute was attached to the simulated instrument section by the use of an eye bolt. The piston was pressurized, the timer set, the parachutes were packed into the split cannister and inserted into the piston sleeve connected to the piston, and the ogive was put in place and four shear pins were installed.

This hardware was connected to the test fixture, as shown in Figure 13, and taken up on a helicopter for a separation and deployment test.

After the helicopter reached an altitude of approximately 500 feet and hovered, the timer was started and the test hardware lowered approximately 20 feet below the aircraft by cables shown in Figure 13. At approximately 65 seconds separation occurred. The test fixture was designed to allow the ogive to move in one direction and the motor and pedestal section to move the opposite direction. However, when the

piston reached the end of its travel, the piston sleeve sheared loose and continued with the split cannister. At about the time the shearing action occurred, the lanyard to the instrument section became taut and its parachute was forced out of the split cannister before the cannister was completely clear of the piston sleeve. This caused higher than expected loads on the eyebolt in the instrumentation section with the end result being a failure of the eyebolt.

The results of this test were as follows:

1) Instrument parachute deployment without the instruments or ogive.
2) Entanglement of motor parachute within the piston sleeve and all its lines cut during the fall to earth (Figure 14).

It was concluded that if actual hardware had been used, structural failure would not have occurred and both parachutes would have deployed properly.

A repeat of this test, using corrected hardware, would not be beneficial. Therefore, the parachute testing program was concluded.

At the conclusion of these tests, a representative of the Structures and Mechanics Laboratory visited the Air Drop Engineering Division, Parachute Equipment Branch, U.S. Army Natick Laboratories, Natick, Massachusetts, with the following questions:

1) Does a similar parachute capable of meeting requirements exist?
2) Is the canopy material most suitable?
3) Can suspension line connections to canopy be altered or improved to allow a different method of production?
4) Will the vent hole size provide sufficient stability?
5) Is the suspension line material most suitable?
6) Will normal production methods require a change in the present design?
7) What packaging or folding method would be best suited?

The answer to question 1 was, "no known parachute exists." Answers to questions 2, 4, 5, and 7 were positive, and questions 3 and 6 could not be answered.

e. Separation Timer

Because of the modification made to the timer for use in actuating the shell in the cartridge actuated separation device, it was

decided that two prototype timers incorporating these modifications would be ordered from M. H. Rhodes, Inc., the timer manufacturer, and used in the last separation test mentioned in Paragraph c. Timers received from the manufacturer are shown in Figure 15. It should be noted that these timers functioned very satisfactorily during separation test.

3. Analysis

a. Dynamic Analysis

During Fiscal Year 1965, dynamic stability studies indicated a need for a computer program to be used for calculating dynamic stability for the two vehicles.

In October, Fiscal Year 1966, this computer program was completed and, using trajectories available at that time, stability calculations were made for both vehicles. The computer program used for these calculations is included in Appendix A.

It should be noted that dynamic stability studies were not conducted for the latest motor designs because performance trajectories were not available until mid-June of Fiscal Year 1966.

b. Thermal Analysis

Thermal analysis for each vehicle using latest airframe designs and trajectories was conducted. The results of these analyses are presented in Appendix B.

4. Airframe Fabrication and Test

Three MDSS vehicle forward sections and one fin-nozzle retainer assembly were fabricated during Fiscal Year 1966. The fin-nozzle retainer was the same as that described in Report No. RS-TN-65-2 and a preliminary test indicates that this assembly will perform satisfactorily.

The forward sections were of the type described in Section III of this report and preliminary tests indicated the following:

1) The pedestal section will withstand flight and handling loads that may be imposed on it.
2) Since there was no change in the ogive material, no tests were conducted.

3) Testing of the separation joint indicated that closer tolerances must be held between pins and groove in pedestal sections to withstand negative acceleration forces.

5. Material Studies

At the time design studies, mentioned in Paragraph 1, were initiated, a closer look was taken at airframe and separation device materials to determine if any new or old materials missed in last years search might exist.

a. Separation Device Materials

The use of polyethylene for the separation piston was dictated by design.

The materials research revealed an off-the-shelf NEMA grade paper phenolic tubing that could be used in place of the aluminum piston sleeve mentioned in the separation test. This paper tube has the advantage of being more economical in production and has better thermal properties than aluminum, thus allowing thermal property requirements of the pedestal section to be relaxed.

b. Airframe

(1) Pedestal Section. The pedestal section described in Report No. RS-TN-65-2 was an asbestos phenolic molding. In discussion with suppliers of molded products, it was determined that this shape would be difficult to mold because of flow problems, and the threads required for motor attachment would be impossible.

The new separation design eliminated the need for threads and since thermal properties could be relaxed, a search was made for an off-the-shelf tubing that could be used in place of the molding.

The result of this search was a NEMA Grade AA asbestos fabric phenolic that is three times as strong as the molding and in production will cost about half as much.

Results of thermal analysis for this material are discussed in Appendix B.

(2) Fin-Nozzle Retainer Assembly. Further studies conducted in this area revealed that there is no better material suited for this application than the steel being considered.

(3) Ogive. Further search for an ogive material with thermal properties equal and mechanical properties better than the properties of the material presently being considered revealed no other materials.

It should be noted that all fabrication and testing consisted of MDSS vehicle components. It is felt by the Structures and Mechanics Laboratory that proven design for the MDSS vehicle can be "scaled" up for the RDT&E vehicle and very little testing required to prove this design. Therefore, very little fabrication and no testing has been carried out for this vehicle.

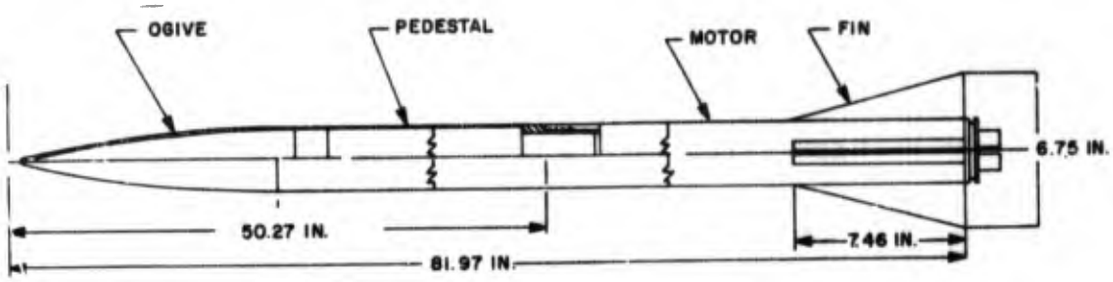

Figure 1. Launcher Test Vehicle

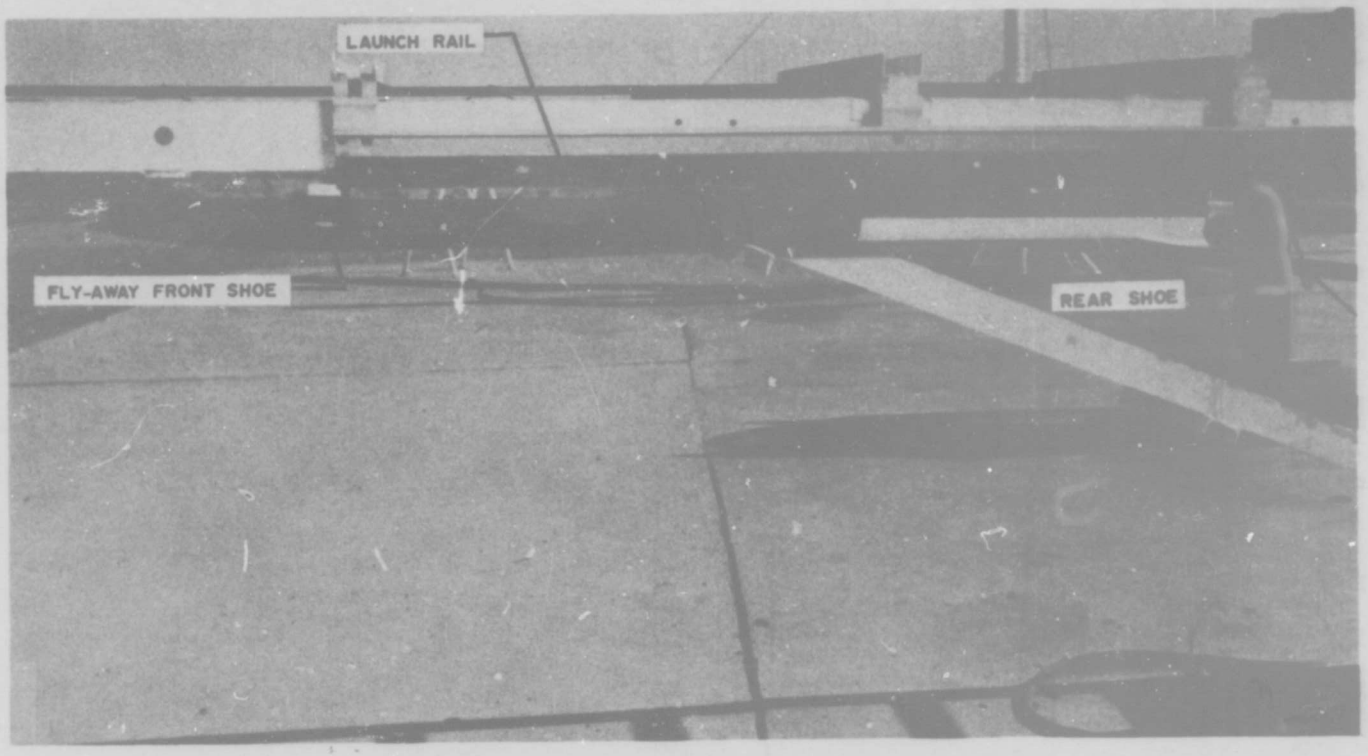

Figure 2. Modified Loki on Launcher

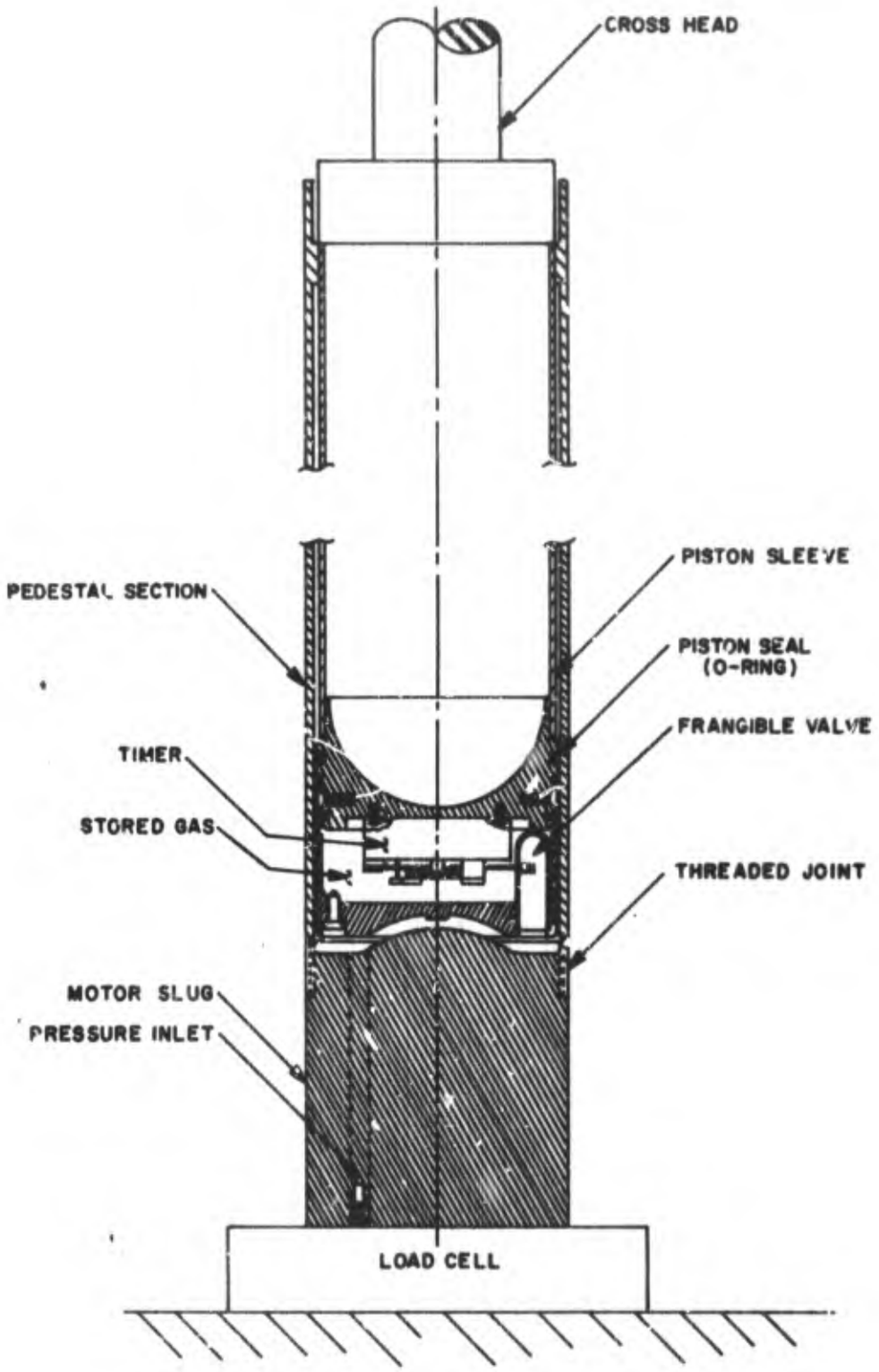

Figure 3. Separation Device In Test Fixture

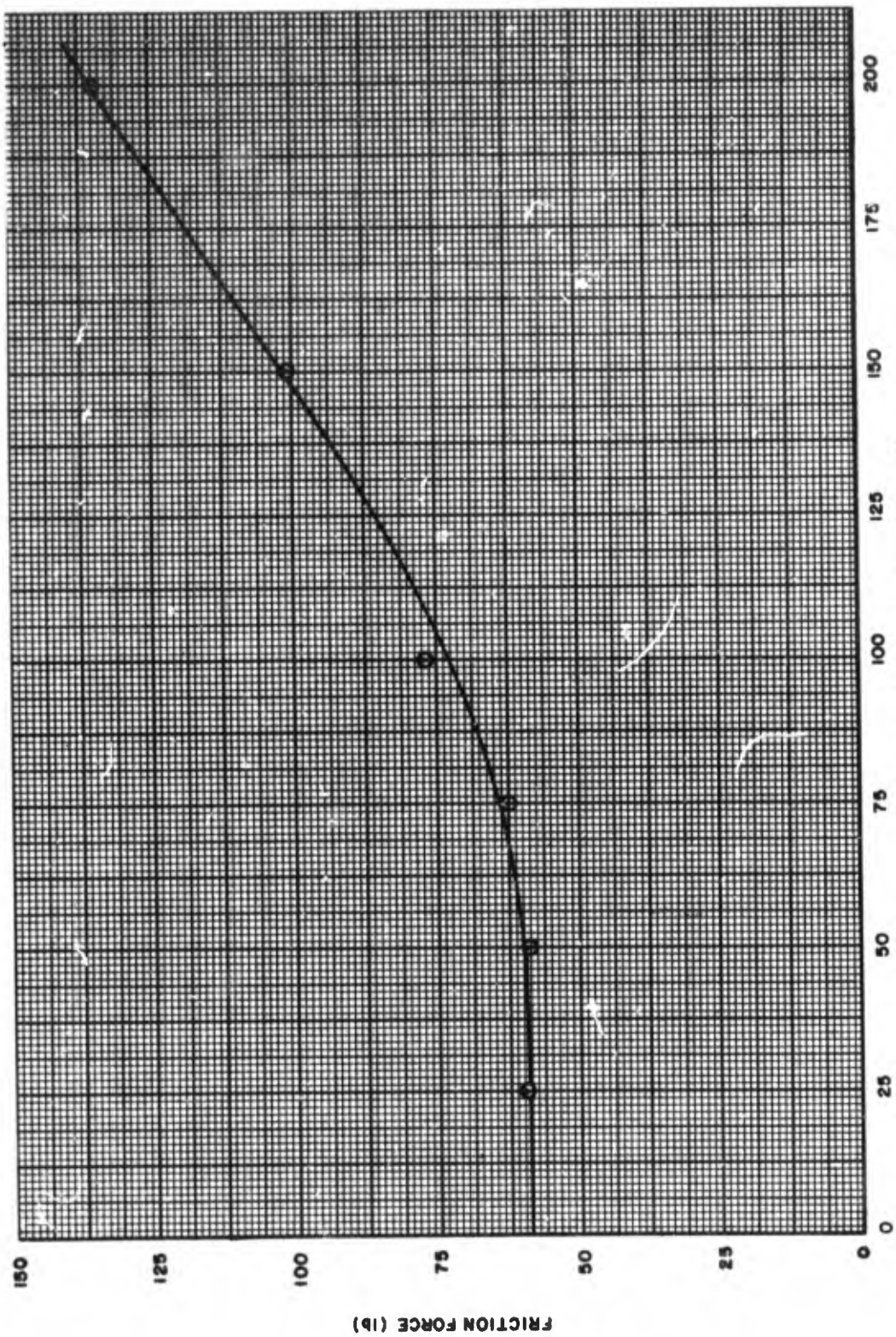

Figure 4. Friction Versus Pressure For Piston-Gas Container

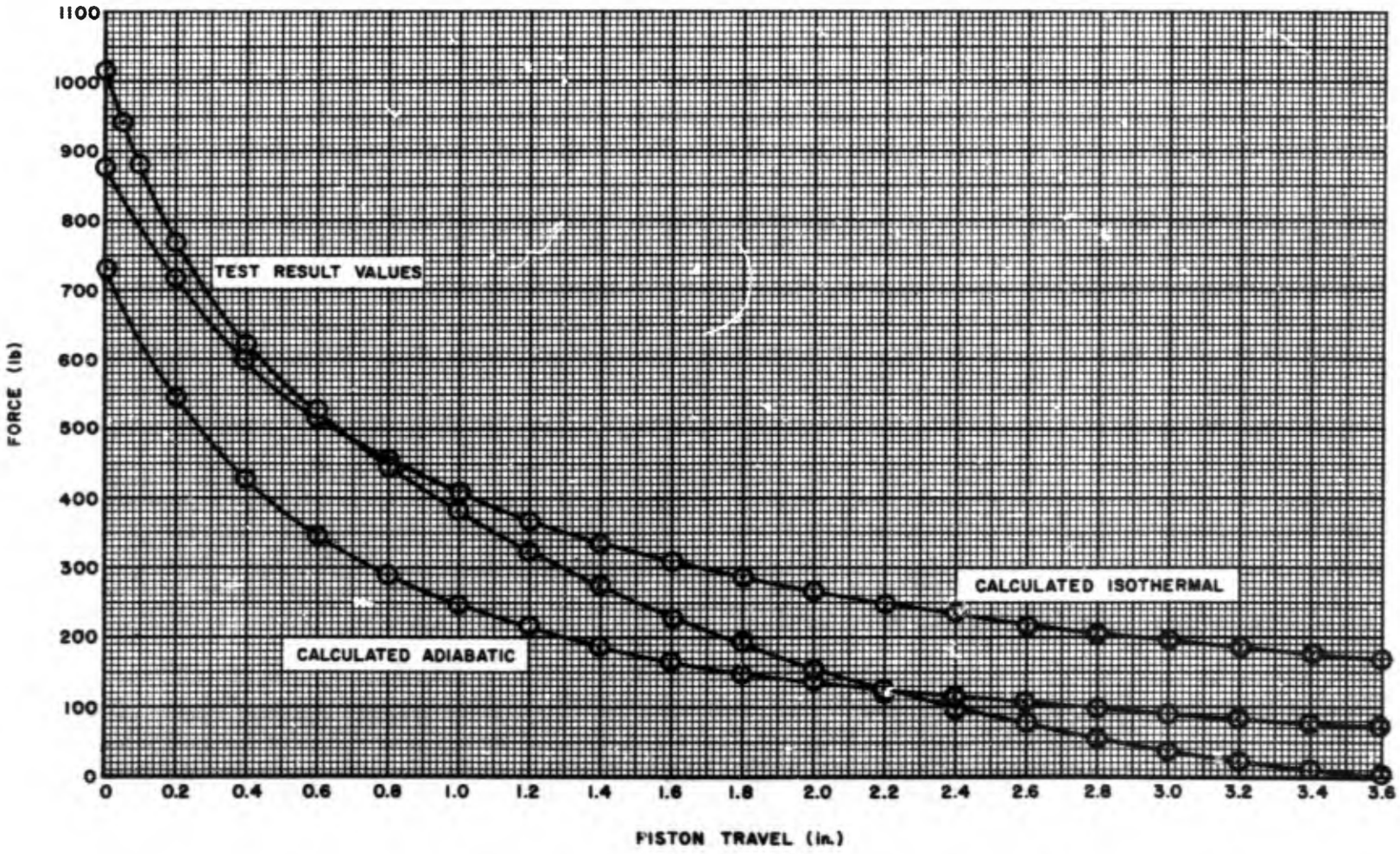

Figure 5. Calculated and Measured Force Versus Piston Travel, Piston-Gas Container

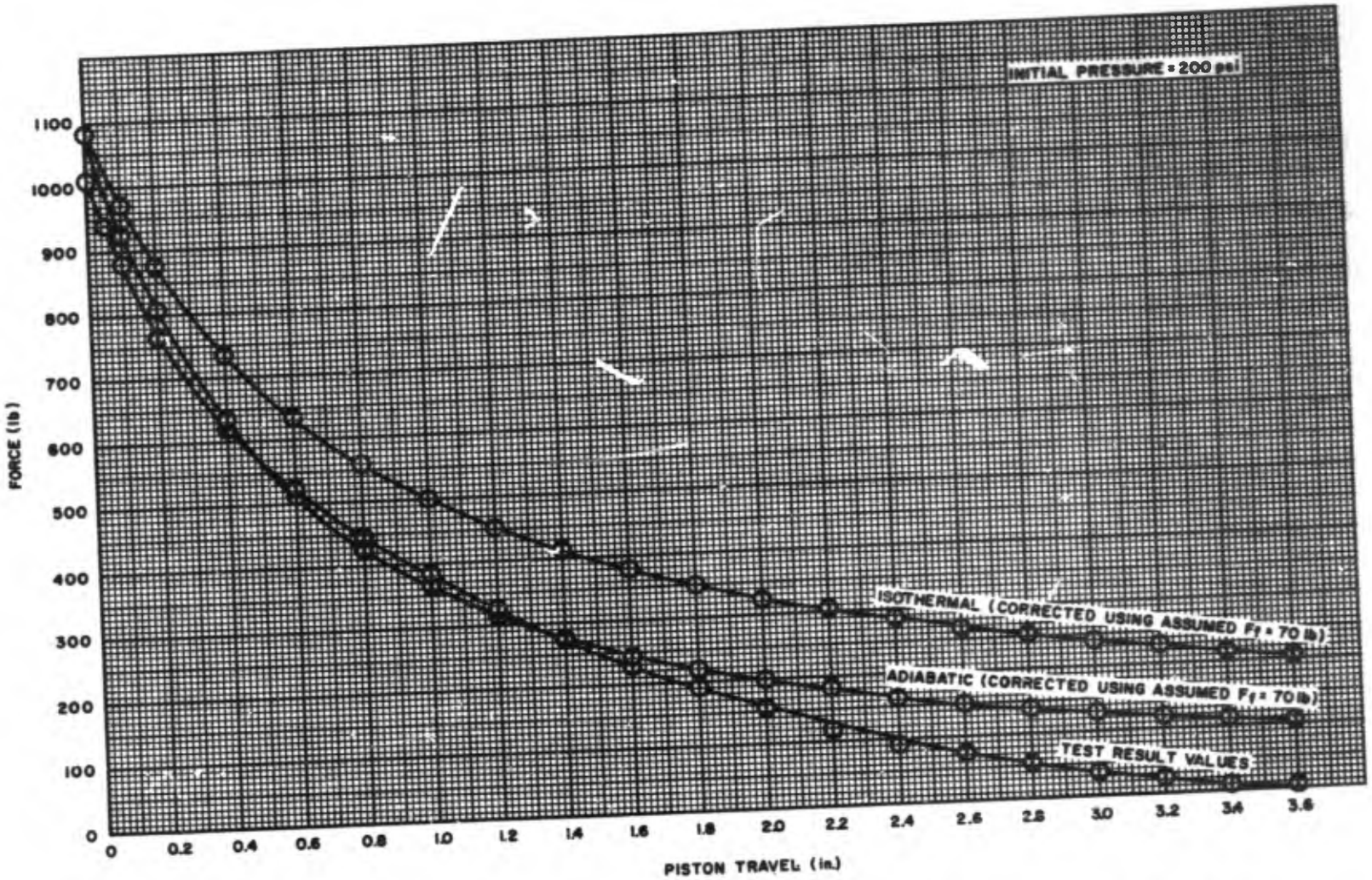

Figure 6. Calculated and Measured Force Versus Piston Travel, With Friction, Piston-Gas Container

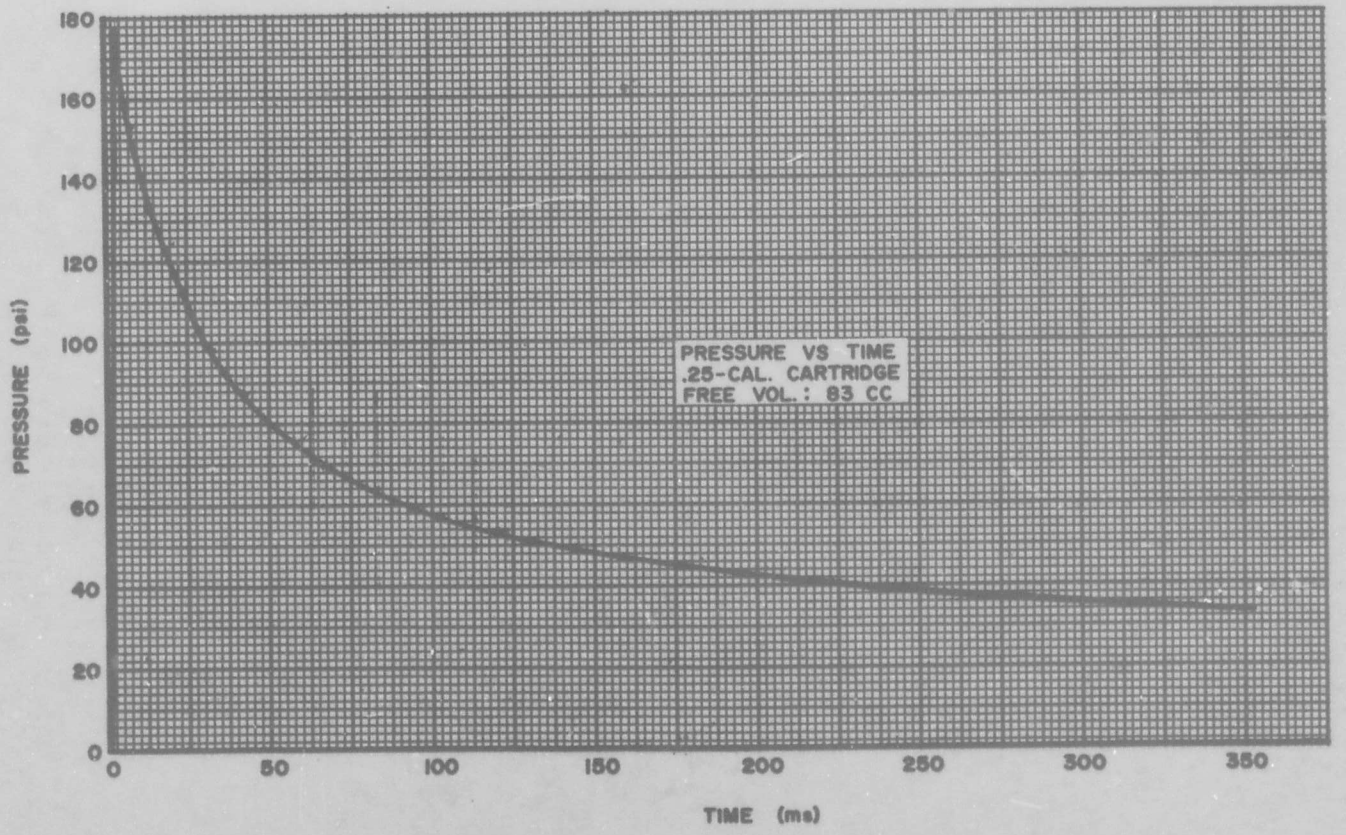

Figure 7. Pressure Versus Time For Separation Device Gas Generator

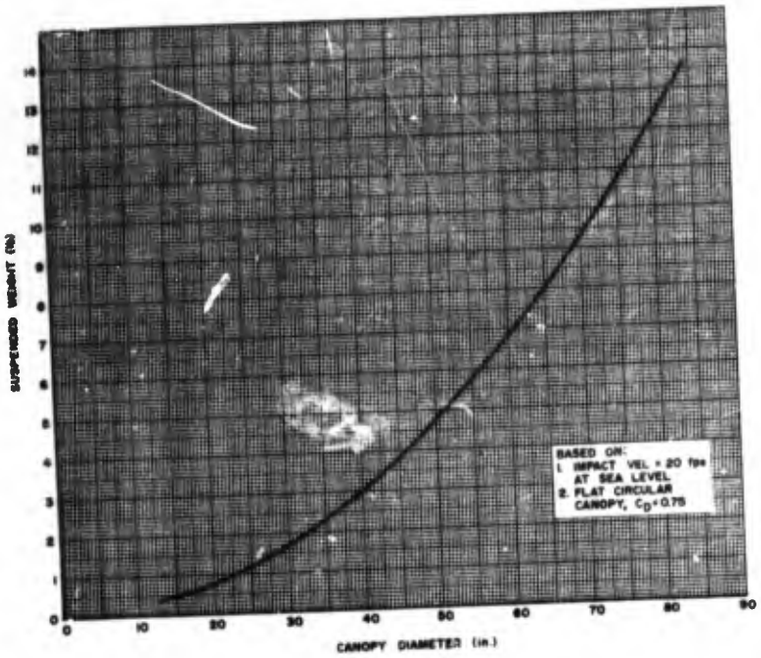

Figure 8. Load Versus Canopy Diameter

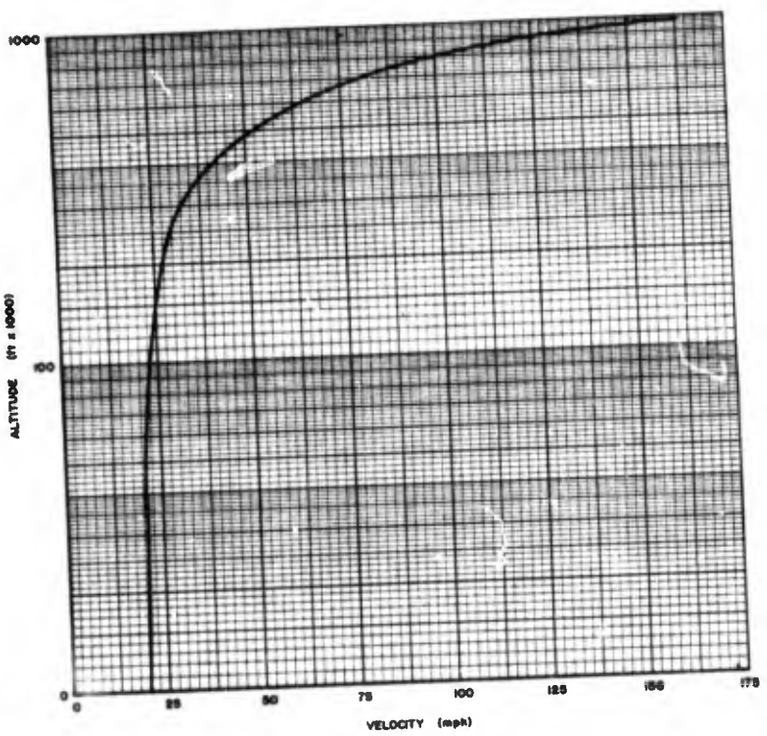

Figure 9. Altitude Versus Velocity, Parachute Diameter - Six Feet, Suspended

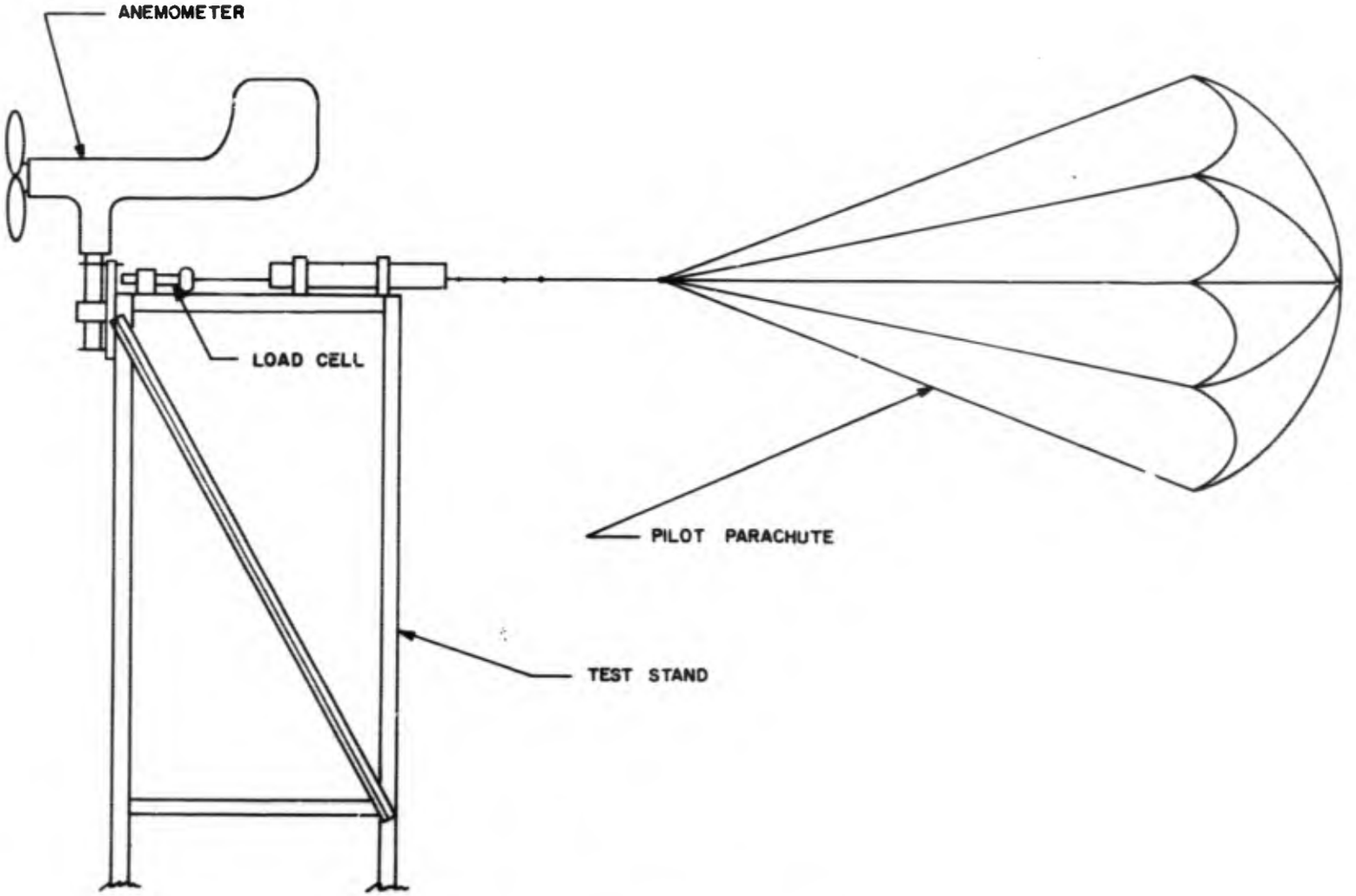

Figure 10. Parachute Test Fixture

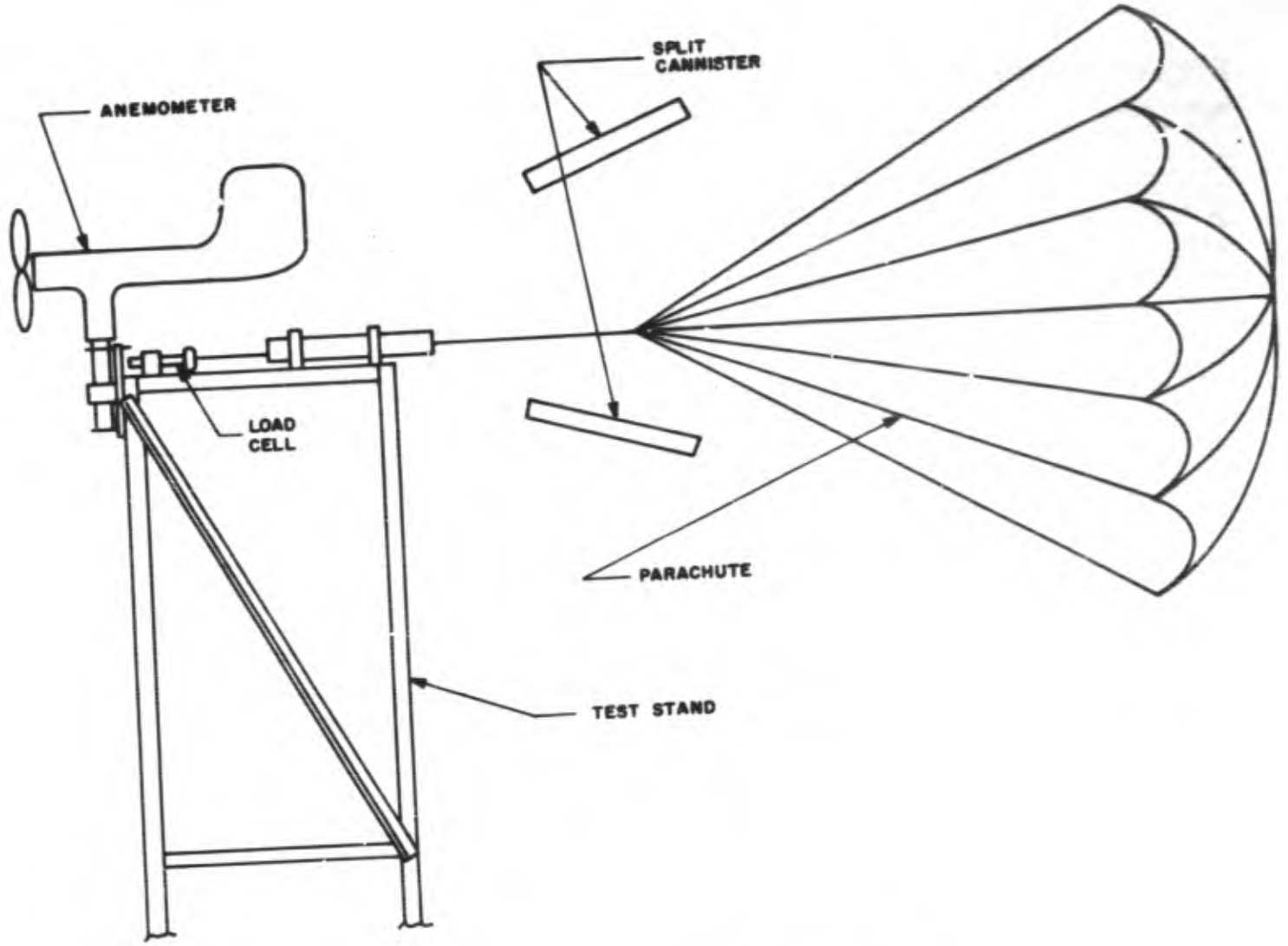

Figure 11. Parachute Deployment

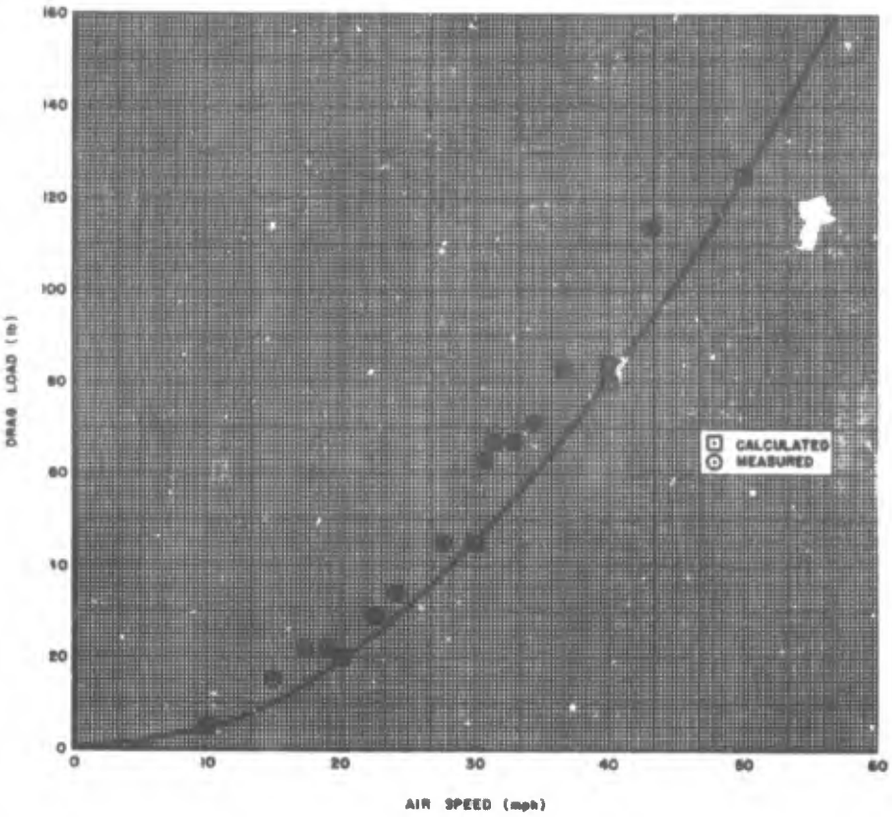

Figure 12. Load Versus Air Speed for Six-Foot Diameter Parachute

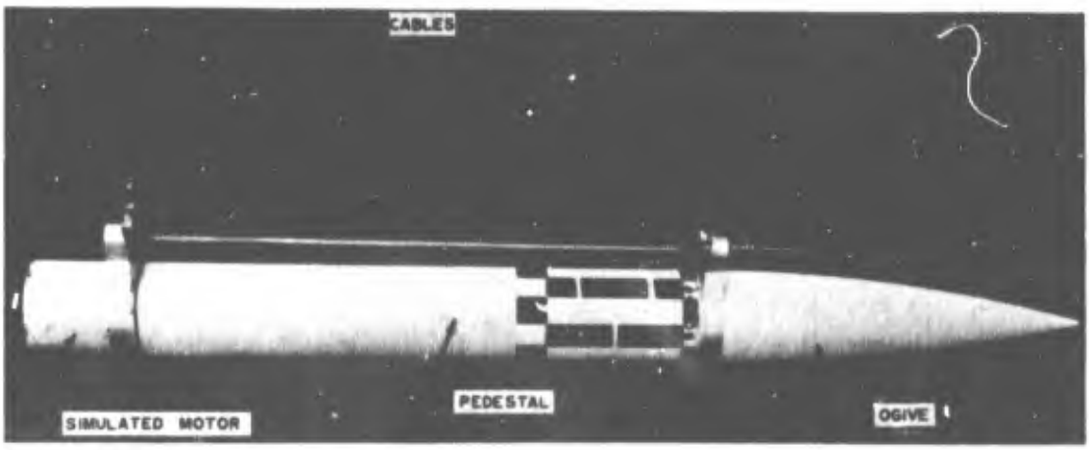

Figure 13. MDSS Forward Section in Test Rig

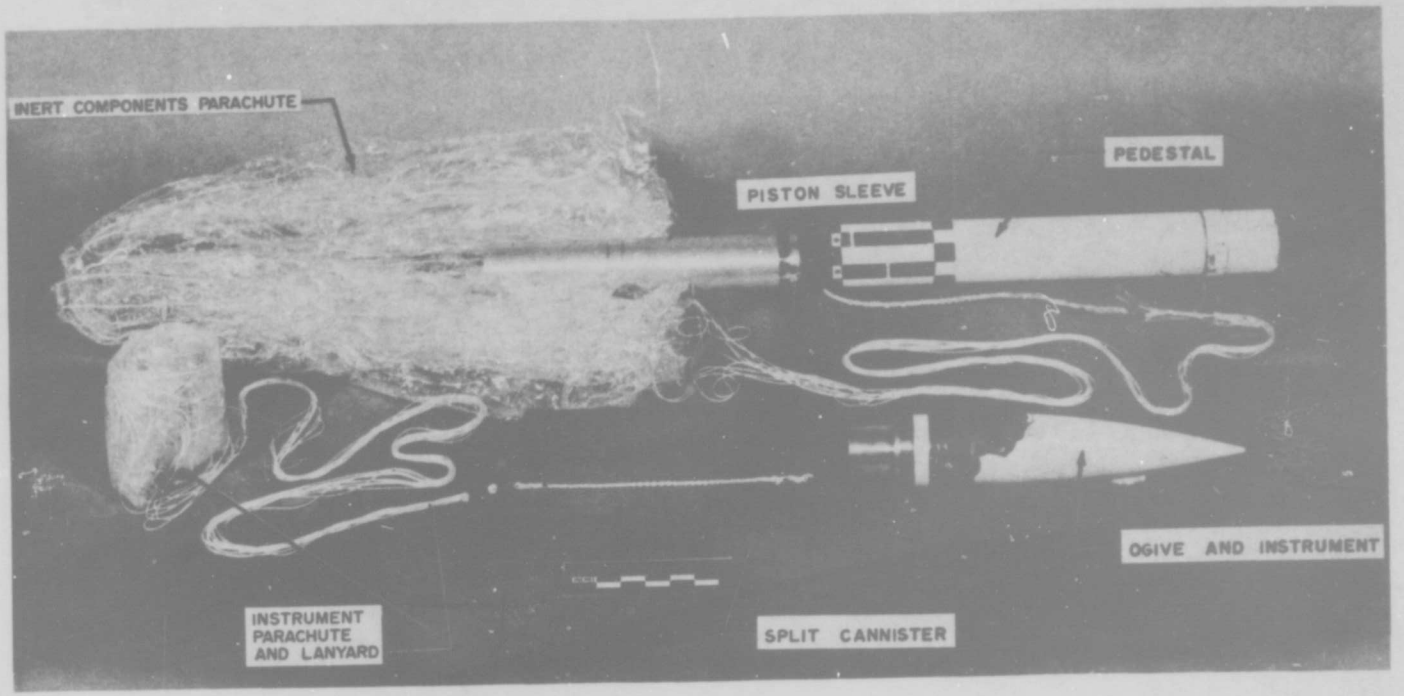

Figure 14. Forward Section After Separation

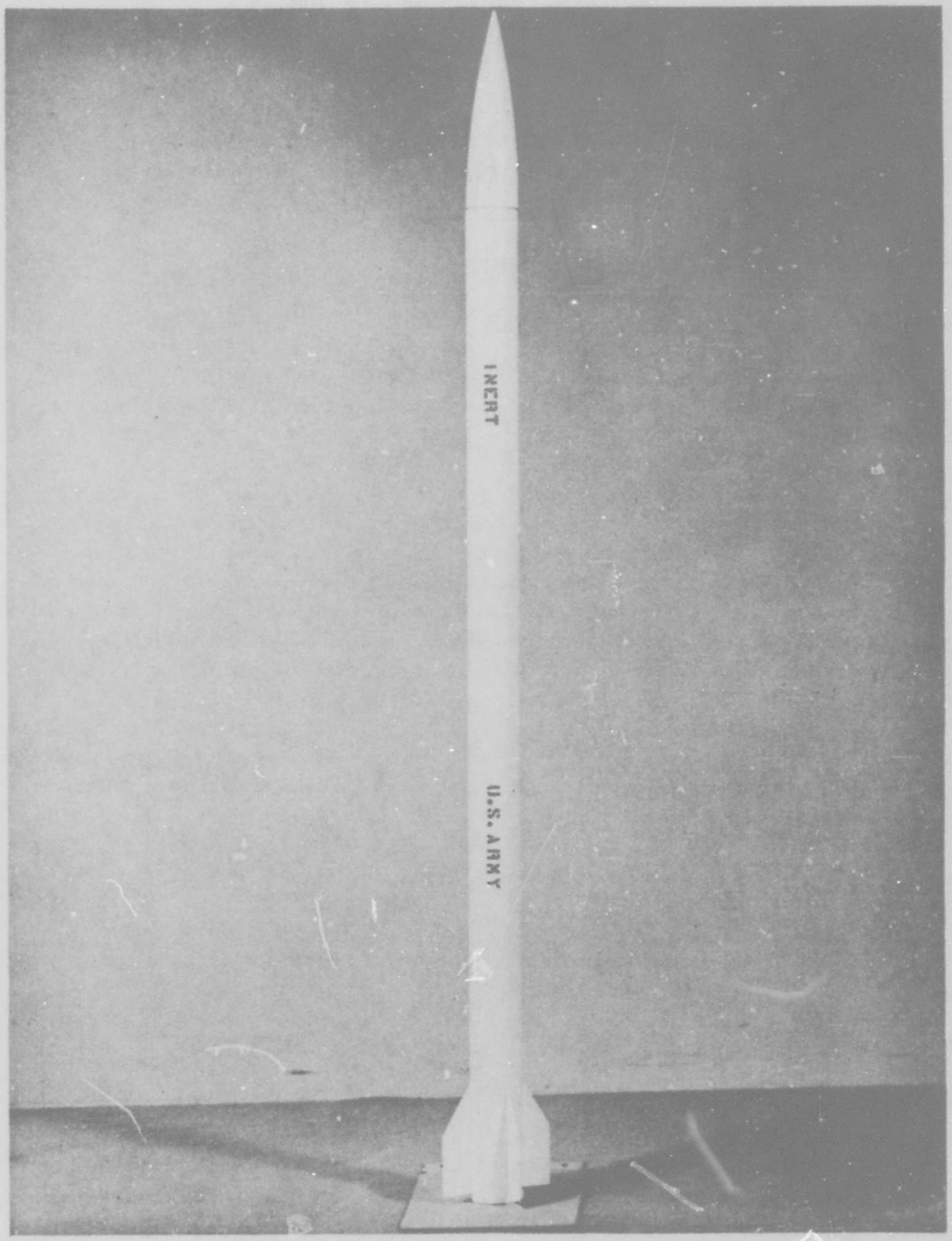

Figure 15. Rocket Vehicle for MDSS

Section III. ROCKET DESCRIPTION

1. Rocket Components for MDSS

The following paragraphs discuss the vehicle configuration resulting from studies mentioned in Section II, Paragraph 1. Figures 16 and 17 are views of the vehicle assembled and separated.

a. Airframe for MDSS Rocket

(1) Ogive Section (Figure 18). The four caliber tangential ogive is to be molded from a nylon-phenolic material. This material with 0.25-inch minimum wall thickness will prevent the payload from exceeding the 150°F maximum temperature specified in the requirements (Appendix B).

The ogive is 15.45 inches in length with a maximum diameter, at the tangent point, of 3.5 inches. This design differs from last years concept in that the ACME threads were removed and replaced by a cylindrical section 1.45 inches long by 3.245 inches in diameter. This section is the female portion of a bayonet connection with the outside being the male connection between ogive and pedestal. The male portion of the bayonet connection is a circular steel spring with two pins 180 degrees apart that lock into the slots in the ogive. With this spring installed, the payload is held in place, within the ogive, and the pins protrude above the 3.245-inch diameter so that when the ogive is placed into the pedestal, these pins snap into a groove inside the pedestal section and hold the ogive in place.

The threads were removed from the ogive for the following two reasons:

1) A homogeneous mixture of fiber and resin would be extremely difficult to achieve in a molding.
2) Removal of the threads allowed for elimination of the intermediate section described in Report No. RS-TN-65-2.

(2) Pedestal Section (Figure 19). The pedestal section which contains the descent vehicle, the parachute, the descent vehicle container, and the separation device is a 19.45 inch long cylinder with a 3.5-inch outside diameter and a 0.125-inch wall thickness. The pedestal is made of standard off-the-shelf tubing, NEMA Grade AA asbestos fabric phenolic. The forward end of the pedestal contains an 0.062-inch radiused groove on the inside diameter, 0.995 inches from the end. This serves as the female portion of the shear joint in which the payload

retainer pins snap into when the ogive is inserted. The aft end of the pedestal connects to the motor bottle by simply slipping it over the forward end of the motor bottle and bonding it into place. (Mass production costs approximately $2.60.)

(3) Fin-Nozzle Retainer Assembly. The fin-nozzle retainer (Figure 20) is the same as presented in Report No. RS-TR-65-2. This assembly consists of four clipped delta fins made of 0.04-inch sheet steel and attached to the retainer ring at the aft end. However, since the motor bottle material was changed to steel, the fin assembly may be welded instead of bonded as originally planned.

This fin arrangement will require an assembly fixture that provides very close alignment so that the three-revolutions per second maximum spin rate of the vehicle is not exceeded.

b. Separation Device

The separation device (Figure 21) evolving from design studies conducted this fiscal year consists of the following components:

1) Polyethylene piston and paper-phenolic sleeve.
2) Mechanical timer with acceleration latch and firing pin (Figure 15).
3) Precussion fired gas generator.
4) Lanyards (one to motor bottle and one to parachute).
5) Parachute (housed in moulded polyethylene split cannister).
6) Piston aft cover.

The device is assembled (Figure 21) with the timer set for the desired time interval (time to apogee). The launch crew receives the rocket in the shipping and storage condition with the instruments and ogive in one container and the remaining hardware in the launch container. As the instruments are being checked, prior to flight, the separation section is pulled from the rocket section, the piston cover removed, and the timer wound and firing pin cocked. The gas generator is then inserted into its place, the cover replaced, and the device reinserted into the pedestal section. The ogive with the instruments is installed on the rocket by first attaching the instrument decent vehicle lanyard to the instrument section and then forcing the ogive into the pedestal until the bayonet pins snap into the groove. At launch, the acceleration of the rocket causes the acceleration latch to release the timer and allows the timer to function. At the end of the preset time interval, the firing pin strikes the primer of the gas generator with the gas occupying the space between the piston and motor head closure. This pressure results in a

force on the piston with the pedestal and rocket motor as the resisting element on one side and the piston sleeve and ogive as the resisting element on the other side. This force between the ogive and the pedestal causes the bayonet pins to tear out of the pedestal section, thus freeing the ogive and instruments from the vehicle.

This piston is still under considerable pressure after the pins tear loose. This pressure will cause motion of the piston such that a relative velocity will be established between the ogive and the separation device as one unit and the pedestal and motor as the other. The separation device will travel forward until it clears the pedestal, at which time it will come to the end of the lanyard connecting it to the motor and stop. The ogive will continue on, pulling the split cannister free of the piston sleeve. This will allow the two halves of the cannister to fall away and the payload decent vehicle and parachute will deploy. The decent vehicle will lower the ogive and instruments, and the parachute will lower the inert components, i.e., motor and pedestal, and separation device as shown in Figure 22. Then two halves of the split cannister will free-fall to earth and, since they weigh very little, will not cause a hazard.

c. MDSS Rocket Physical and Performance Characteristics

Tables I and II present the rocket physical and performance characteristics.

2. Rocket Vehicle for RDT&E

The following paragraphs discuss the RDT&E Vehicle (Figure 23) resulting from studies mentioned in Section II, Paragraph 1.

a. Airframe

(1) Ogive Section (Figure 24). During design and material studies, it was determined that the one-piece forward section, proposed for the RDT&E rocket, would be extremely difficult to fabricate. Also, there would be problems in achieving homogenous strength throughout the structure. For these reasons, the forward section was made in two pieces, the ogive and the pedestal.

The ogive is a four-caliber tangent molded from nylon-phenolic. It is 19 inches long with a base diameter of 4.75 inches and has a minimum wall thickness of 0.25 inch to protect the payload from the high temperature experienced during flight (Appendix B). The aft end of the ogive contains a 1.25-inch long cylinder, 4.495 inches in diameter, which serves as the male portion of the joint between the ogive and the pedestal.

Table I. MDSS Vehicle Physical Characteristics

Rocket	
Diameter (in.)	3.50
Length (in.)	80.14
Weight (lb)	
Total	38.74
Burned	18.84
Center of Gravity from Nose (in.)	
Total	48.30
Burned	43.20
Moments of Inertia (lb-in.^{2})	
Roll	
Total	77.29
Burned	44.98
Pitch-Yaw	
Total	16,114.33
Burned	12,263.15
Ogive	4 Earlier
Fins	
Number	4
Planform	Clipped Delta
Span (in.)	7.50

Table II. MDSS Vehicle Performance Characteristics

Altitude at Apogee (ft), 80 deg QE from Missile	109,870
Time to Apogee (sec)	77.33
Burning Time (sec)	3.50
Velocity at Burnout (ft/sec)	4945
Mach Number at Burnout	4.45
Altitude at Burnout (ft)	7286
Maximum Acceleration (g)	70.94
Launch Acceleration (g)	28.00
Acceleration of Payload at Separation (g)	21.00
Maximum Amp Temperature (°F)	146
Spin (rps)	3

(2) Pedestal Section (Figure 25). The pedestal is a cylindrical section 4.75 inches in diameter and 12.75 inches long with a wall thickness of 0.125 inch which contains the instrument parachute. It is made of off-the-shelf asbestos fabric-phenolic tubing. The pedestal is fixed at its forward end to the ogive through a bonded joint and is attached at its aft end to the motor-pedestal adapter by shear pins.

(3) Pedestal-Motor Adapter (Figure 26). The adapter is made of steel tubing and is 4.75 inches in diameter, 3.95 inches long, and has a wall thickness of 0.075 inch. Four aluminum shear pins, five-thirtyseconds of an inch in diameter, connect the adapter to the pedestal section. The adapter connects to the front end of the motor through a bayonet connection.

The purpose of the adapter is to allow removal of the forward section without special tools.

(4) Fin-Nozzle Retainer Assembly (Figure 27). Through studies conducted during the year, it was learned that the fin presented in Report No. RS-TN-65-1 was not large enough to retain rocket stability under certain conditions.

The Advanced Systems Laboratory recalculated the fin force and the resulting required area is shown in Figure 24. The varying thickness of fin cross section is an attempt to reduce flutter with the least weight possible.

The fin will necessarily be fabricated of steel because of aerodynamic heating and will be welded to the nozzle retainer ring, four fins per ring. This assembly will be held to the motor bottle with a special alignment fixture and welded in place.

b. Separation Device (Figure 28)

The separation device is located within the adapter section of the RDT&E vehicle (Figure 25) and consists of the following components:

1) Mechanical timer with firing pin (Figure 21).
2) Polyethylene piston.
3) Piston sleeve.
4) Lanyards.
5) Snap line.
6) Parachute.
7) Split cannister.

The mechanical timer and gas cartridge are the same as those used in the MDSS vehicle. The polyethylene pistons are of the same design but utilize a different configuration for lanyard connections and seal. The parachute is the same as that used in ARCAS vehicles and the split cannister is a scaled version of the MDSS cannister.

It is anticipated that the rocket will be stored and shipped as two units, the rocket motor with fins as one package and forward section containing the other components as the other. A plastic closure will be provided for the open end of the forward section which will retain the components. The gas cartridge will be handled as a separate item, thus making the forward section inert. Prior to launch, the plastic closure will be used as a base while the forward section is removed for a final instrumentation check (Figure 29). After the components are replaced in the forward section and the plastic closure is removed, the piston closure is removed, the timer wound and firing pin set, and the gas cartridge installed. If separation is not required, this phase will be left out. The lanyard on the aft end of the piston will be taken loose and looped through the motor bottle bayonet pins and then refastened. The forward section will then be inserted on the motor bottle and locked into place. At this point, the rocket will be sensitive to longitudinal "g" loading and must be handled with care.

The acceleration of the rocket at launch will initiate the timer to which, after a preset time, will allow the firing pin to strike the cartridge, thus causing separation to occur. The piston force due to high pressure will shear the pins in the shear joint. There will be sufficient piston travel, while the gases are expanding, to accelerate the two bodies in opposite directions. When the lanyard between the piston and motor becomes taut, the piston travel changes directions (Figure 30) taking slack out of the snap line between the piston and parachute. The snap line pulls the split cannister and parachute from the forward section allowing the split cannister to separate, freeing the parachute. As the lanyard between the parachute and payload becomes taut, the snap line breaks away and the parachute deploys dragging the instrument section out of the forward section (Figure 31). The motor, adapter, piston, and split cannister free-fall to earth as one unit and the forward section as the other. The payload is lowered, at a controlled rate, by the parachute.

d. <u>RDT&E Rocket Physical and Performance Characteristics.</u>

Tables III and IV present the rocket physical and performance characteristics.

Table III. RDT&E Physical Characteristics

Rocket	
Diameter (in.)	4.75
Length (in.)	99.35
Weight (lb)	
Total	88.99
Burned	36.06
Center of Gravity, Location from Nose (in.)	
Total	60.405
Burned	57.27
Moments of Inertia (lb-in.^{2})	
Roll	
Total	351.62
Burned	300.39
Pitch-Yaw	
Total	47,722.40
Burned	31,775.91
Ogive	4 Caliber Tangent
Fins	
Number	4
Planform	Clipped Delta
Span (in.)	30.75

Table IV. RDT&E Performance Characteristics

Altitude at Apogee (ft) (80° QE from Msl)	235,595
Time to Apogee (sec)	120.96
Burning Time (sec)	5.3
Velocity at Burnout (ft/sec)	6151.83
Mach Number at Burnout	5.78
Altitude at Burnout (ft)	13,273
Maximum Acceleration (g)	69.86
Launch Acceleration (g)	21.53
Acceleration at Separation (g)	20 (Approx)
Maximum Payload Temperature (°F)	150
Spin (rps)	9

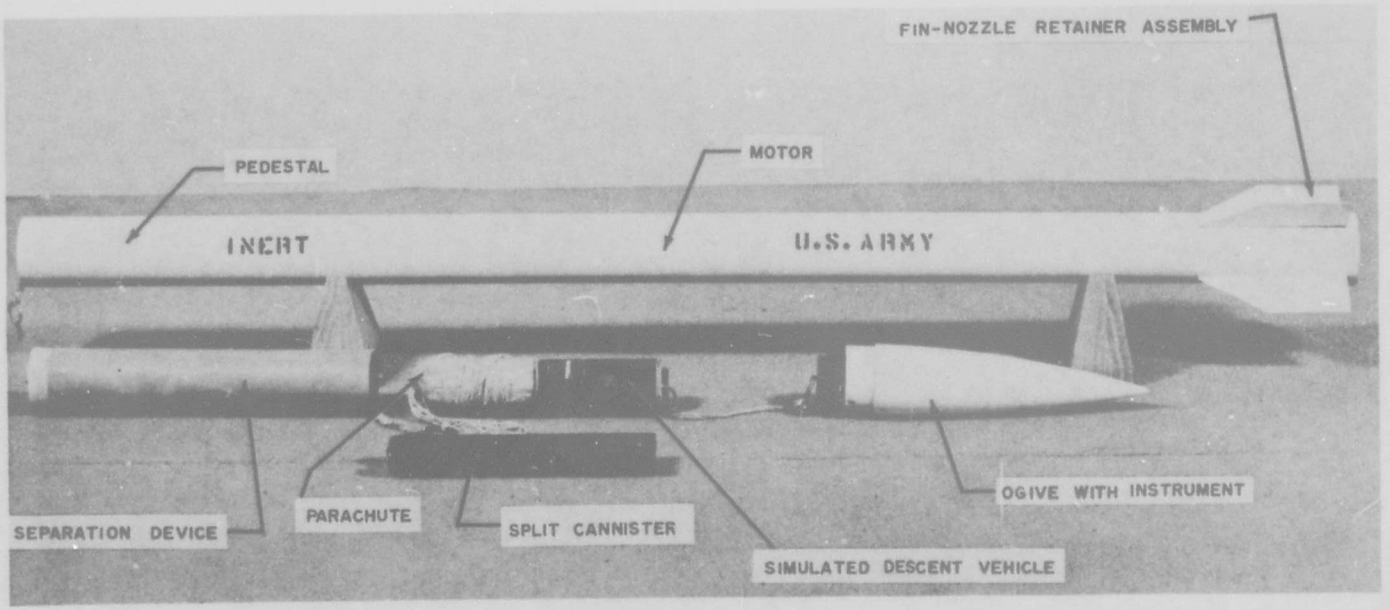

Figure 16. MDSS Vehicle, Separated

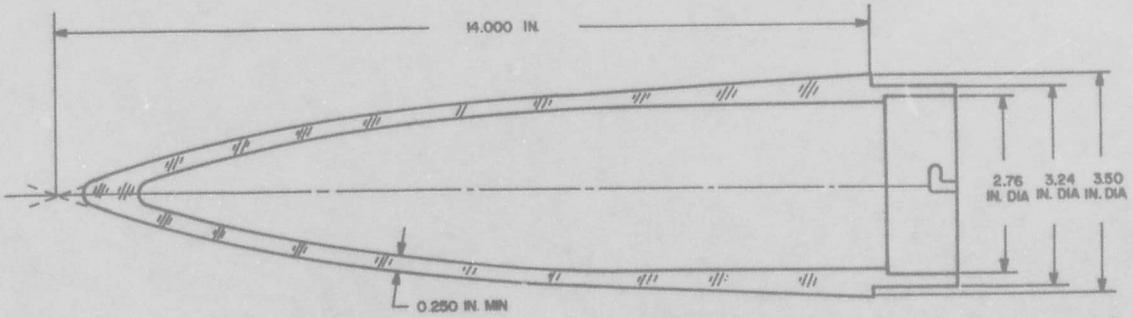

Figure 17. Ogive Section, MDSS

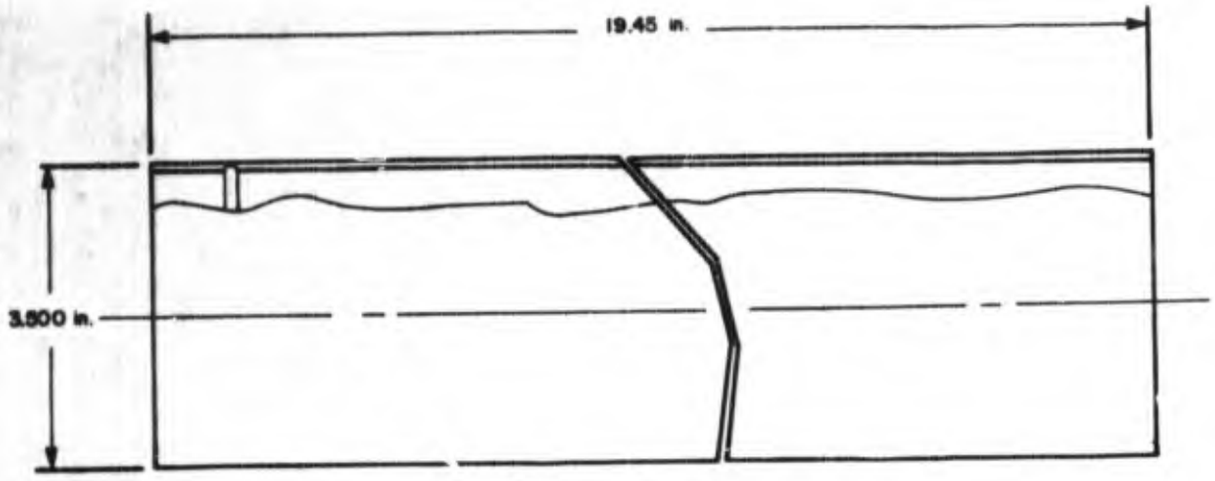

Figure 18. Pedestal Section, MDSS

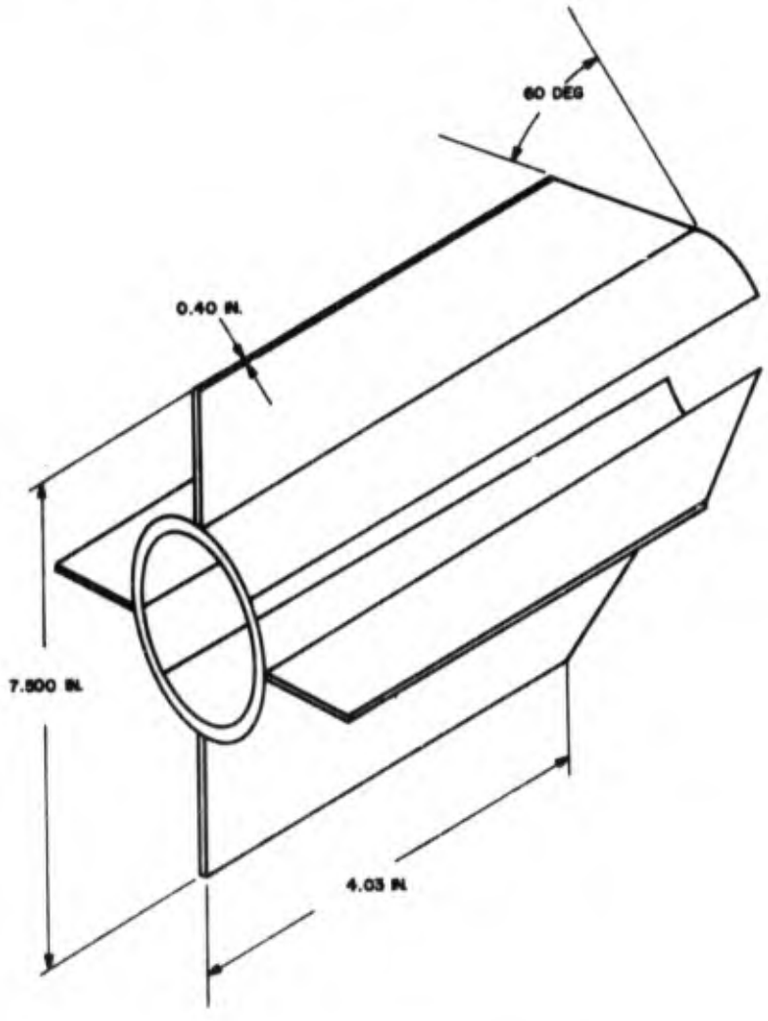

Figure 19. Fin Assembly, MDSS

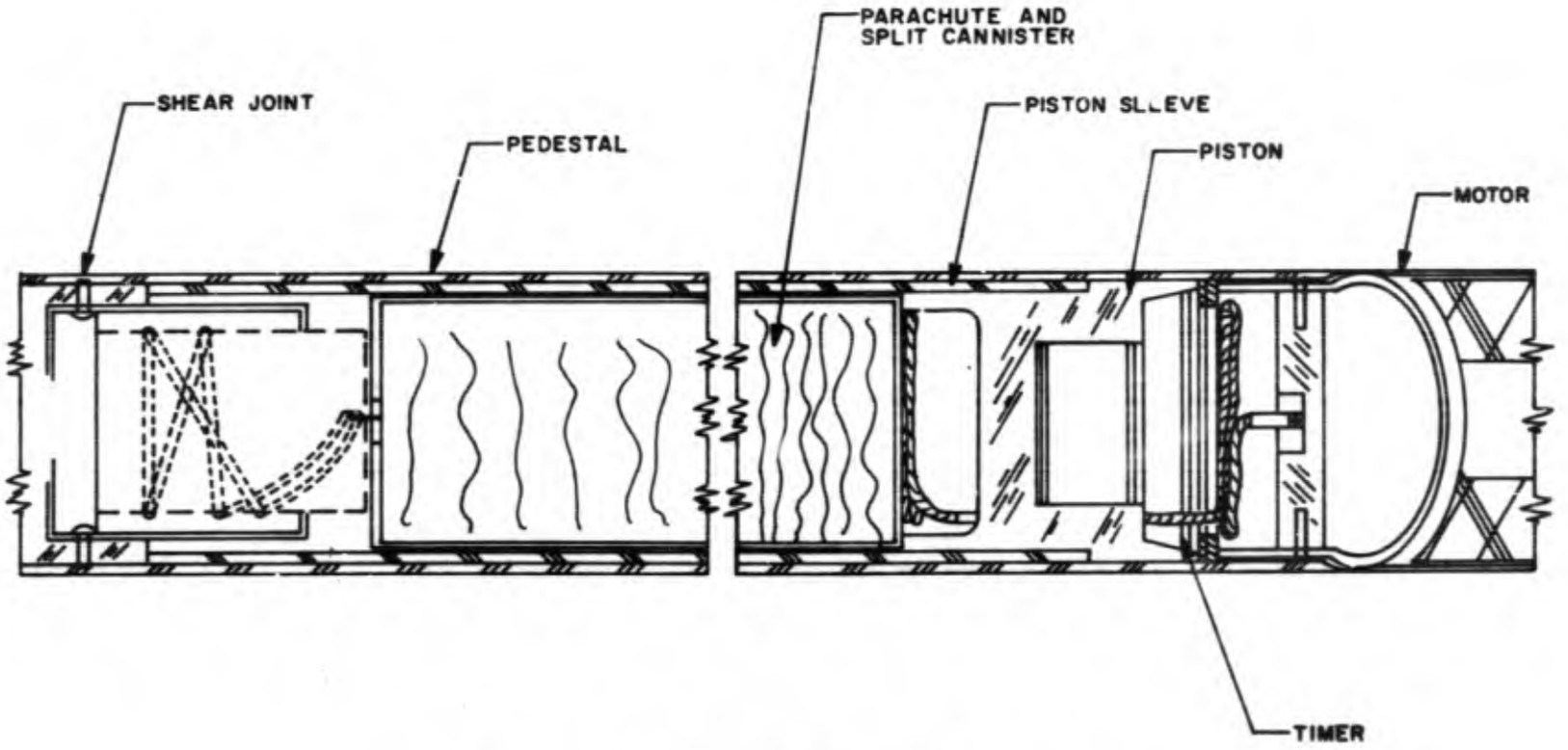

Figure 20. Separation Device, MDSS

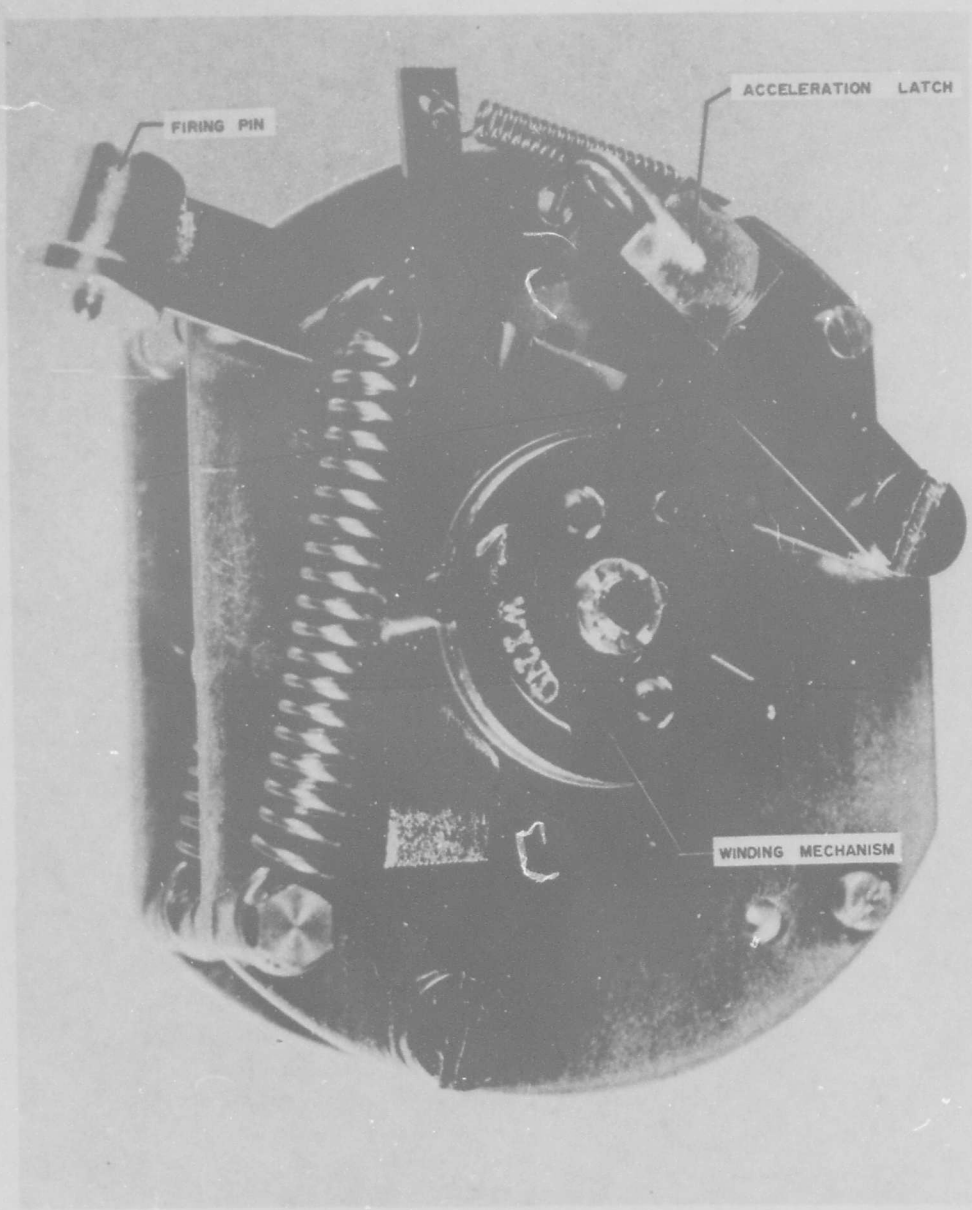

Figure 21. Mechanical Timer

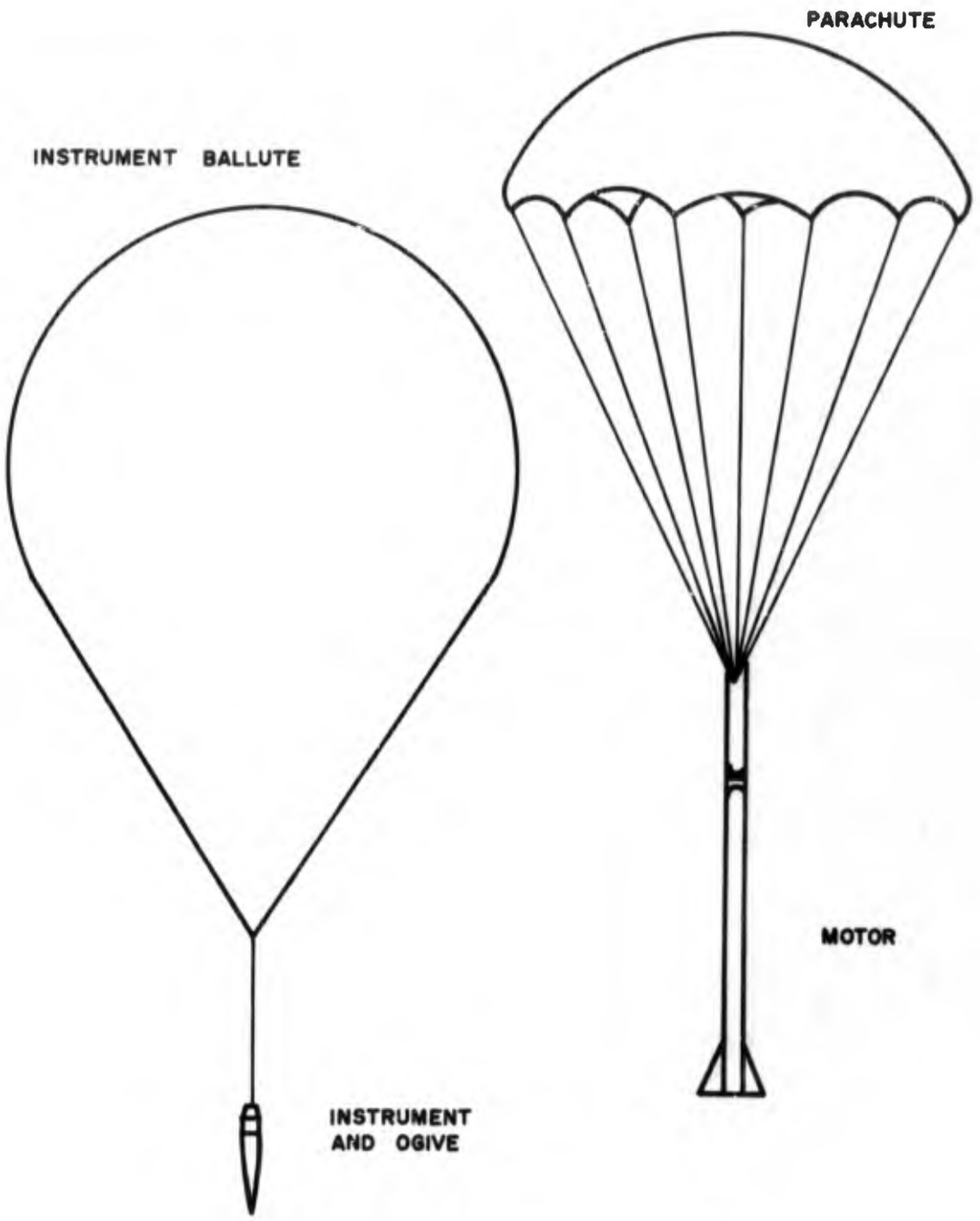

Figure 22. Separation of MDSS

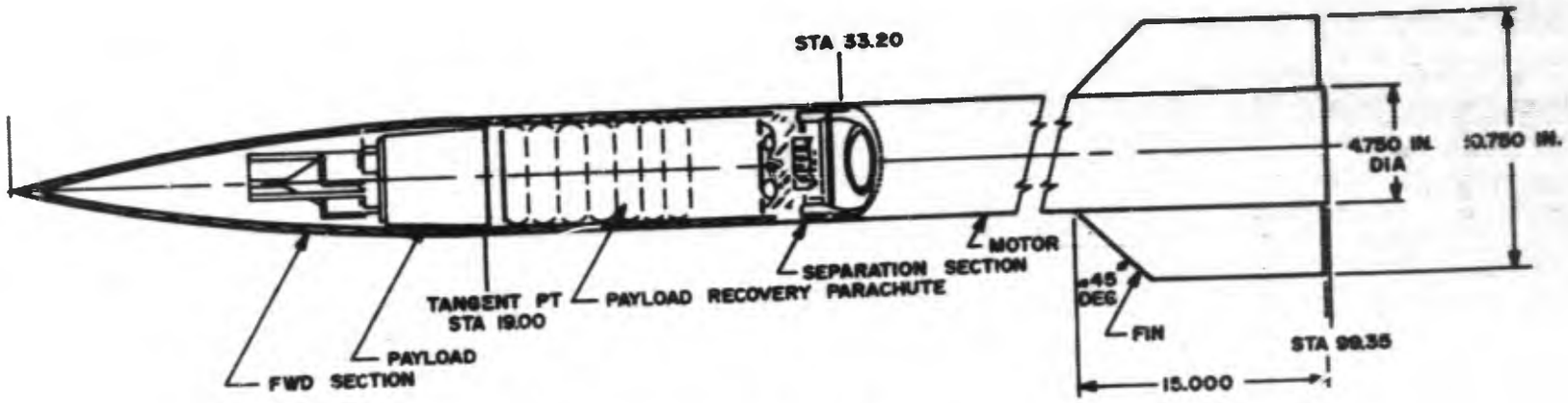

Figure 23. RDT&E Rocket

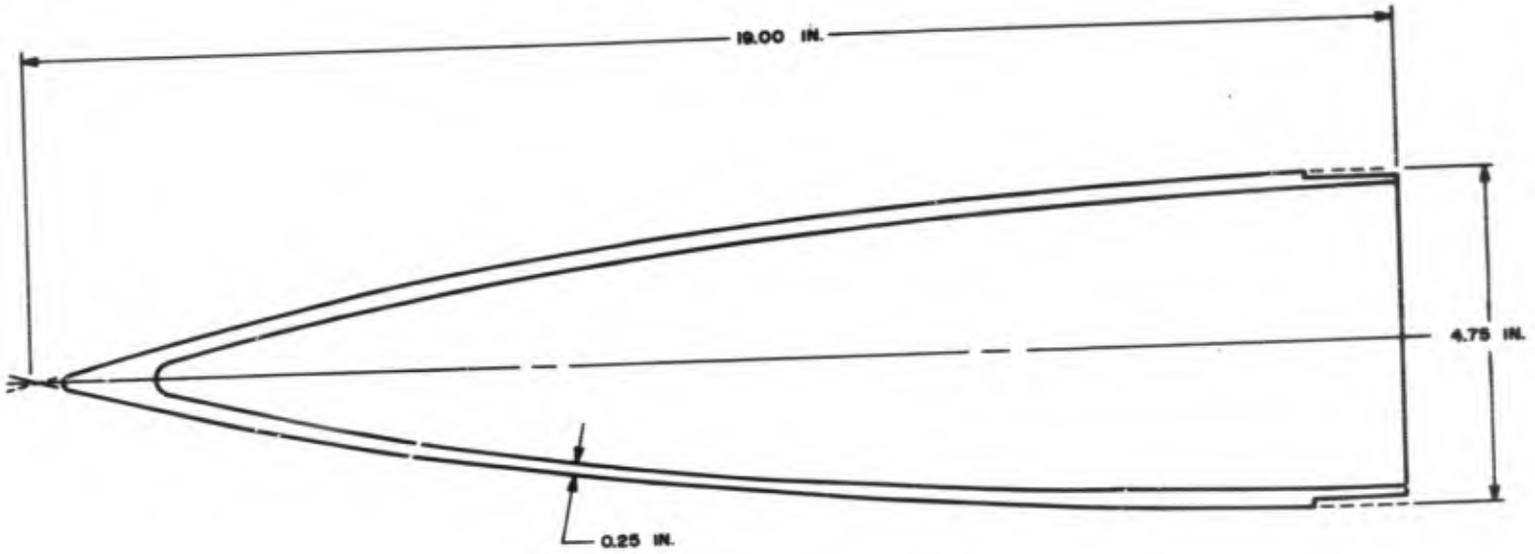

Figure 24. Ogive, RDT&E Vehicle

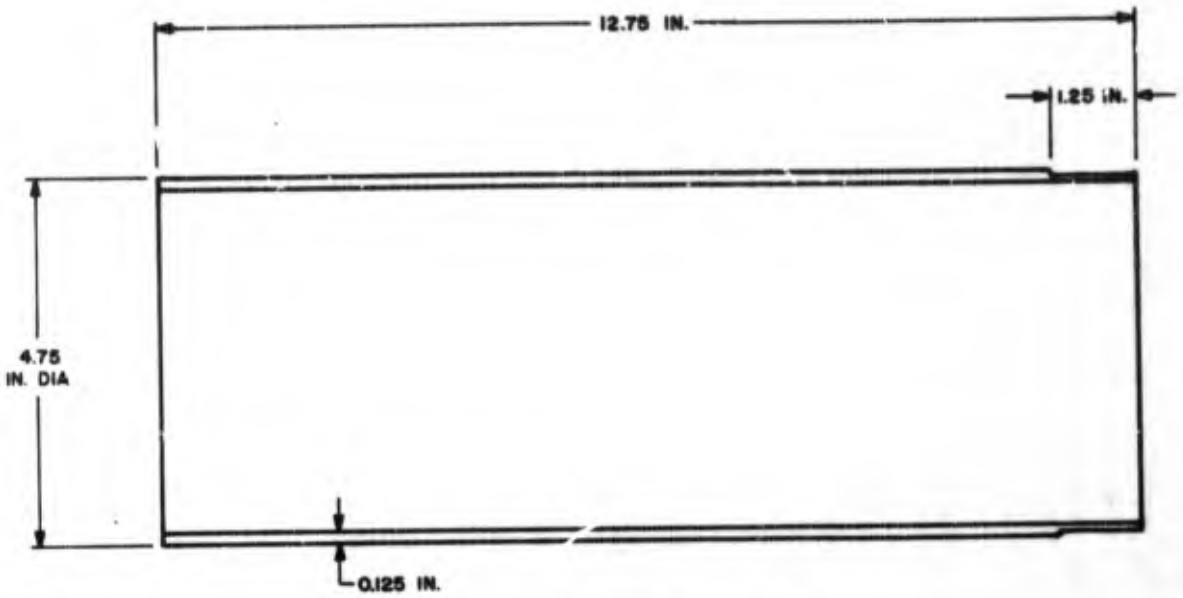

Figure 25. Pedestal, RDT&E

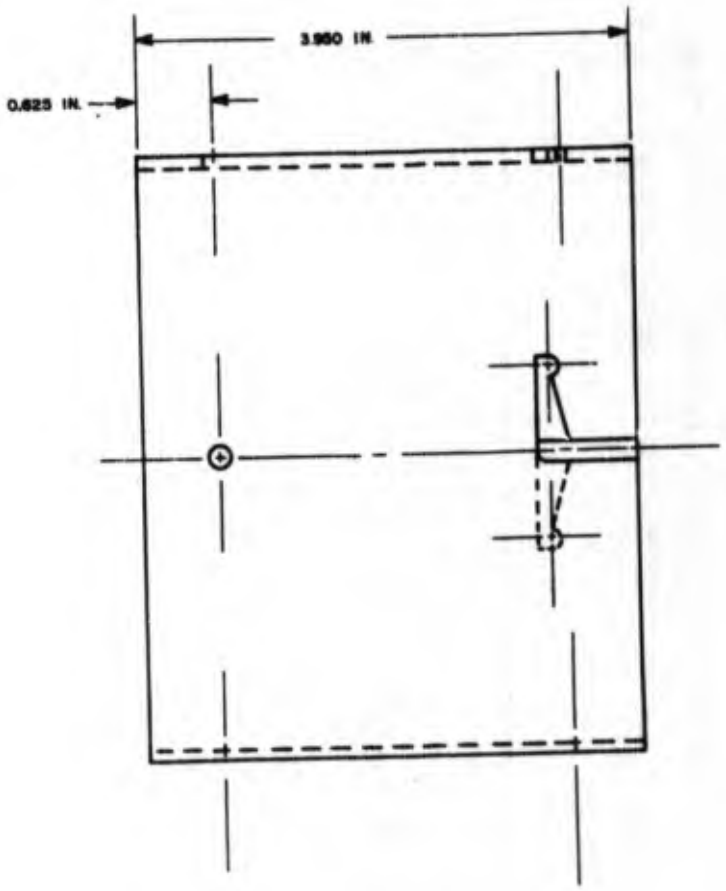

Figure 26. Adapter, RDT&E

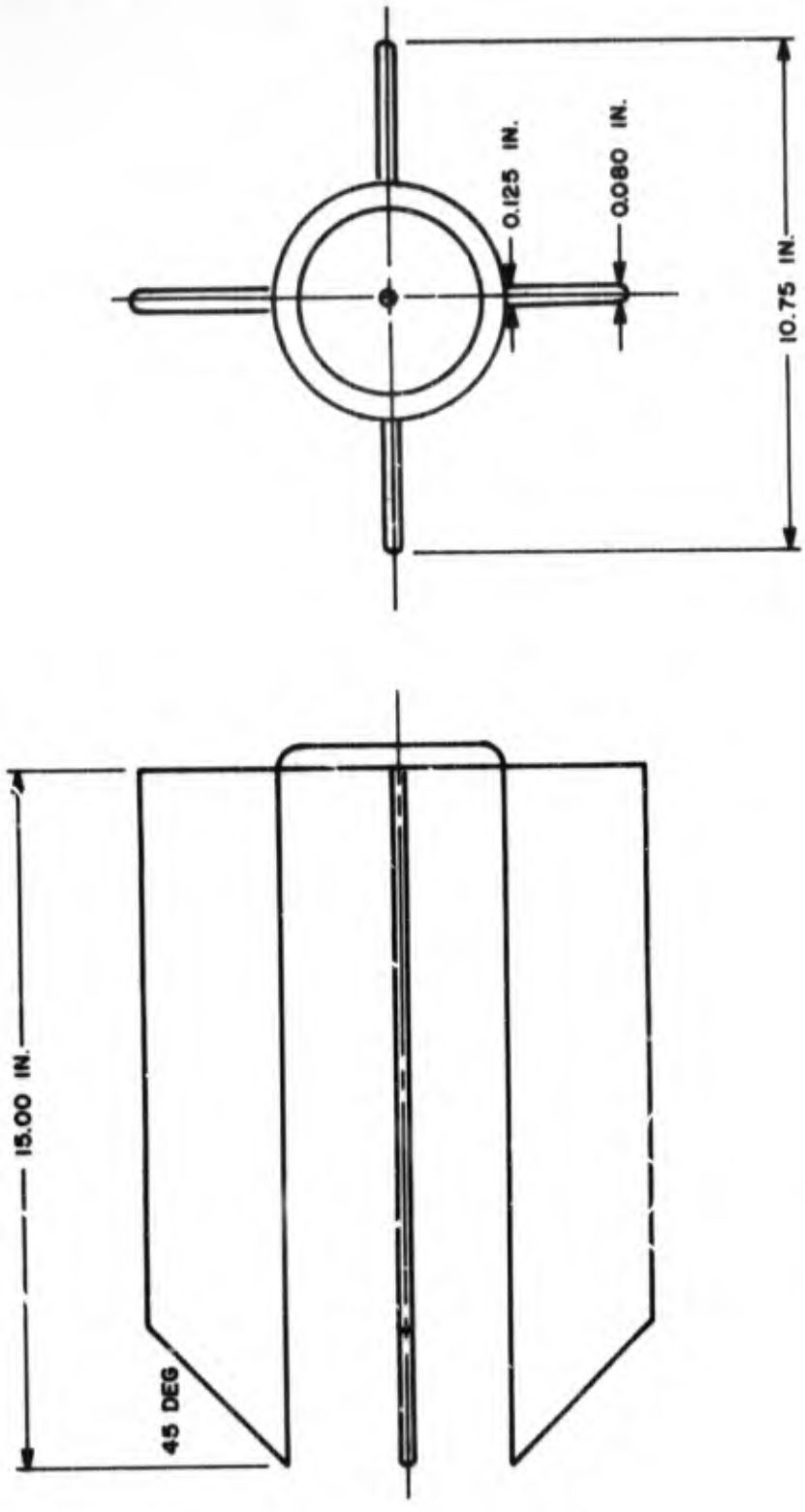

Figure 27. Fin-Nozzle Retainer, RDT&E

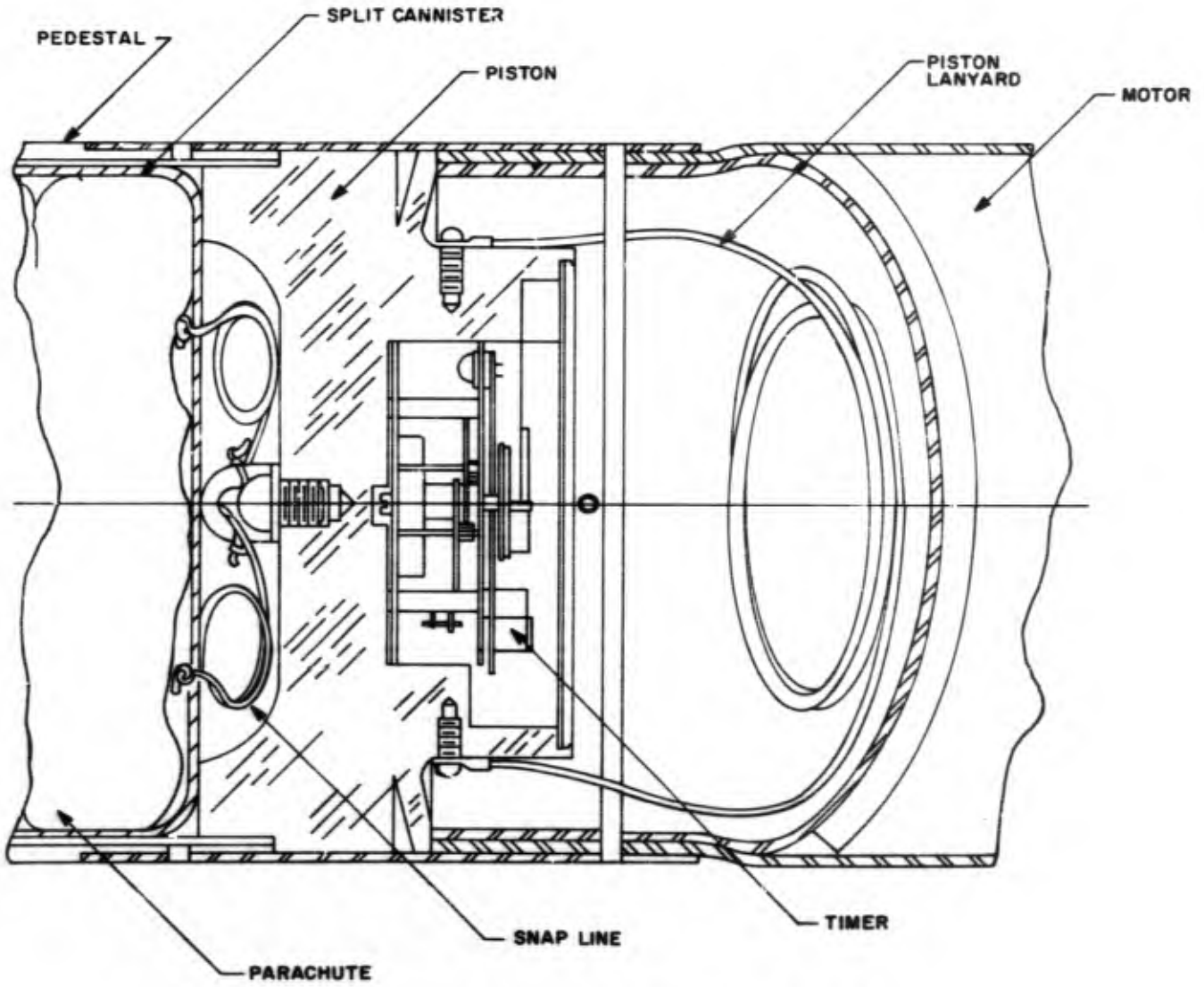

Figure 28. Separation Device, RDT&E

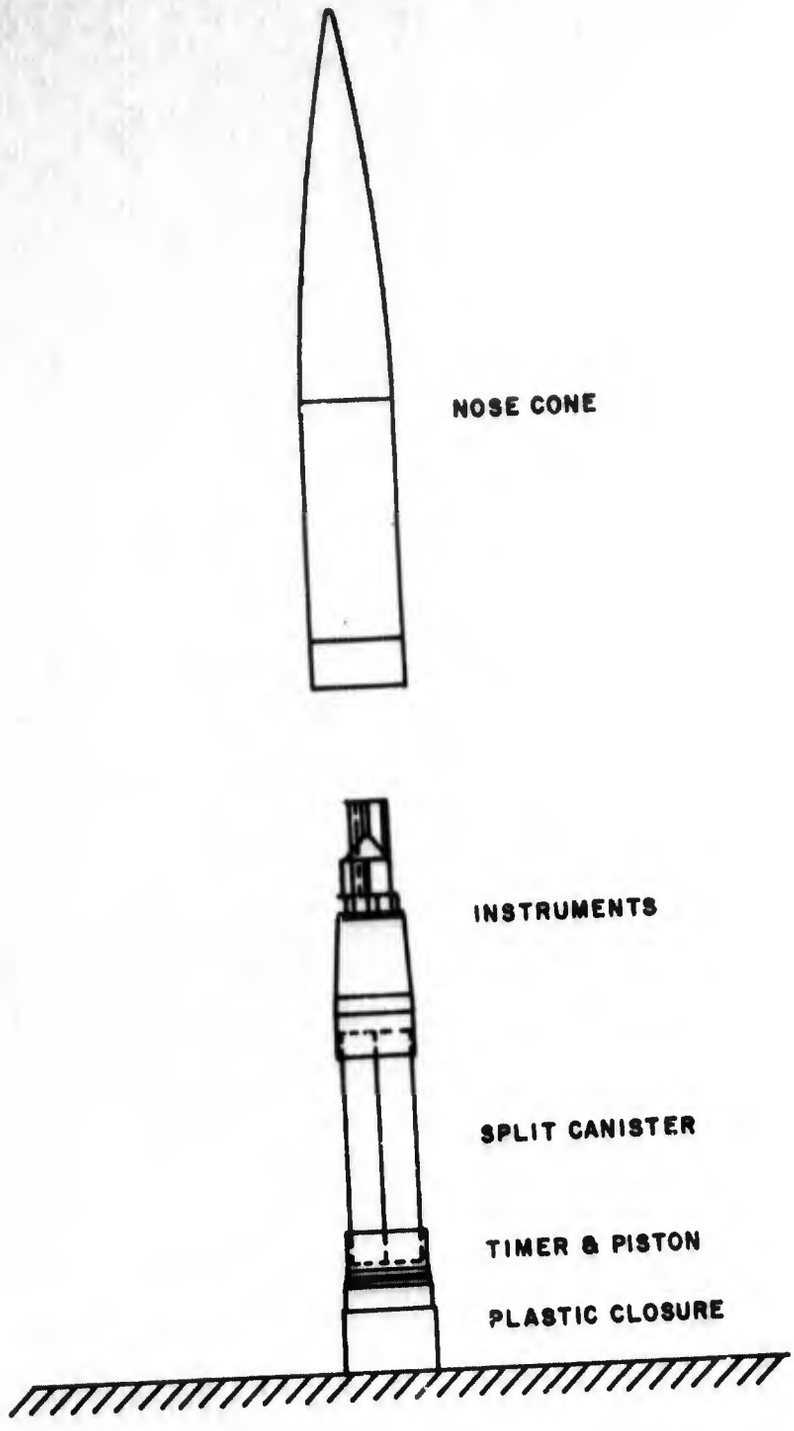

Figure 29. Instrumentation Checkout

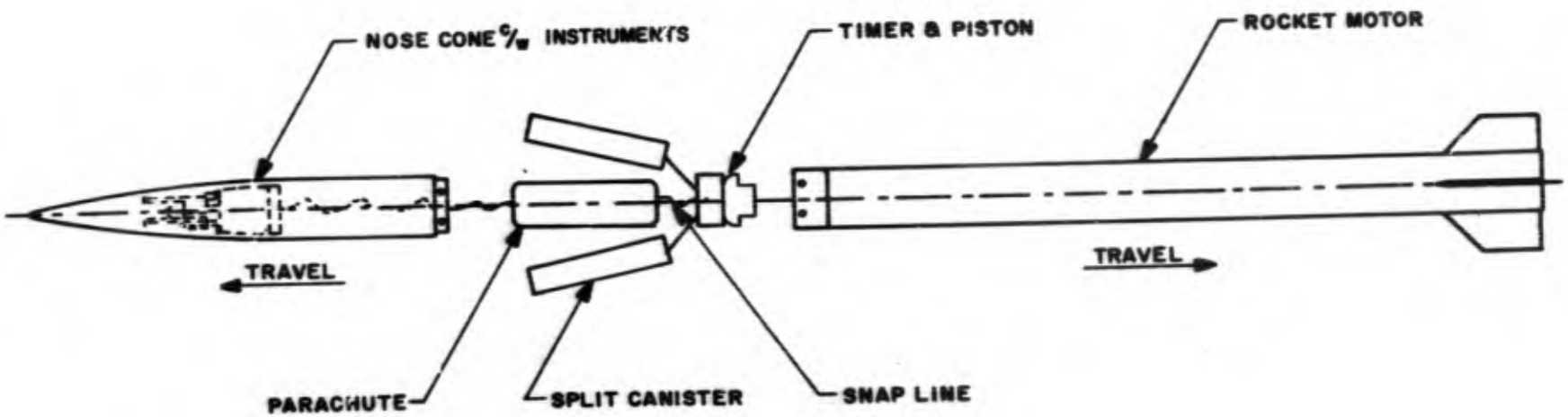

Figure 30. Partial Separation

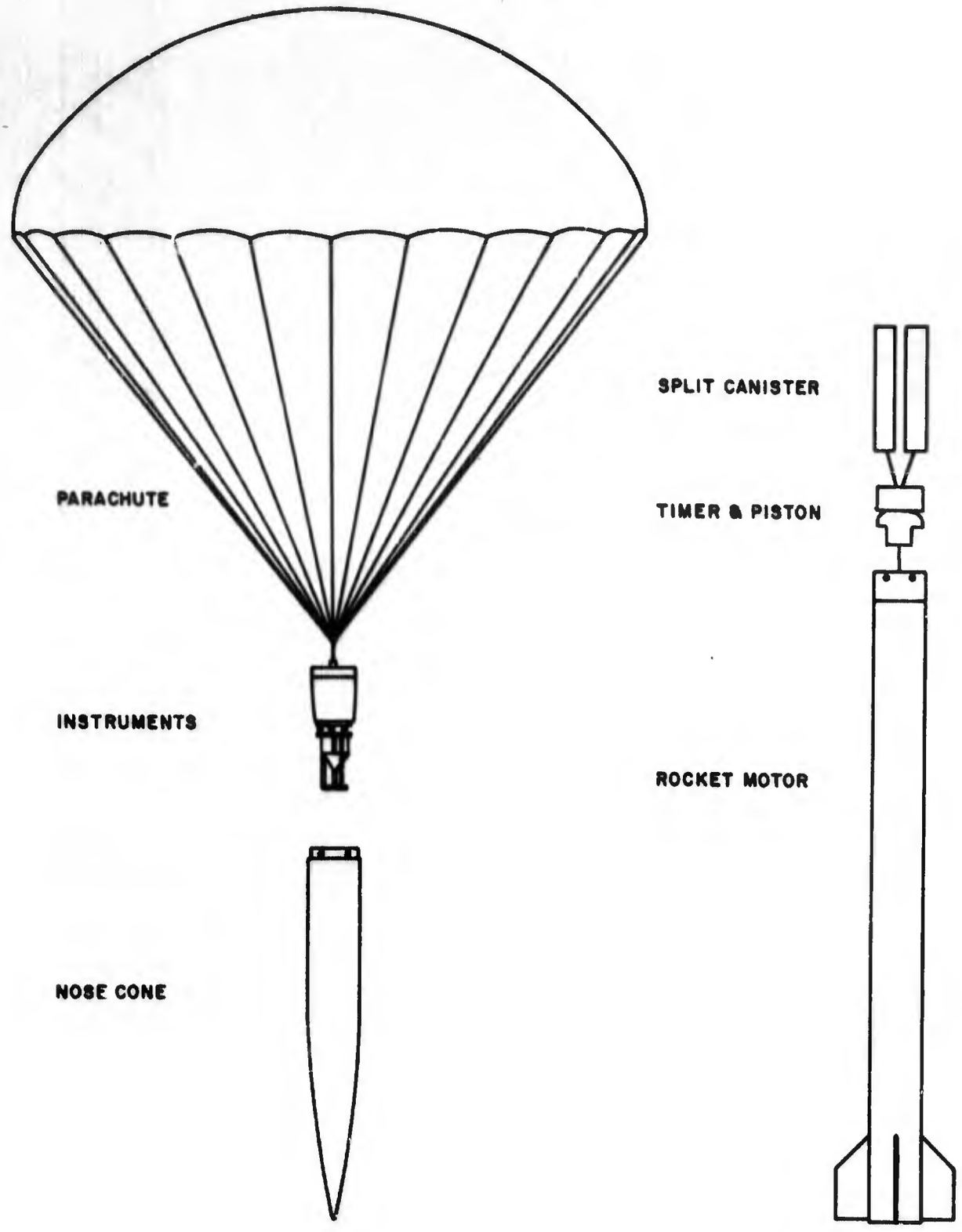

Figure 31. Separation Device In Test Fixture

Appendix A

THE DYNAMIC STABILITY OF AN UNGUIDED FLEXIBLE MISSILE

by

Joe C. Walters

This appendix defines a method of calculating the dynamic stability of an unguided, undamped, flexibile missile considering the structural dynamics and aerodynamics of the missile. This method of analysis applies to a constant missile velocity and utilizes a time dependent integration. A computer program has been written for this type of analysis and is described in this appendix.

1. Introduction

In the design of an unguided missile, care is exercised to make certain that the center of pressure of the missile is always aft of the center of gravity. Therefore, an induced angle of attack, which could result from a gust of wind, will create a restoring moment that tends to reduce the angle of attack to zero.

A flexibile missile is the natural resultant when an effort is made to utilize inexpensive materials and lightweight design. If a relatively flexible missile encounters a gust, the missile bending deflection may be such that the center of pressure will shift forward of the center of gravity. This would result in an overturning moment that tends to increase the missile angle of attack. If the missile is too flexibile, it will become unstable and encounter violent in-flight oscillations or suffer a structural failure.

This appendix outlines a method of analysis which permits a definition of the limits of missile flexibility and aerodynamics required for stability. A computer program which is described in this appendix was written to determine these limitations.

2. Analysis Procedure

In the conventional missile design, the center of pressure is aft of the center of gravity. This is a requirement for missile stability. Thus, any induced angle of attack, such as a gust, will cause a restoring moment to act on the missile about the center of gravity. This restoring moment reduces the angle of attack and the missile is then stablized. If a missile was perfectly rigid, then the center of pressure would remain aft of the center of gravity and the stability of the missile would be assured.

A flexibile missile will be subjected to in-flight bending vibration with the aerodynamic loads acting as forcing functions. This vibration will cause each missile section to have a different angle of attack than its adjacent sections. This results in a set of forces acting on the missile sections that are different from those forces acting on the undeflected missile. This new set of forces can cause the center of pressure to shift forward of the center of gravity which is a condition of instability.

During a single vibration cycle in which this phenomenom occurs, the center of pressure will instantaneously coincide with the center of gravity, and will be either fore or aft of the center of gravity during the remaining vibration time period. This means that a moment will be acting on the missile about the center of gravity which will tend to either overturn (increase the angle of attack) or restore (decrease the angle of attack) the missile steady state conditions depending on whether the center of pressure is fore or aft of the center of gravity, respectively.

To illustrate the foregoing paragraphs, assume a missile with the mass concentrated at the midspan and the aerodynamic forces acting on the nose and tail fins only (Figure 32). The aerodynamic forces F_n and F_f are a function of the normal force coefficients C_n and C_f for the nose and fins, respectively, and of the angle of attack, "α." The force F_r is a resultant of F_n and F_f. For the rigid missile, the force F_r tends to restore the missile to zero angle of attack. For a flexibile missile in a deflected position (Figure 33), the angles of attack on the nose and fin sections have changed and the forces have changed in proportion to the changes in the angles of attack. Thus, F_n has increased and F_f has decreased, causing a shift of the center of pressure forward of the center of gravity and the missile is in a temporary condition of instability.

The stability of a missile is dependent on the magnitude and duration of the restoring and overturning moments occurring during a single bending vibrational period. To determine the missile stability, an initial angle of attack is assumed, such as would result from a gust or some

other condition. The time dependent numerical integration is applied to the missile through a single period of vibration. If at the end of this period, the angle of attack for the missile in an undeflected condition has decreased or remains the same as the initial angle of attack, the missile is considered stable. If the angle of attack is greater than the initial angle of attack, the missile is considered unstable. Since no damping has been included in the analysis, a missile will be somewhat more stable than the results of the program would indicate.

In determining the center of pressure location and the moment acting on the missile, the aerodynamic lift and crossflow forces acting normal to missile axis have been considered.

The drag forces contribute a small normal force component to the missile when it is in a deflected condition. This has been neglected due to the magnitude as compared to the lift forces.

The missile structural characteristics are determined by the mass distribution and from the "EI" or stiffness distribution, which is the product of the modulus of elasticity and moment of inertia. These values are required for calculation of the missile natural bending frequency and the missile response to the aerodynamic loads.

The missile stability analysis is based on a time dependent integration of the missile parameter variables. This approach is necessary due to the continuous variation of the angle of attack at each of the missile sections and the resulting variation in the aerodynamic loads.

The computer program uses the following routine to determine the missile stability:

1) Input data are read including aerodynamics, structural dynamics, time intervals for integration, deflection coefficients, and initial conditions imposed on the missile.
2) Aerodynamic loads are computed for each missile section. The initial and final load calculations are on an undeflected missile with all intervening load calculations being made for the missile in the various deflected positions encountered during a single vibration period.
3) The loads are applied to the missile sections for a specified time interval. The missile rotational and translational accelerations, velocities, and displacements are determined.
4) The aerodynamic loads and missile accelerations are used to calculate the forces on each of the missile sections.

5) Shear, moment, slope, and deflection are calculated using the calculated forces and structural characteristics of the missile.
6) The missile is allowed to deflect a predetermined specified percentage of the deflection calculated in step 5 above. The percentage of deflection permitted during each time interval is a function of the time interval of integration and corresponds to the deflection - time relationship of simple harmonic motion or free vibration.
7) New angles of attack are then calculated considering the missile rotation and deflections occurring in the preceding time interval.

Steps 2 through 7 above are repeated until the missile bending deflection is equal to the amplitude of the missile deflection under forced vibration conditions. When this point is reached, steps 2 through 7 are repeated until the missile bending deflections are reduced to the initial undeflected position.

After a single complete vibration cycle has been analyzed, the final conditions are compared to the initial conditions imposed on the missile. If the final values of the nonsteady state conditions are the same or less than the initial values, the missile is considered to be stable at the particular velocity and altitude of the analysis. If the final nonsteady state conditions are greater than the initial values, the missile is considered unstable.

There will be a certain amount of damping present in the missile flight that has not been taken into account in the analysis. For this reason, the missile may tend to be more stable than the analysis predicts. The complexity of aerodynamic and structural damping factors along with the storage capacity limitations of the computer (IBM 1620) have dictated their omission in this program.

3. Equations

The missile is divided into sections as dictated by the variation in stiffness, mass distribution, forces, and structural considerations. A station is a point on the missile where input data defining the missile characteristics are given. A station should be located at each significant change in stiffness, at each mass concentration, at each aerodynamic load point, and where the structural analysis will require the missile internal loads. The stations divide the missile into a number of sections that are used in the analysis.

The symbols for the equations are listed below.

A_i	Angle of attack, station i
A_r	Reference area
A_n	Missile acceleration, normal to missile axis
A_{ro}	Missile rotational acceleration
A_{lc}	Launch angle cosine
A_{ni}	Acceleration, normal to missile axis, station i
A_{ra}	Angle between missile reference axis and axis through station 1
C_{li}	Coefficient of lift, station i
C_{cfi}	Coefficient of cross flow acting on station i
$C_{(j)}$	Slope-time factor, harmonic vibration
D_n	Missile displacement, normal to missile axis
D_{ro}	Missile rotational displacement
D_t	Integration time interval
D_i	Deflection, station i
D_o	Deflection of station 1, relative to nodal axis
D_{ni}	Normalized deflection, relative to nodal axis at station i
EI_i	Stiffness factor, modulus of elasticity times moment of inertia, station i
F_{nt}	Total normal force on the missile

F_{ni}	Normal force, station i
G	Gravitational acceleration constant
I_{ri}	Pitching moment of inertia for missile section, station i
I_{rt}	Pitching moment of inertia, total missile
L_i	Length of section between stations
M_i	Moment, station i
M_t	Mass, missile total
P_d	Dynamic pressure
Q_i	Shear, station i
S_i	Slope, station i
S_{ti}	Slope referred to missile axis and varying with time, station i
V_{ro}	Missile rotational velocity
V_n	Missile velocity, normal to missile axis
W_t	Total missile weight
W_i	Weight at station i
X_{cg}	Missile center of gravity location
X_i	Station location, station i
X_{cp}	Missile center of pressure location
X_f	Station of forward nodal point
X_r	Station of rear nodal point

The weight and distance from a zero reference point at the forward tip of the missile are given for each missile station. The total weight, mass, and center of gravity are then calculated.

$$W_t = \sum W_i \tag{1}$$

$$M_t = \frac{W_t}{G} \tag{2}$$

$$X_{cg} = \frac{\sum W_i \cdot X_i}{W_t} \tag{3}$$

The pitching moment of inertia is given by

$$I_{rt} = \sum W_i \left(X_{cg} - X_i\right)^2 + I_{ri} \quad . \tag{4}$$

Missile section pitching moment of inertia I_{ri} is given by the following. Right circular cylinder of radius r, length L_i, and density ρ

$$I_{ri} = \frac{\pi r^2 L_i \rho}{12} (3r^2 + L_i^2) = \frac{W_i}{12} (3r^2 + L_i^2) \; ; \tag{5}$$

hollow right circular cylinder with outer radius, r_o, and inner radius, r_i

$$I_{ri} = \frac{\pi (r_o^2 - r_i^2) L_i \rho}{4} \left(r_o^2 + r_i^2 + \frac{L_i^2}{3}\right) = \frac{W_i}{4} \left(r_o^2 + r_i^2 + \frac{L_i^2}{3}\right) ; \tag{6}$$

and thin wall right circular cylinder of radius, r, and thickness, t

$$I_{ri} = \pi r t L_i \rho \left(r^2 + \frac{L_i^2}{6}\right) = \frac{W_i}{2} \left(r^2 + \frac{L_i^2}{6}\right) . \tag{7}$$

The aerodynamic forces acting on the missile can be resolved into normal and axial forces referenced to the missile axis. The axial or drag forces contribute a very small normal force component when the missile has a bending deflection. The drag forces are therefore neglected. The normal forces and center of pressure are written as

$$F_{ni} = P_d \cdot A_r \cdot A_i \left(C_{li} + C_{cfi} \cdot A_i\right) \tag{8}$$

$$F_{nt} = \sum F_{ni} \tag{9}$$

$$X_{cp} = \frac{\sum F_{ni} \cdot X_i}{F_{nt}} \tag{10}$$

The forces and moments acting on the missile will cause the following normal and rotational acceierations, velocities, and displacements of the missile referenced to the center of gravity.

$$A_n = \frac{F_{nt}}{M_t - A_{lc} \cdot G} \tag{11}$$

$$V_n = V_n + A_n \cdot D_t \tag{12}$$

$$D_n = D_n + \frac{V_n \cdot D_t}{2} \tag{13}$$

$$A_{ro} = \frac{M_t\left(A_n \cdot G \cdot A_{lc}\right)X_{cg} - \sum F_{ni} \cdot X_i}{I_{rt}} \tag{14}$$

$$V_{ro} = V_{ro} + A_{ro} \cdot D_t \tag{15}$$

$$D_{ro} = D_{ro} + \frac{V_{ro} \cdot D_t}{2} \tag{16}$$

The normal acceleration at each station including rotational acceleration is

$$A_{ni} = A_n + A_{ro} + \left(X_{cg} - X_i\right) \tag{17}$$

The shear, moment, slope,and deflection for each missile station are defined according to Figure 34 as follows.

$$Q_{i+1} = Q_i - F_{n_{i+1}} + \frac{W_{i+1} \cdot A_{n_{i+1}}}{G} \tag{18}$$

$$M_{i+1} = M_i + Q_i \cdot L_i + W_{i+1} \frac{I_{r_{i+1}} \cdot A_{ro}}{2G} \tag{19}$$

$$S_{i+1} = S_i + \frac{M_i \cdot L_i}{EI_i} - \frac{Q_i \cdot L_i^2}{2EI_i} \tag{20}$$

$$D_{i+1} = D_i - S_i \cdot L_i + \frac{Q_i \cdot L_i^3}{3EI_i} - \frac{M_i \cdot L_i^2}{2EI_i} \tag{21}$$

The forward tip of the missile is station 1 and used as a reference point for the missile. The shear, moment, slope, and deflection are zero at this station.

The forward tip on the missile is for station 1 and the reference point for the missile slope and deflection. The shear, moment, slope, and deflection are zero at this station.

Since the missile will be vibrating and the missile axis will not be a straight line, a new definition of the missile axis is required for the relationship of the missile rotations and displacements. The missile axis is therefore defined as the line passing through the missile nodal points of the first bending mode of vibration at stations X_f and X_r for the station nearest the forward and rearward points of the missile, respectively. The value of D_i for the stations X_f and X_r will be D_f and D_r, respectively. The angle between the nodal point reference axis and the reference axis through the forward tip of the missile, station 1, is shown in Figure 35 and defined as

$$A_{ra} = \left(\frac{D_f - D_r}{X_r - X_f}\right) \tag{22}$$

The aerodynamic angle of attack of each missile section is a time dependent variable shown in Figure 36 and defined by the sum of

$$A_i = D_{ro} + \sum_0^j \left(S_i - A_{ra}\right) C_{(j)} \tag{23}$$

The term $C_{(j)}$ is a time dependent factor which governs the slope of the missile sections as a function of time and is related to simple harmonic motion. An overall missile configuration is shown in Figure 37.

The following relationships are used to establish a normalized deflection curve based on the deflection at station 1 relative to the missile axis through the nodal points, as shown in Figure 35.

$$D_o = - D_f - A_{ra} \cdot X_f \tag{24}$$

$$D_{ni} = \frac{D_o + D_i + X_i \cdot A_{ra}}{D_o} \qquad (25)$$

4. Computer Program

The Fortran program statements do not permit the use of symbols in the same manner as used in the equations. The symbols defined for the program are listed below.

Symbol	Fortran Symbol	Symbol	Fortran Symbol
A_i	AT	F_{ni}	FN(N)
A_r	AR	G	G
A_n	AN	I_{rt}	RIT
A_{ro}	ARO	L_i	DL
A_{lc}	ALC	M_i	OM(N)
A_{ni}	ANI	P_d	PD
A_{ra}	ARA	Q_i	Q(N)
C_{li}	CL(N)	S_i	SL(N)
C_{cfi}	CC(N)	S_{ti}	AI(N)
$C_{(j)}$	CJ(J)	V_{ro}	VRO
D_n	DN	V_n	VN
D_{ro}	DRO	W_t	WT
D_t	DT	W_i	W(N)
D_i	DF(N)	X_{cg}	XCG
D_o	DF(1)	X_i	X(N)
D_{ni}	DIN	X_{cp}	XCP
EI_i	EI(N)	X_f	XF
F_{nt}	FNT	X_r	XR

PROGRAM SOURCE STATEMENTS

```
      DIMENSION X(100),W(100),EI(100),RI(100),CL(100),CC(100),P(100)
      DIMENSION Q(100),OM(100),SL(100),DF(100)
      DIMENSION AI(100),CJ(50),FN(100)
      READ 1,XF,XR,VN,DN,VRO,DRO
    1 FORMAT(6F10.5)
      READ 1,PD,AR,TI,DT,G,ALC
      READ 2,NUM,JINL
    2 FORMAT(2I10)
      DO 4 N=1,NUM
      READ 3,X(N),W(N),EI(N),RI(N),CL(N),CC(N),P(N)
    3 FORMAT(F10.4,F10.4,F15.0,F5.1,F10.4,F10.4,F10.4)
    4 AI(N)=0.
      DO 5 J=1,JINL
      READ 6,CJ(J)
    6 FORMAT(F10.6)
    5 CONTINUE
      J=1
      ARA=0.
      Q(1)=0.
      OM(1)=0.
      DF(1)=0.
      RIT=0.
      FNT=0.
      FNTM=0.
      WT=0.
      WTM=0.
      DO 7 N=1,NUM
      WT=WT+W(N)
    7 WTM=WTM+W(N)*X(N)
      XCG=WTM/WT
      TM=WT/G
      DO 8 N=1,NUM
      RIT=RIT+W(N)*.5*RI(N)/G+W(N)*(XCG-X(N))**2/G
      AI(N)=0.
    8 SL(N)=0.
      PRINT 14,WT,RIT,XCG
   14 FORMAT(F10.4,8X,F12.6)
   16 DO 9 N=1,NUM
      AI(N)=AI(N)+(SL(N)-ARA)*CJ(J)
      AT=AI(N)+DRO
      FN(N)=PD*AR*(CL(N)+CC(N)*AT)*AT
      FNT=FNT+FN(N)
    9 FNTM=FNTM+FN(N)*X(N)
      AN=FNT/TM-G*ALC
      VN=VN+AN*DT
      DN=DN+VN*DT/2.
      ARO=(TM*(AN-G*ALC)*XCG-FNTM)/RIT
      VRO=VRO+ARO*DT
```

PROGRAM SOURCE STATEMENTS (CONCLUDED)

```
      DRO=DRO+VRO*DT/2.
      XCP=FNTM/FNT
      FNT=0.
      FNTM=0.
      NU=NUM-1
      DO 12 N=1,NU
      DL=X(N+1)-X(N)
      DLL=DL*DL
      DLLL=DLL*DL
      ANI=AN+ARO*(XCG-X(N+1))
      Q(N+1)=Q(N)-FN(N+1)+W(N+1)*ANI/G
      OM(N+1)=OM(N)+Q(N)*DL+W(N+1)*.5*RI(N+1)*ARO/G
      SL(N+1)=SL(N)+OM(N)*DL/EI(N)-Q(N)*DLL/(2.*EI(N))
      DF(N+1)=DF(N)-SL(N)*DL+Q(N)*DLLL/(3.*EI(N))-OM(N)*DLL/(2.*EI(N))
      IF(XF-X(N))10,11,12
   10 IF(XR-X(N))12,13,12
   11 DFF=DF(N)
      GO TO 12
   13 DRR=DF(N)
   12 CONTINUE
      ARA=(DFF-DRR)/(XR-XF)
      DIO=-DFF-ARA*XF
      TI=TI+DT
      J=J+1
      PRINT 23,TI,XCP,DIO
   23 FORMAT(F10.4,4X,F8.3,4X,F12.6)
      PRINT 15,ARO,VRO,DRO
   15 FORMAT(F10.2,2X,F10.4,4X,F10.5)
      IF(SENSE SWITCH 2)22,24
   22 PRINT 15,AN,VN,DN
      N1=1
      DO 17, N=1,NUM
      IF(P(N))18,17,18
   18 DIN =(DIO+DF(N)+X(N)*ARA)/DIO
      PRINT 19,X(N),Q(N),OM(N),AI(N),DIN
   19 FORMAT(F8.3,2X,F10.4,2X,F10.2,2X,F8.5,2X,F8.5)
   17 CONTINUE
   24 IF(SENSE SWITCH 3)25,16
   25 PUNCH 23,TI,XCP,DIO
      PUNCH 15,AN,VN,DN
      PUNCH 15,ARO,VRO,DRO
      N1=1
      DO 26 N=1,NUM
      IF(P(N))27,26,27
   27 DIN=(DIO+DF(N)+X(N)*ARA)/DIO
      PUNCH 19,X(N),Q(N),OM(N),AI(N),DIN
   26 CONTINUE
      GO TO 16
      END
```

5. **Preparation of Data**

a. XF, Station at Forward Nodal Point

The value of XF is the distance from the missile nose to the first nodal point of the first bending vibrational frequency. A station value of X(N) must be read in at the exact value of XF since the program must identify and use this point in the calculations.

b. XR, Station at Rearward Nodal Point

The value of XR is the distance from the missile nose to the second nodal point of the first bending vibrational frequency. A station value of X(N) must be read in for XR also.

c. VN, Missile Velocity Normal to Missile Axis

VN is the missile velocity in a direction approximately normal to the missile flight path for small angles of attack. This is usually read in as zero.

d. DN, Missile Displacement, Normal to Missile Axis

DN can be used when a calculation is made for determining a change in missile position. It is normally read in as zero.

e. VRO, Missile Rotational Velocity

The missile rotational velocity can be specified in cases where required. It is usually read in as zero.

f. DRO, Missile Rotational Displacement

DRO determines the initial value for the missile angle of attack. In this example. an angle of one degree is selected and the value of DRO is 0.01745 radian.

g. PD, Dynamic Pressure

The PD is a function of altitude and velocity and is constant in this program. The analysis must be performed for every altitude and velocity desired.

$$PD = \frac{a}{2} M^2 P_\infty$$

where

α = Gas constant for air, 1.4

M = Mach number

P_∞ = Atmospheric pressure at given altitude

$$PD = \frac{1.4}{2} (4.35)^2 \frac{2120.0 \text{ lb/ft}^2}{144 \text{ in}^2/\text{ft}^2}$$

$$= 194.9 \text{ lb/in.}^2$$

h. AR, Reference Area

AR is the cross sectional area of the missile body section or when diameter = D = 3.50 inches,

$$AR = \pi \cdot \frac{D^2}{2} = 9.62 \text{ inches}^2$$

i. TI, Initial Time

TI is an arbitrary value and is chosen as the burnout time in this problem, or four seconds.

j. DT, Integration Time Interval

The integration time interval, DT, is a function of the natural frequency of the missile and the number of intervals of integration.

The natural frequency of the missile was determined in a separate program and found to be 478.5 radians per second, or 76 cycles per second.

The vibration time period is, therefore, one-seventy-sixth of a second or 0.0132 second per cycle.

If 40 time intervals are used for the integration of one complete cycle, then $DT = \frac{0.0132}{40} = 0.00033$ second.

k. G, Gravitational Acceleration Constant

Gravitational acceleration constant, G, is consistent with units of area and pressure. The value of G is 386.4 inches per second per second.

l. ALC, Launch Angle Cosine

The launch angle is measured from the horizontal, thus a missile travelling vertically has a launch angle of 90 degrees. The launch angle cosine of 90 degrees is zero in this case.

m. NUM, Number of Stations

The value of NUM is the number of station values read in for the missile.

n. JINL, Number of Time Integrations

The number of time integrations is related to the determination of DT. In the example, 40 was selected for the number of time divisions of a single vibrational period. Since the original rigid body conditions are desired, and additional integration is performed the value of JINL is 41 which is also the number of CJ(J) cards.

o. X(N), Station Locations

Station locations, X(N), are selected according to structural considerations, lumped masses, and external loading points. A station must be located at each of the missile vibrational nodal points, XF for the forward point and XR for the rearward point. The station value of X(N) must be exactly the same as XF and XR in the program to identify these points.

p. W(N), Section Weight

The weight, W(N), at a station X(N) should include the distributed weight for half the distance to the next station on each side of X(N), and any concentrated weight at X(N).

q. EI(N), Stiffness Factor

The stiffness factor, EI(N), is defined as the modulus of elasticity times moment of inertia. The value of EI(N), to be entered at X(N), is for the section of the missile between stations X(N-1) and X(N). It is assumed constant between these stations. Therefore, a station must be located at any abrupt change in the value of EI(N). If a gradually changing value of EI(N) occurs, such as in an ogive section, an average value between the stations should be used.

r. RI(N), Pitching Moment of Inertia Factor

Pitching moment of inertia factor, RI(N), is a factor which is used in the program to determine the value of the pitching moment of inertia at station X(N). In the program, the pitching moment of inertia at X(N) is calculated as

$$I_p = \frac{W(N)}{2} RI(N)$$

The factor RI(N) was chosen for a read in value as a matter of convenience rather than calculating I_p for each station. The value of L at X(N) is the sum of half the distances to the adjacent stations, and r is assumed constant. If r is varying, an average value is used and a station should be located at any abrupt changes.

The values for RI(N) are right circular cylinder of radius r, length L,

$$RI(N) = \frac{3r^2 + L^2}{6}$$

Hollow circular cylinder, outer radius, r_o, inner radius, r_i, and length L;

$$RI(N) = \frac{r_o^2 + r_i^2 + \frac{L^2}{3}}{2}$$

Thin wall cylinder of radius, r, and length, L,

$$RI(N) = r^2 + \frac{L^2}{6}$$

s. CL(N), Coefficient of Lift

The coefficient of lift is used to calculate the normal forces on the missile sections;

$$FN(N) = PD \cdot AR \cdot CL(N) \cdot AT$$

Where FN(N) is the aerodynamic force acting on station X(N), PD is dynamic pressure, and AT is angle of attack. The units of CL(N) must be consistent with these factors. The section of the missile used to determine FN(N) acting at X(N) includes half the distances to the adjacent stations and is derived from aerodynamic data of the overall missile.

t. CC(N), Cross Flow Coefficient

The cross flow coefficient is used to calculate a normal force acting on the missile sections;

$$FN(N) = PD \cdot AR \cdot CC(N) \cdot AT^2$$

The value of CC(N) could be included in CL(N) if it was not a function of AT which yields an AT^2 when calculating FN(N).

u. P(N), Printing Code

The printing code is a print out of the values of Q(N), OM(N), AI(N), and DIN (shear moment, slope, and deflection, respectively) for station X(N), which can be obtained by using a value P(N) ≠ 0 at station X(N) in the read-in data, and turning on computer sense switch 2. The ends of the missile and the nodal points, XF and XR, would normally be desirable along with other stations as required.

v. CJ(J), Harmonic Motion Factor

The harmonic motion factor relates the missile sections angle of attack to the vibrational frequency and the integration time intervals, DT.

DATA FORMAT

	XF	XR	VN	DN	VRO	DRO
17.		64.0	0.0	0.0	0.0	0.01745

	PD	AR	TI	DT	G	ALC
194. 9		9.62	4.0	.00033	386.	0.0

	NUM	JINL
	39	41

	X(N)	W(N)	EI(N)	RI(N)	CL(N)	CC(N)	P(N)
0.	0	.0	1000.	0.0	.0	.0	1.0
	745	.008	1000.	.1	.039	.0	.0
1.	74	.022	9300.	.2	.117	.0	.0
			ETC.				

	CJ(J)
.0	
.0	123
.0	366
ETC.	

XF 17.0 XR 64.0 VN 0.0 DN 0.0 VRO 0.0 DRO 0.01745

PD 94.9 AR 9.62 TT 4.0 DT .00033 386.4 G 0.0 AIC

NUM 39 JINL 41

X(N)	W(N)	EI(N)	RI(N)	CL(N)	CC(N)	P(N)	CJ(J)
.0	.0	1000.	.0	.00	.0	1.0	.000
.745	.008	1000.	.1	.039	.0	.0	.0123
1.74	.022	9300.	.2	.117	.0	.0	.0366
2.84	.035	36000.	.4	.172	.0	.0	.0601
3.94	.048	90000.	.7	.209	.0	1.0	.0820
5.05	.074	190000.	1.0	.230	.0	.0	.1019
6.12	.079	320000.	1.5	.238	.0	.0	.1193
7.29	.090	460000.	1.7	.234	.0	.0	.1338
8.35	.092	600000.	2.0	.223	.0	1.0	.1449
9.65	.148	900000.	2.6	.205	.09	.0	.1527
10.62	.147	1100000.	2.8	.183	.0	.0	.1564
11.75	.170	1400000.	3.0	.159	.03	.0	.1564
12.87	.193	1600000.	3.0	.135	.03	1.0	.1527
13.85	.213	1600000.	3.0	.080	.09	.0	.1449
14.00	4.410	1600000.	4.0	.000	.0	.0	.1338
15.61	.275	2900000.	3.0	.240	.18	.0	.1193
17.00	.000	2900000.	.00	.00	.0	1.0	.1019
18.4	.412	2900000.	4.00	.189	.30	.0	.0820
21.1	.375	2900000.	4.00	.151	.48	.0	.0601
23.9	.412	2900000.	4.00	.118	.54	1.0	.0366
26.7	.308	2900000.	4.00	.093	.81	.0	.0123
28.0	.258	2900000.	4.00	.00	.0	.0	-.0123
29.4	.696	2900000.	4.00	.073	.96	1.0	-.0366
32.2	.535	9700000.	4.00	.058	.84	1.0	-.0601
35.0	.330	9700000.	4.00	.046	1.53	.0	-.0820
37.8	.275	9700000.	4.00	.036	1.47	.0	-.1019
40.6	.440	9700000.	5.0	.028	1.68	1.0	-.1193
45.4	.660	9700000.	9.0	.060	2.37	1.0	-.1338
52.3	.660	9700000.	9.0	.051	5.70	1.0	-.1449
57.0	.550	9700000.	7.0	.042	4.95	1.0	-.1527
62.0	.440	9700000.	6.0	.033	3.99	.0	-.1564
64.0	.000	9700000.	.0	.00	.0	1.0	-.1564
66.0	.440	9700000.	6.0	.024	3.96	.0	-.1527
70.0	.440	9700000.	6.0	.015	.0	1.0	-.1449
70.3	.00	9700000.	.00	4.250	.0	1.0	-.1338
71.2	2.260	9700000.	2.0	.000	.0	.0	-.1193
71.5	1.000	9700000.	3.0	.000	.0	.0	-.1019
74.0	.275	9700000.	4.0	.005	.0	.0	-.0820
74.5	.000	9700000.	.0	.005	.0	1.0	-.0601
							-.0366
							-.0123

ω - graph

ωt = 0°
Σ CJ(J) = ①

ωt = 180°
Σ CJ(J) = 2.0

ωt = 360°
Σ CJ(J) = 0

6. Operation of Computer Program

The lift coefficient, CL(1), for the first station of the read-in data should always be read in as zero. A dummy station should be used if necessary. This requirement is due to the shear equation which uses the aerodynamic force, FN(N+1), in the determination of the shear, Q(N+1). Since the numerical integration begins at N = 1, the first value of FN(N) is FN(2). Thus, FN(1) would never be recognized in the shear equation and would lead to a constant error in shear throughout the missile length.

The stiffness factor, EI(N), must never be zero since it is used for division in the program.

The initial value of CJ(J) must be zero if the initial missile conditions, prior to the dynamic response, are to be obtained. This should be considered when the time is printed during the calculation and is related to the vibration cycle.

The program may be compiled so that sense switch 4 will cause the results of calculation to be printed on the typewriter, whereby the value on the left of the "equal signs" in the program will be typed. Any peculiarities in the program results can thus be traced throughout the program and errors identified. This feature is usually unnecessary after the program has been checked and is operational.

The computer program will always type the values for total weight, rotational inertia, and center of gravity. These are the first items typed and will not be repeated.

The next six values to be typed will be time, XCP, and DIO on one line and ARO, VRO, and DRO on another line. These values will automatically be typed for each time interval and provide a means of knowing to what point the calculations have progressed and when a maximum or minimum deflection occurs in the vibration cycle. The station values of shear, moment, slope, and deflection can then be obtained when required.

Sense switch 2 is turned on when the typed values of AN, VN, and DN are required, and for the typed values of shear, moment, slope, and deflection, or Q(N), OM(N), AI(N), and DIN, respectively. The stations for which this data are typed will be specified under the code "P(N)" in the read data.

The use of the typewriter on the 1620 computer is a time consuming routine and the alternative of providing the same data on punched cards

is available. Sense switch 3 on will provide the data on punched cards and is much faster than the typewriter. Data output on punched cards will include TI, XCP, and DIO; AN, VN, and DN; ARO, VRO, and DRO; and station data Q(N), OM(N), AI(N), and DIN. This will normally be required for a vibration cycle at the initial undeflected conditions, maximum deflection, and at the completion of a vibration cycle.

EXAMPLE OF TYPED OUTPUT.

WT	RIT
16.7700	24.964116

TI	XCP	DIO
4.0003	45.749	.080778

AN	VN	DN
6230.21	2.0559	.00033

ARO	VRO	DRO
-86.64	-.0285	.01744

X(N)	Q(N)	OM(N)	AI(N)	DIN
.000	.0000	.00	.00000	1.00000
3.940	-16.6293	-17.78	.00000	.73792
8.350	-43.8159	-136.86	.00000	.44606
12.870	-59.5003	-366.24	.00000	.18863
17.000	-17.1432	-479.24	.00000	.00000
23.900	-18.0165	-607.90	.00000	-.23110
29.400	-6.7404	-700.64	.00000	-.33527
32.200	-1.1572	-719.75	.00000	-.35562
40.600	9.5019	-707.88	.00000	-.34932
45.400	17.9596	-662.94	.00000	-.31625
52.300	25.8317	-539.68	.00000	-.23077
57.000	32.8737	-418.70	.00000	-.14923
64.000	39.0031	-176.62	.00000	.00000
70.000	55.6244	84.14	.00000	.14325
70.300	-83.4256	100.82	.00000	.15062
74.500	-.0000	-.00	.00000	.25286

$\sum CJ(J) = 0.$

TI	XCP	DIO
4.0006	45.687	.080976

AN	VN	DN
6230.48	4.1120	.00101

ARO	VRO	DRO
-85.97	-.0569	.01743

4.0009	45.503	.081587
-84.01	-.0846	.01742
4.0013	45.198	.082605
-80.78	-.1113	.01740
4.0016	44.779	.084018
-76.32	-.1365	.01738

ARO	VRO	DRO
4.0019	44.252	.085811
-70.72	-.1598	.01735
4.0023	43.627	.087962
-64.04	-.1810	.01732
4.0026	42.913	.090444
-56.41	-.1996	.01729
4.0029	42.126	.093217
-47.95	-.2154	.01725
4.0033	41.281	.096239
-38.81	-.2282	.01721
4.0036	40.397	.099445
-29.20	-.2378	.01717
4.0039	39.494	.102766
-19.32	-.2442	.01713
4.0042	38.595	.106123
-9.40	-.2473	.01709
4.0046	37.725	.109417
.27	-.2472	.01705
4.0049	36.905	.112551
9.45	-.2441	.01701
4.0052	36.161	.115420
17.85	-.2382	.01697
4.0056	35.513	.117920
25.21	-.2299	.01693
4.0059	34.982	.119953
31.26	-.2196	.01690
4.0062	34.583	.121436
35.81	-.2078	.01686
4.0066	34.331	.122297
38.67	-.1950	.01683

TI	XCP	DIO
4.0069	34.232	.122497
AN	**VN**	**DN**
6498.31	44.0711	.07928
ARO	**VRO**	**DRO**
39.74	-.1819	.01680

X(N)	Q(N)	OM(N)	AI(N)	DIN	
.000	.0000	.00	.01191	1.00000	
3.940	-28.3562	-29.91	.01381	.73451	
8.350	-73.3471	-231.46	.01231	.43904	
12.870	-96.3354	-609.98	.01010	.18276	
17.000	-17.6745	-760.72	.00782	.00000	
23.900	-16.5855	-888.64	.00487	-.21590	$\sum CJ(J) = 2.0$
29.400	-1.5638	-969.52	.00206	-.30813	
32.200	5.3804	-973.79	.00049	-.32444	MAXIMUM
40.600	17.1737	-901.68	-.00093	-.31235	VALUE
45.400	25.0455	-818.94	-.00175	-.27989	
52.300	31.7465	-645.82	-.00289	-.20156	

X(N)	Q(N)	OM(N)	AI(N)	DIN
57.000	37.2147	496.41	-.00352	-.12932
64.000	41.5109	227.18	-.00421	.00000
70.000	51.4968	39.72	-.00448	.12298
70.300	-46.9458	55.17	-.00448	.12930
74.500	-.0001	-.00	-.00445	.21746

4.0072	34.230	.122019
38.98	-.1690	01677
4.0075	34.504	.120874
36.44	-.1570	01675
4.0079	34.869	.119099
32.19	-.1464	01672
4.0082	35.372	.116763
26.41	-.1377	01670
4.0085	35.999	.113950
19.92	-.1313	01668
4.0089	36.729	.110760
11.18	-.1276	01666
4.0092	37.542	.107300
2.25	-.1268	01664
4.0095	38.413	.103683
-7.15	-.1292	01662
4.0099	39.318	.100008
-16.77	-.1347	.01659
4.0102	40.230	.096382
-26.32	-.1434	.01657
4.0105	41.126	.092888
-35.56	-.1552	.01654
4.0108	41.986	.089594
-44.29	-.1698	.01652
4.0112	42.787	.086568
-52.29	-.1870	.01649
4.0115	43.513	.083850
-59.44	-.2067	.01645
4.0118	44.149	.081475
-65.61	-.2283	.01641
4.0122	44.684	.079468
-70.70	-.2516	.01637
4.0125	45.108	.077842
-74.65	-.2763	.01633
4.0128	45.416	.076606
-77.41	-.3018	.01628
4.0132	45.602	.075766
-78.95	-.3279	.01622

TI	XCP	DIO
4.0135	45.663	.075319
AN	VN	DN
5761.23	84.3522	.29598
ARO	VRO	DRO
-79.26	-.3540	.01616

X(N)	Q(N)	OM(N)	AI(N)	DIN
.000	.0000	.00	.00002	1.00000
3.940	-15.4808	-16.55	.00001	.73797
8.350	-40.7951	-127.41	.00002	.44616
12.870	-55.4132	-340.99	.00003	.18872
17.000	-16.0582	-446.45	.00004	.00000
23.900	-16.8967	-566.99	.00004	-.23134
29.400	-6.4254	-654.00	.00002	-.33571
32.200	-1.2396	-672.21	.00001	-.35614
40.600	8.7545	-662.28	.00000	-.35001
45.400	16.6377	-620.87	-.00001	-.31696
52.300	24.0943	-506.68	-.00002	-.23140
57.000	30.7593	-393.83	-.00003	-.14968
64.000	36.5492	-167.21	-.00005	-.00000
70.000	52.0052	77.30	-.00005	.14381
70.300	-76.8799	2.90	-.00005	.15120
74.500	-.0000	-.00	-.00005	.25389

CJ(J) = 0.

VIBRATION CYCLE COMPLETED

EXAMPLE OF PUNCHED CARD OUTPUT

4.0003	45.749	.080778		
6230.21	2.0559	.00033		
-86.64	-.0285	.01744		
.000	.0000	.00	.00000	1.00000
3.940	-16.6293	-17.78	.00000	.73792
8.350	-43.8159	-136.86	.00000	.44606
12.870	-59.5003	-366.24	.00000	.18863
17.000	-17.1432	-479.24	.00000	.00000
23.900	-18.0165	-607.90	.00000	-.23110
29.400	-6.7404	-700.64	.00000	-.33527
32.200	-1.1572	-719.75	.00000	-.35562
40.600	9.5019	-707.88	.00000	-.34932
45.400	17.9596	-662.94	.00000	-.31625
52.300	25.8317	-539.68	.00000	-.23077
57.000	32.8737	-418.70	.00000	-.14923
64.000	39.0031	-176.62	.00000	.00000
70.000	55.6244	84.14	.00000	.14325
70.300	-83.4256	100.82	.00000	.15062
74.500	-.0000	-.00	.00000	.25286
4.0069	34.232	.122497		
6498.31	44.0711	.07928		
39.74	-.1819	.01680		
.000	.0000	.00	.01191	1.00000
3.940	-28.3562	-29.91	.01381	.73451
8.350	-73.3471	-221.46	.01231	.43904
12.870	-96.3354	-609.98	.01010	.18276
17.000	-17.6745	-760.72	.00782	.00000
23.900	-16.5855	-888.64	.00487	-.21590
29.400	-1.5638	-969.52	.00206	-.30813
32.200	5.3804	-973.79	.00049	-.32444
40.600	17.1737	-901.68	-.00093	-.31235
45.400	25.0456	-818.94	-.00175	-.27989
52.300	31.7463	-645.82	-.00289	-.20156
57.000	37.2147	-496.41	-.00352	-.12932
64.000	41.5109	-227.18	-.00421	.00000
70.000	51.4968	39.72	-.00448	.12298
70.300	-46.9458	55.17	-.00448	.12930
74.500	-.0001	-.00	-.00445	.21746
4.0135	45.663	.075319		
5761.23	84.3522	.29598		
-79.26	-.3540	.01616		
.000	.0000	.00	.00002	1.00000
3.940	-15.4808	-16.55	.00001	.73797
8.350	-40.7951	-127.41	.00002	.44616
12.870	-55.4132	-340.99	.00003	.18872
17.000	-16.0582	-446.45	.00004	.00000
23.900	-16.8967	-566.99	.00004	-.23134
29.400	-6.4254	-654.00	.00002	-.33571
32.200	-1.2396	-672.21	.00001	-.35614
40.600	8.7545	-662.20	.00000	-.35001
45.400	16.6377	-620.87	-.00001	-.31696
52.300	24.0943	-506.68	-.00002	-.23140
57.000	30.7593	-393.83	-.00003	-.14968
64.000	36.5492	-167.21	-.00005	-.00000
70.000	52.0052	77.30	-.00005	.14381
70.300	-76.8799	92.90	-.00005	.15120
74.500	-.0000	-.00	-.00005	.25389

7. Discussion of Results

The missile used in this example is a version of a proposed tactical meteorological rocket. The results were obtained on punched cards and a print of these cards has been shown previously in this appendix.

An indication of stability is shown by a plot of XCG and XCP versus time in Figure 38. XCG will be a constant and XCP will vary throughout the vibration period. The value of "XCG -XCP" is directly related to the rotational acceleration, ARO. A plot of rotational displacements, DRO versus time, shows the missile rotational response of the missile. An assesment of the rotational velocity, VRO and DRO, at the end of the missile vibrational period indicates the missile stability. Examples of these are shown in Figures 38 and 39.

The values of shear, moment, slope, and deflection are shown in Figures 40 through 43. It should be noted that these terms do not necessarily represent the true values in the normal meaning of these terms.

The shear, Q(N), is the value that would exist from a "steady state" condition, i. e., when the external aerodynamic forces are in equilibrium with the acceleration forces of the missile. Vibration forces are not considered in this shear value.

The moment, OM(N), is the value that would exist from a "steady state" condition, i. e., when the external aerodynamic forces are in equilibrium with the acceleration forces of the missile and the moment results from the slopes associated with these forces in equilibrium. A more meaningful value of moment could be obtained, if desired, from the relationship $OM(N+1) = \frac{[AI(N+1) - AI(N)] * EI(N+1)}{X(N+1) - X(N)}$. This utilizes the slopes, AI(N), of the missile during the vibration cycle. The slope, AI(N), has been calculated throughout the vibration cycle. The calculation omits the shear forces caused by vibratory motion accelerations about the missile nodal axis.

The final values of AI(N) are not exactly zero or back to the original undeflected positions. This can be explained by noting the values of DIO. These are seen to vary throughout the vibration cycle. This indicates a variation in SL(N), since they are directly related. If SL(N) remained constant, then AI(N) would vary uniformly as harmonic motion since CJ(J) which governs AI(N) is based on harmonic motion as indicated in this appendix. A comparison of the residual values of AI(N) with the maximum values of AI(N) is an indication of how closely the vibration follows harmonic motion.

The deflection, DIN, is the normalized value that would exist from the same "steady state" condition used for calculating the shear and moment. The normalized values are based on the deflection at station 1 and are referenced to the nodal axis of the missile, as previously defined. To get the original values of deflection, the normalized values can be multiplied by the deflection at station 1, DIO.

The problem of determining the deflection geometry of the missile at a given instant is discussed in this appendix. The solution is based on the assumption that the missile will vibrate at its natural frequency and follow a simple harmonic vibratory motion. The forcing function for the motion is the aerodynamic loading that is experienced by the sudden application of an angle of attack.

The deflection geometry of the missile is determined in the program for steady state condition using the aerodynamic loads. This deflection pattern and time-deflection relationship in harmonic vibratory motion are then used to determine the slope of the missile at each station, X(N), for each time during the numerical integration. This slope in turn is used to calculate the angles of attack for each missile station for the forces used in the next cycle of the integration. The forced vibration equation is used to establish the required time-deflection relationship.

The equation of forced vibration is

$$\frac{W}{g}\frac{d^2x}{dt^2} + \beta\frac{dx}{dt} + kx = F(t)$$

If the damping, $\beta = 0$, and the forcing function, F(t), is constant, and

$$\frac{W}{g} = m;\ m\frac{d^2x}{dt^2} + kx = F,$$

$$\frac{d^2x}{dt^2} + \frac{k}{m}x = \frac{F}{m},$$

$$\text{let } \frac{k}{m} = A,\ \frac{F}{m} = B,$$

$$\frac{d^2x}{dt^2} + Ax = B$$

For a complimentary solution to the differential equation, when F = 0, and D is a differential operator;

$$(D^2 + A)\, x = 0$$

$$(D - i\sqrt{A})\ (D + i\sqrt{A})\, x = 0$$

and

$$X_c = C_1\ e^{i\sqrt{A}t} + C_2\ e^{i\sqrt{A}t}$$

or

$$X_c = C_3\ \sin\sqrt{A}t + C_4\ \cos\sqrt{A}t$$

To find x such that

$$\frac{d^2x}{dt^2} + Ax = B,$$

let

$$X = e^{i\sqrt{A}t} + \frac{B}{A}$$

$$\frac{dx}{dt} = i\sqrt{A} \cdot e^{i\sqrt{A}t}$$

$$\frac{d^2x}{dt} = -A \cdot e^{i\sqrt{A}t}$$

Substitution gives

$$-A \cdot e^{i\sqrt{A}t} + A\left(e^{i\sqrt{A}t} + \frac{B}{A}\right) = B$$

$$(-A + A)\ e^{i\sqrt{A}t} + B = B$$

and the value chosen for x satisfies the differential equation. The desired equation is the sum of the complimentary and particular solutions

$$X = C_3\ \sin\sqrt{A}t + C_4\ \cos\sqrt{A}t + e^{i\sqrt{A}t} + \frac{B}{A}$$

but

$$e^{i\sqrt{A}t} = \cos\sqrt{A}t + i\ \sin\sqrt{A}t$$

and

$$x = (C_3 + i) \sin \sqrt{At} + C_5 \cos \sqrt{At} + \frac{B}{A}$$

Initial conditions

for $t = 0$, $x = 0$

$$0 = (C_3 + i) \sin \sqrt{At} + C_5 \cos \sqrt{At} + \frac{B}{A}$$

$$0 = 0 + C_5 \cdot 1 + \frac{B}{A}$$

$$C_5 = -\frac{B}{A}$$

for

$$t = 0, \frac{dx}{dt} = 0$$

$$\frac{dx}{dt} = \sqrt{A}\,(C_3 + i) \cos \sqrt{At} + \sqrt{A} C_5 \frac{B}{A} \sin \sqrt{At} = 0$$

$$0 = \sqrt{A}(C_3 + i) \cdot 1 + 0$$

$$C_3 + i = 0 \ .$$

The equation, therefore, reduces to

$$X = -\frac{B}{A} \cos \sqrt{At} + \frac{B}{A}$$

and upon substitution for A and B

$$X = -\frac{F}{k} \left(\cos \sqrt{\frac{kt}{m}} - 1 \right)$$

The natural frequency of a simple undamped spring-mass system is given by

$$\omega = \sqrt{\frac{k}{m}}$$

and

$$x = -\frac{F}{k} (\cos \omega t - 1)$$

when

$\cos \omega t = 1,\ x = 0$

$x = 0$ when $\omega t = 0,\ 2\pi,\ 4\pi,\ 2n\pi$

when

$\cos \omega t = -1,\ x = 2$, maximum displacement

x = maximum when $\omega t = \pi,\ 3\pi,\ 5\pi,\ \text{---}\ (2n + 1)\pi$.

The time required to go from zero to maximum displacement is

$$\omega t = \pi,\ t = \frac{\pi}{\omega}$$

and time to return to the original position,

$$t = \frac{2\pi}{\omega t}$$

The arbitrary value of 40 time increments for a complete period of vibration was selected. CJ(J) is defined as the change in the value of (cos θn - 1.0) for θn and θn + 1.

Let $\theta = \omega t$ $\qquad \theta = \frac{2\pi}{40}$

θ°	Cos θ	Cos θ -1.	J	CJ(J)
o	1.0	.0	1	.0123
9	.9877	-.0123	2	.0489
18	.9511	-.0484	3	.0601
27	.8910	-.1090	4	.0820
.	.	.	.	.
.	.	.	.	.
.	.	.	.	.
171	-.9877	-1.9877	19	.0489
180	-1.0	-2.0000	20	.0123
189	-.9877	-1.9877	21	-.0123
.	.	.	.	.
.	.	.	.	.
.	.	.	.	.
342	.9511	-.0489	38	-.0601
351	.9877	-.0123	39	-.0366
360	1.00	-.0000	40	-.0123
				$\sum CJ(J) = 0.0$

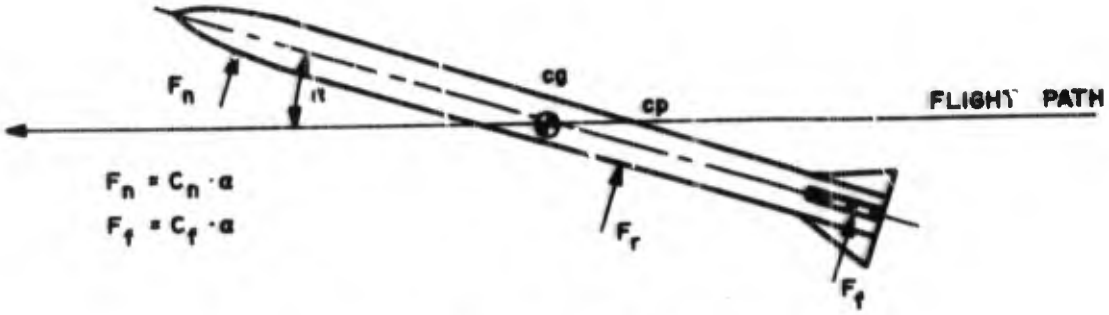

Figure 32. Rigid Missile

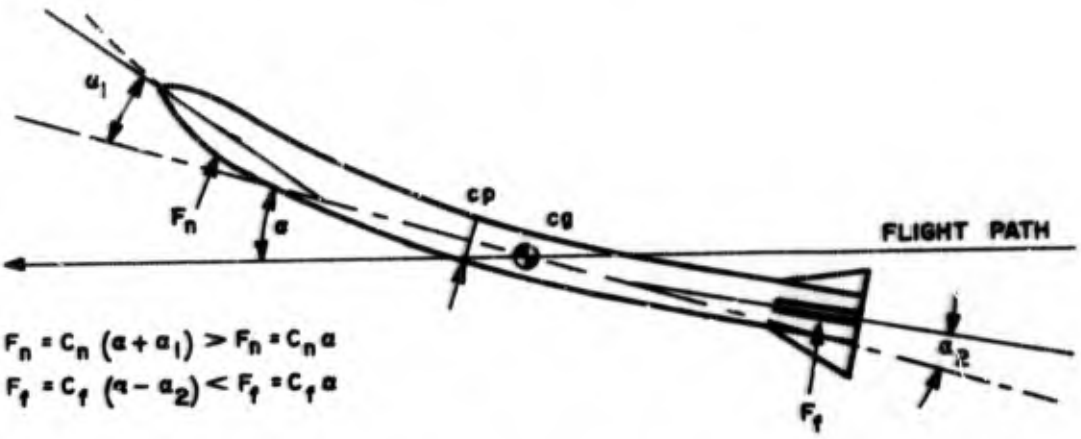

Figure 33. Flexible Missile

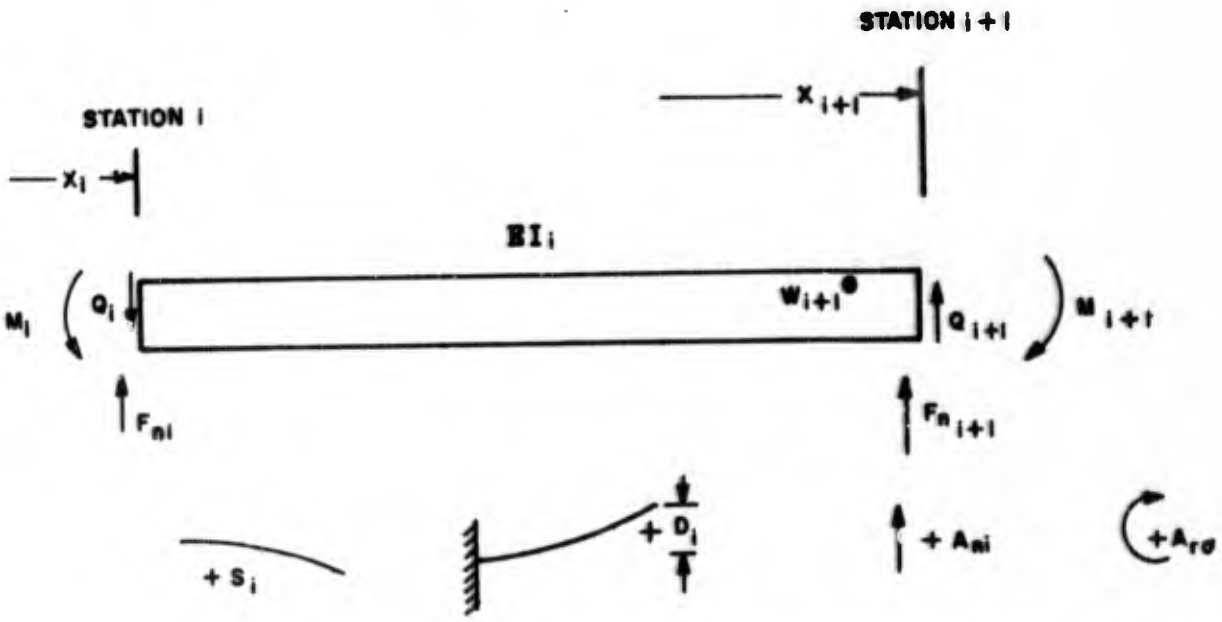

Figure 34. Missile Section With Sign Convention (All Shown Positive).

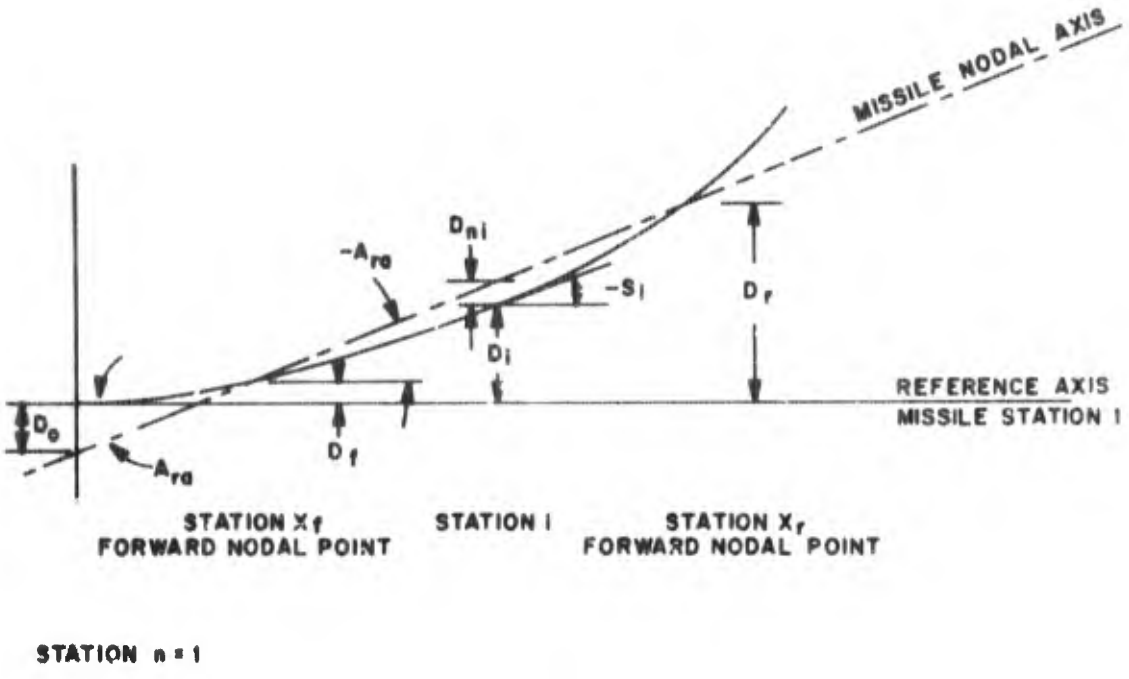

Figure 35. Definition of Missile Slopes and Deflections.

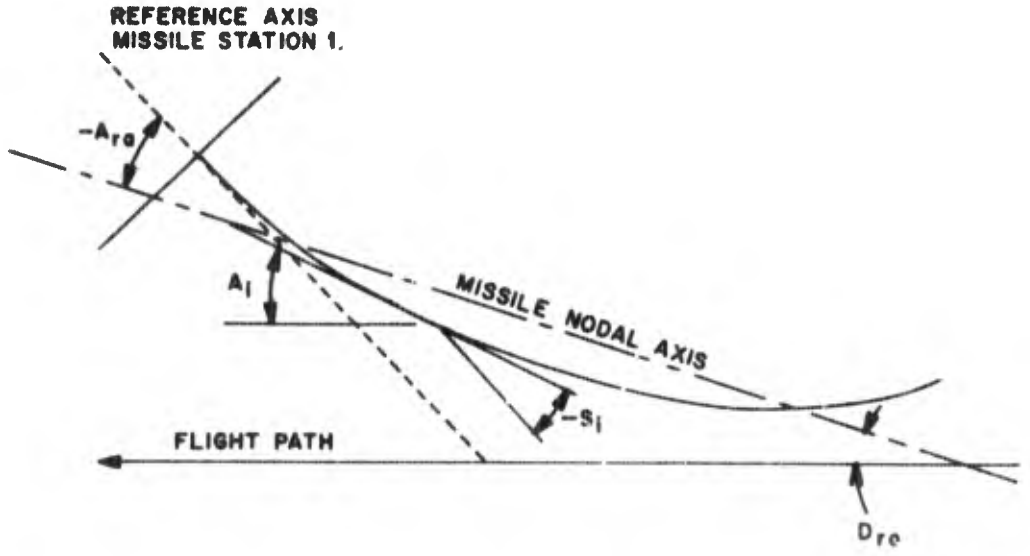

Figure 36. Missile Angle of Attack, Station i

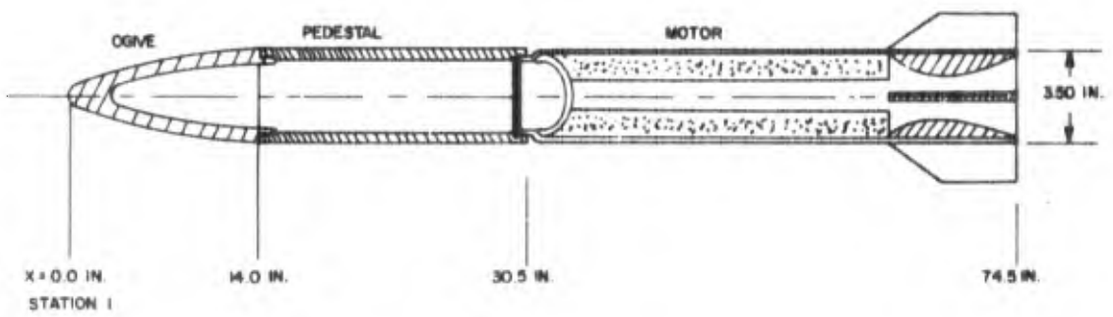

Figure 37. Missile Configuration

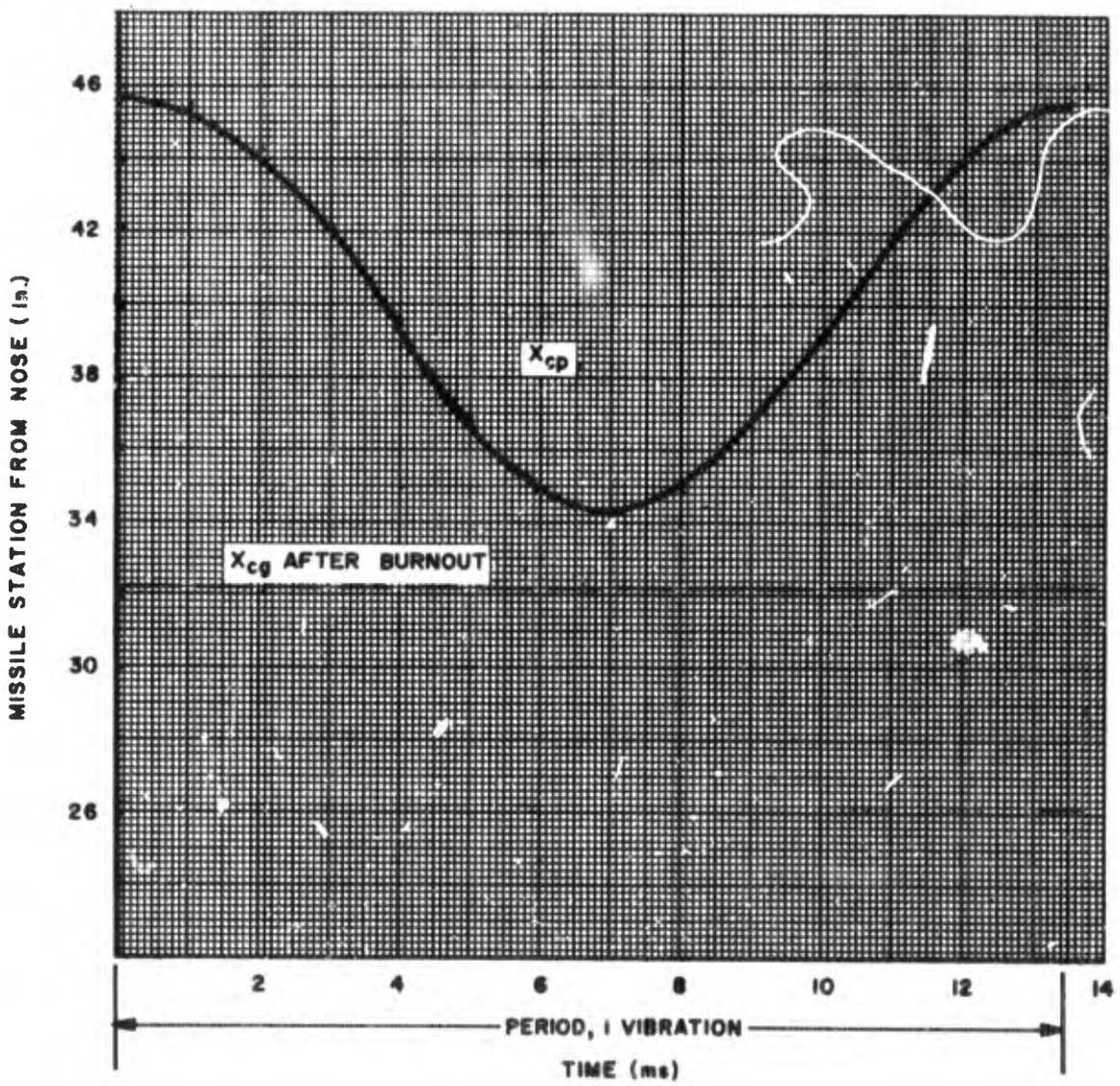

Figure 38. X_{cg} and X_{cp} Versus Time

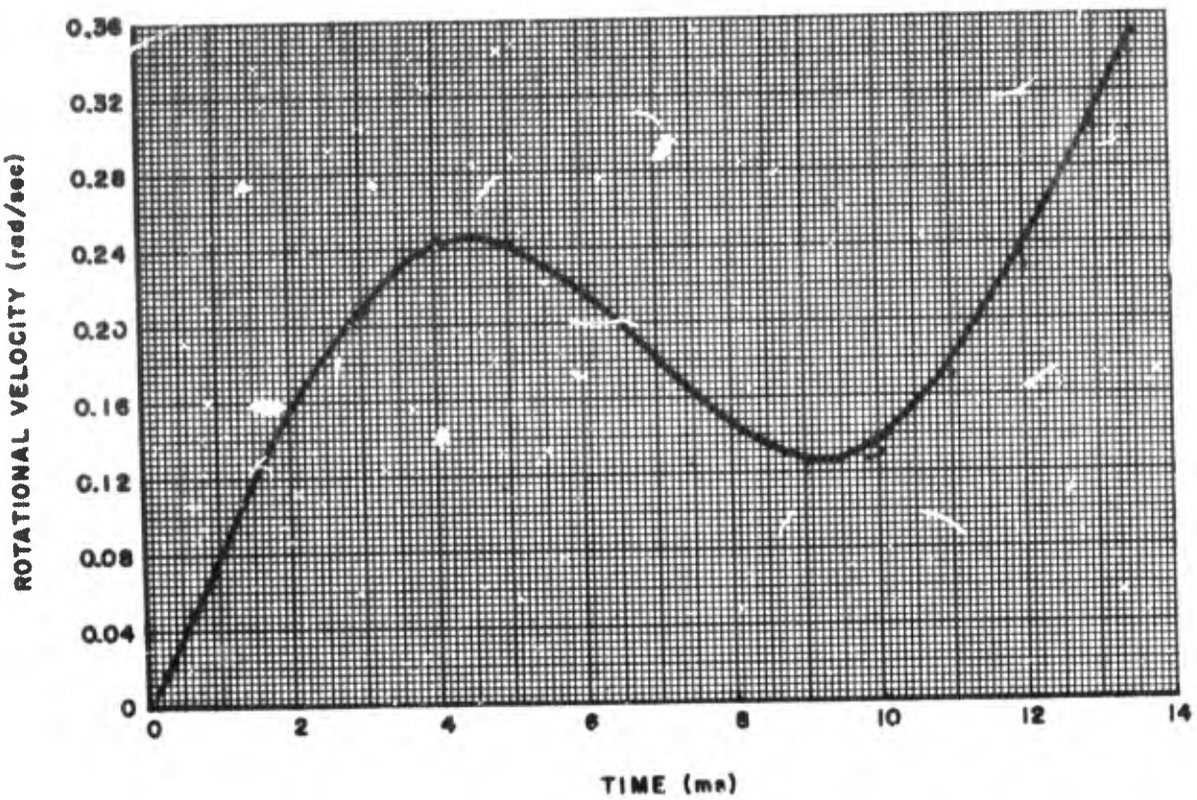

Figure 39. Rotational Velocity Versus Time

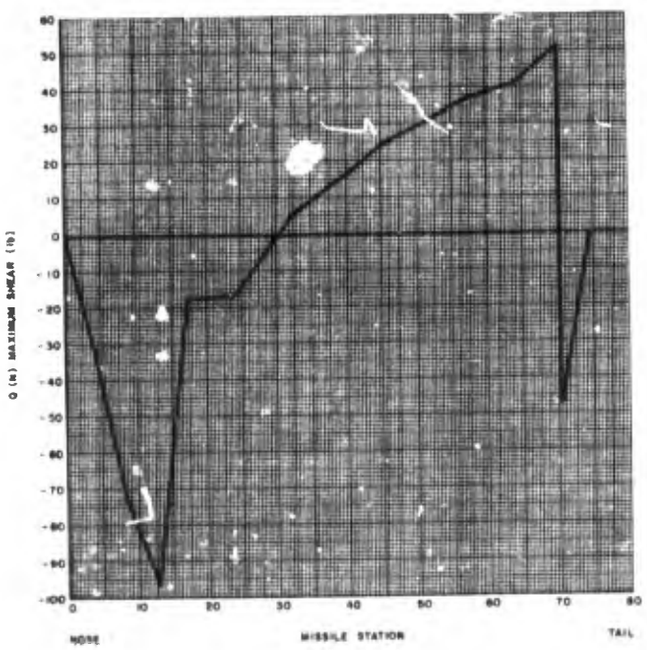

Figure 40. Maximum Shear Versus Station

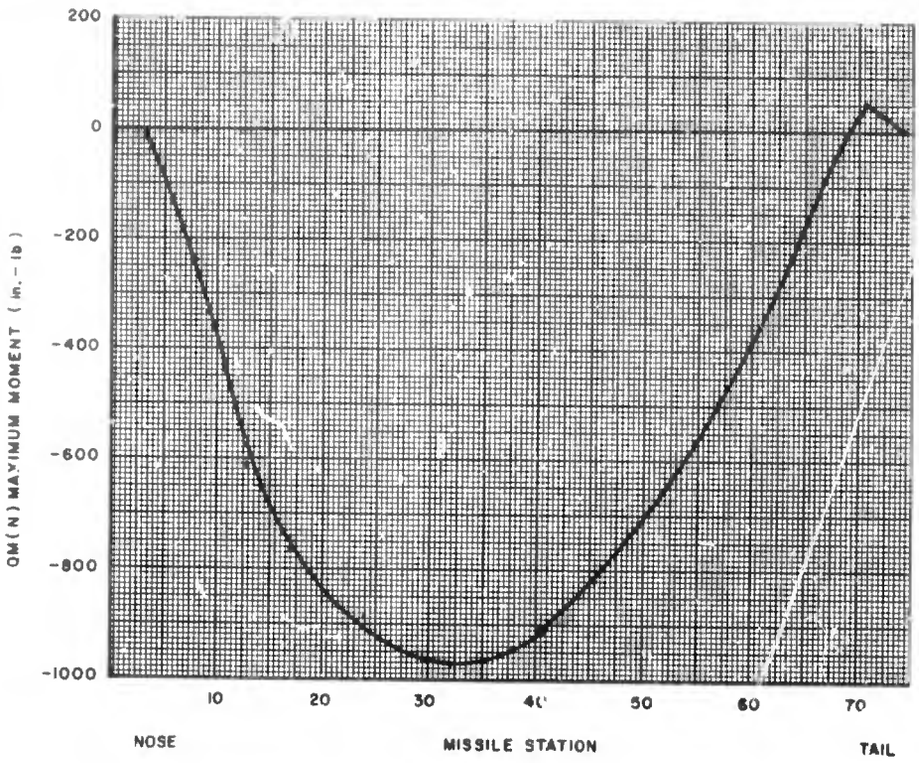

Figure 41. Moment Versus Station

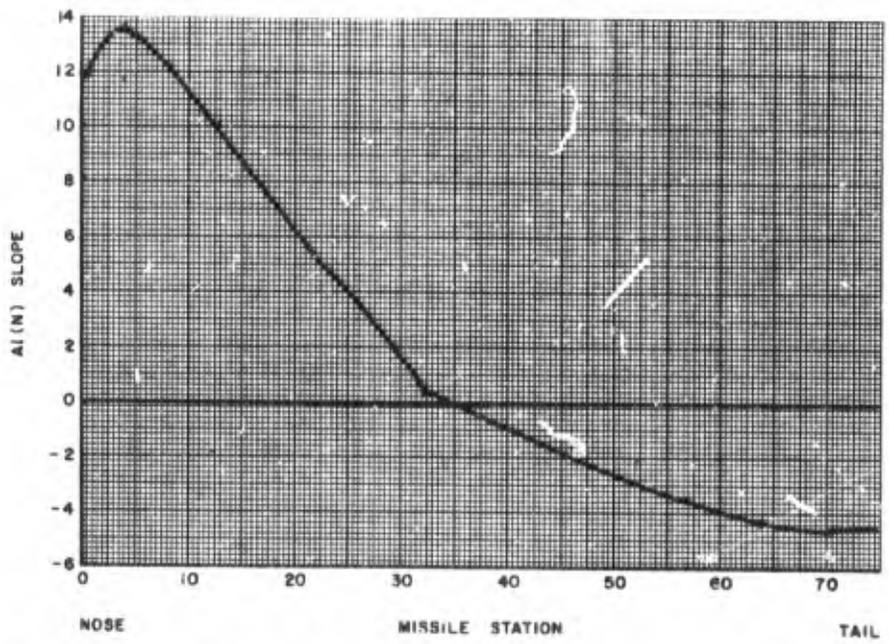

Figure 42. Slope Versus Station

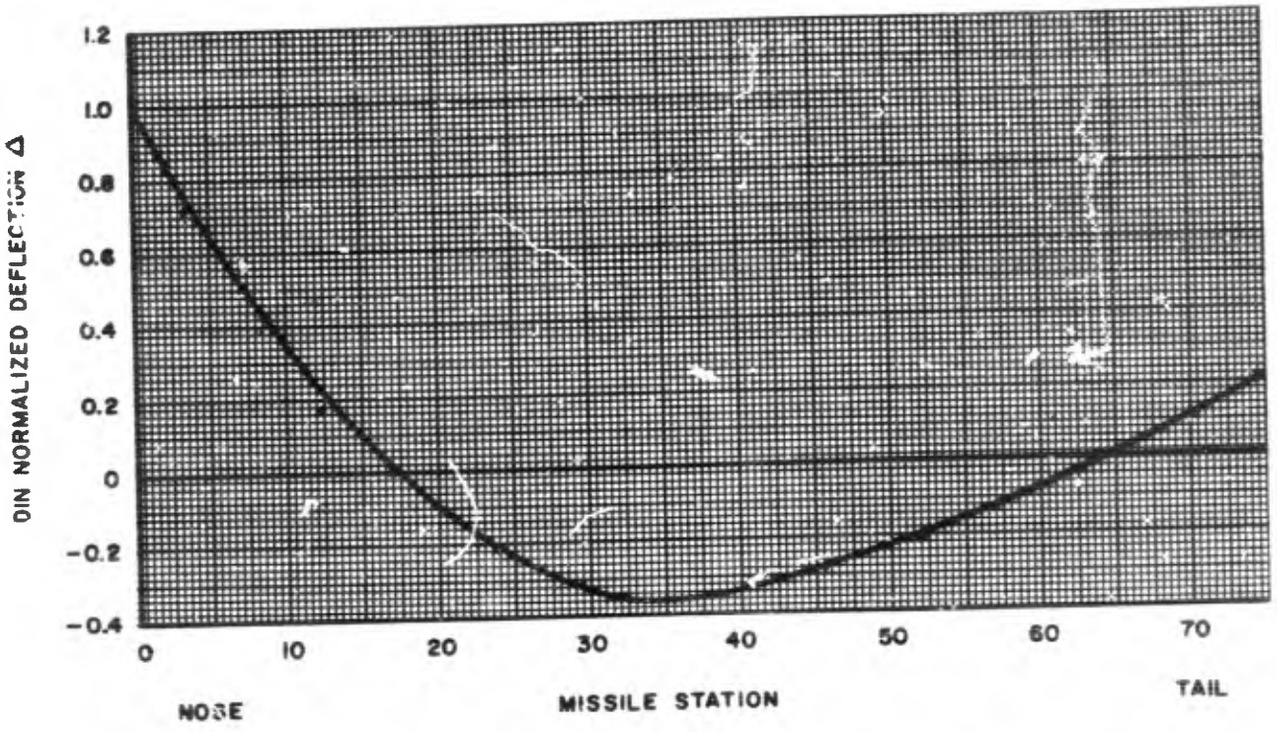

Figure 43. First Mode Bending Deflection

Appendix B

THERMODYNAMIC ANALYSIS FOR ROCKET COMPONENTS FOR MDSS AND RDT&E VEHICLES

Analysis of aerodynamic heating of the two vehicles (MDSS and RDT&E) produced the temperature histories presented in Figures 44 through 51.

Exterior and interior surface temperatures of the nylon-phenolic molded ogive are presented in Figure 44 for one station, L_x = 8 inches. Maximum internal temperature rise for this configuration is 6°F at 80 seconds. Internal temperature rise for the RDT&E ogive (nylon-phenolic molding), at L_x = 12 inches, is 28°F at 120 seconds (Figure 48).

Internal wall temperatures for the pedestal section for the vehicles are shown in Figures 45 and 49. Maximum temperature for the MDSS vehicle (L_x = 20 inches) occurs at 23 seconds and is 269°F. Maximum temperature for the RDT&E vehicle (L_x = 24 inches) occurs at 37 seconds and is 455°F. As stated earlier in the report, these temperatures will not be felt by the descent vehicles because of the split cannister and paper phenolic piston sleeve between the parachute and pedestal wall.

Motor bottle temperatures for the two vehicles are presented in Figures 46 and 50. Analysis of the motors did not take into consideration the internal insulation which might cause temperature to be higher.

Fin leading edge temperatures for the rockets are presented in Figures 47 and 51. This analysis was performed before fin redesign for the RDT&E vehicle; therefore, results show temperature much higher than would actually exist on the present design.

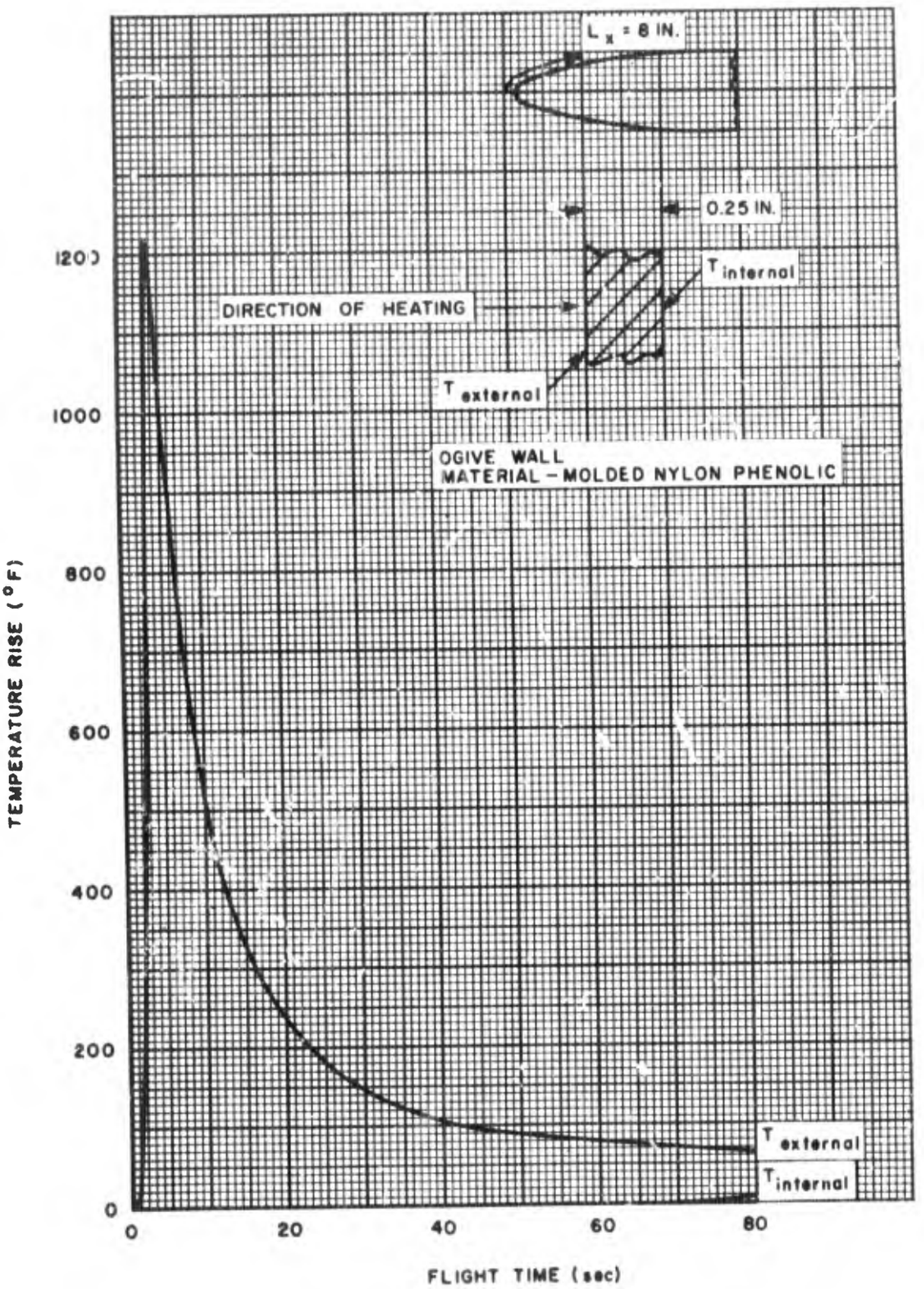

Figure 44. MDSS Rocket Ogive Wall Temperatures

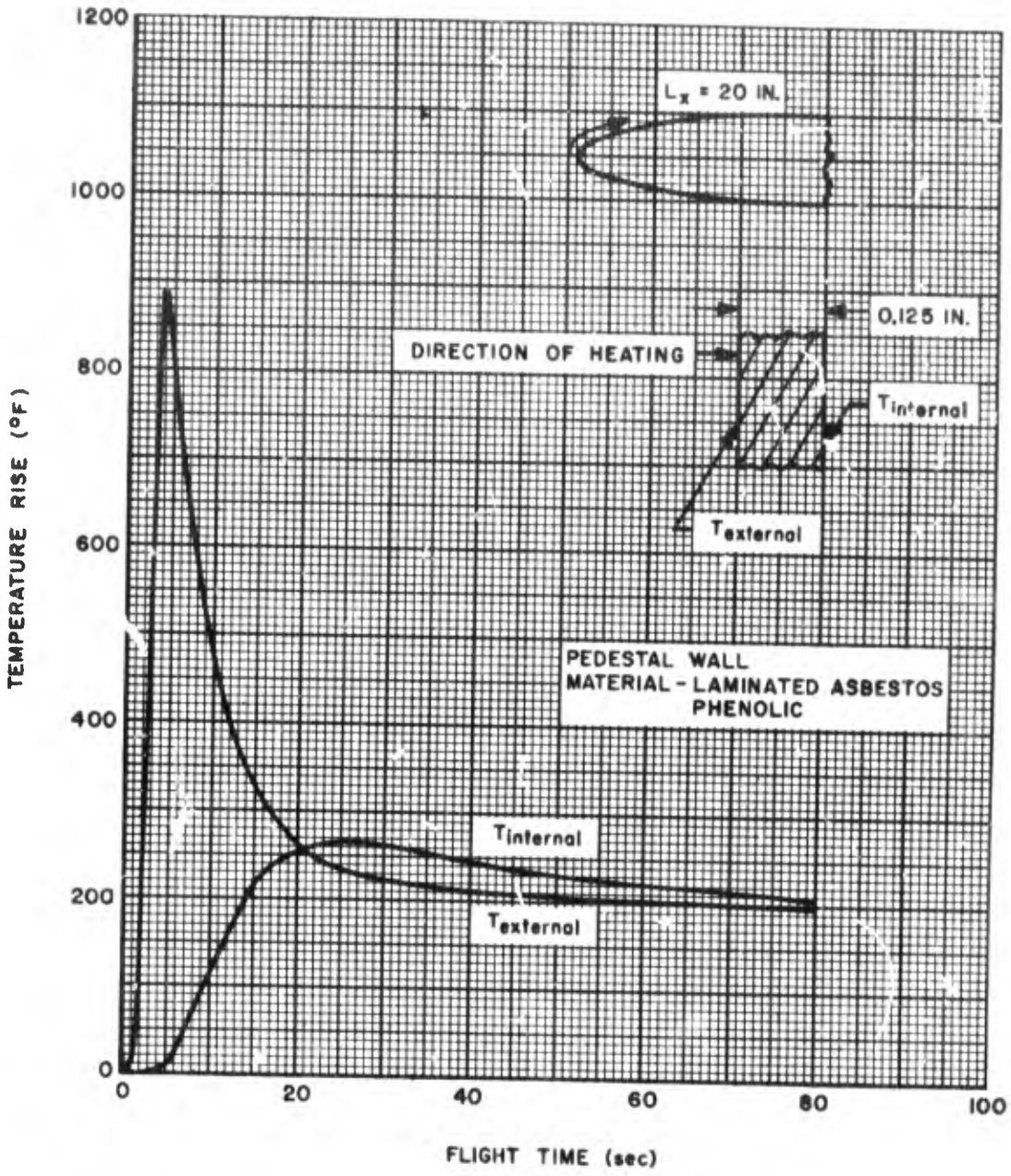

Figure 45. MDSS Rocket Pedestal Wall Temperatures

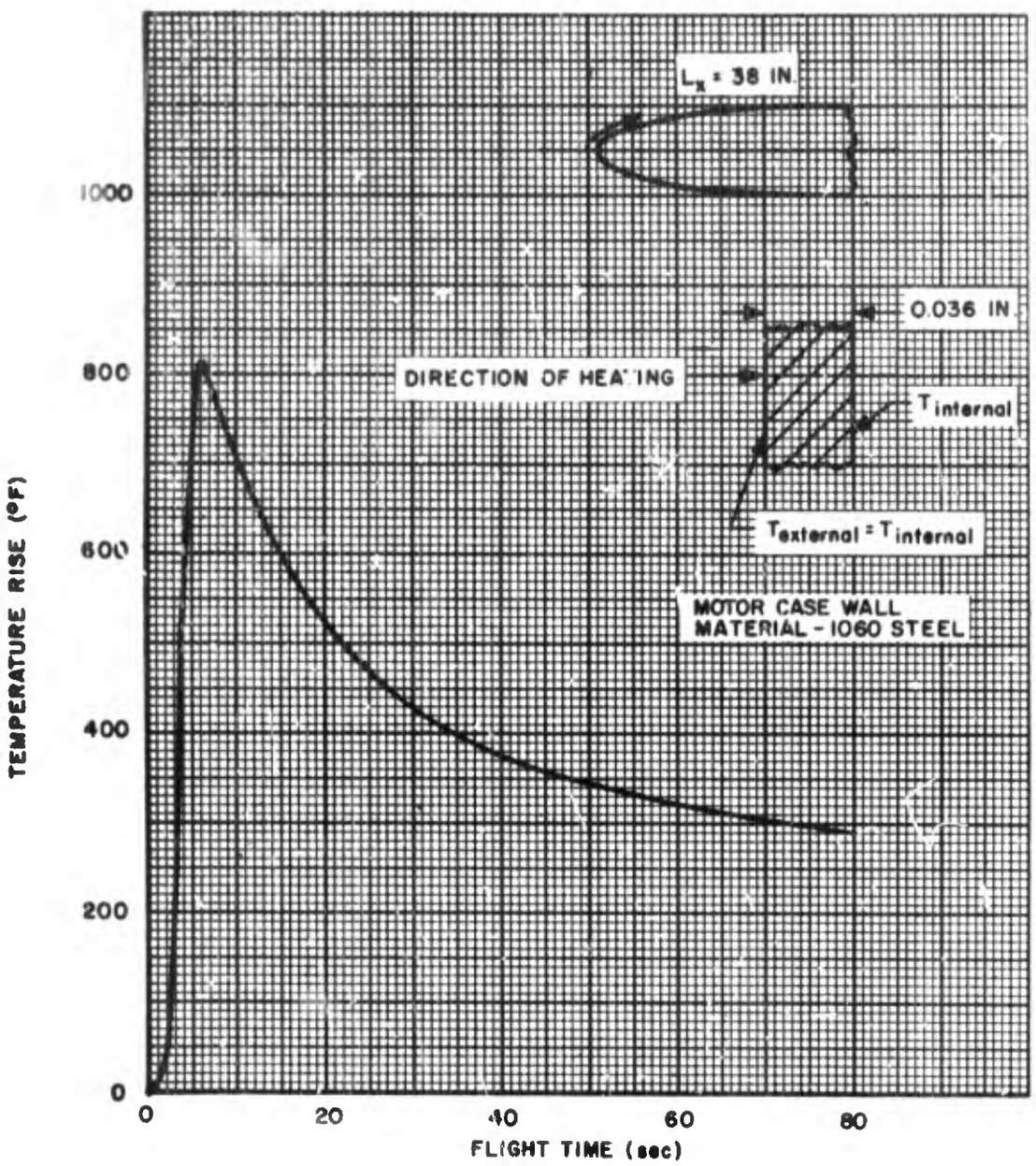

Figure 46. MDS[illegible]ket Motor Case Wall Temperatures

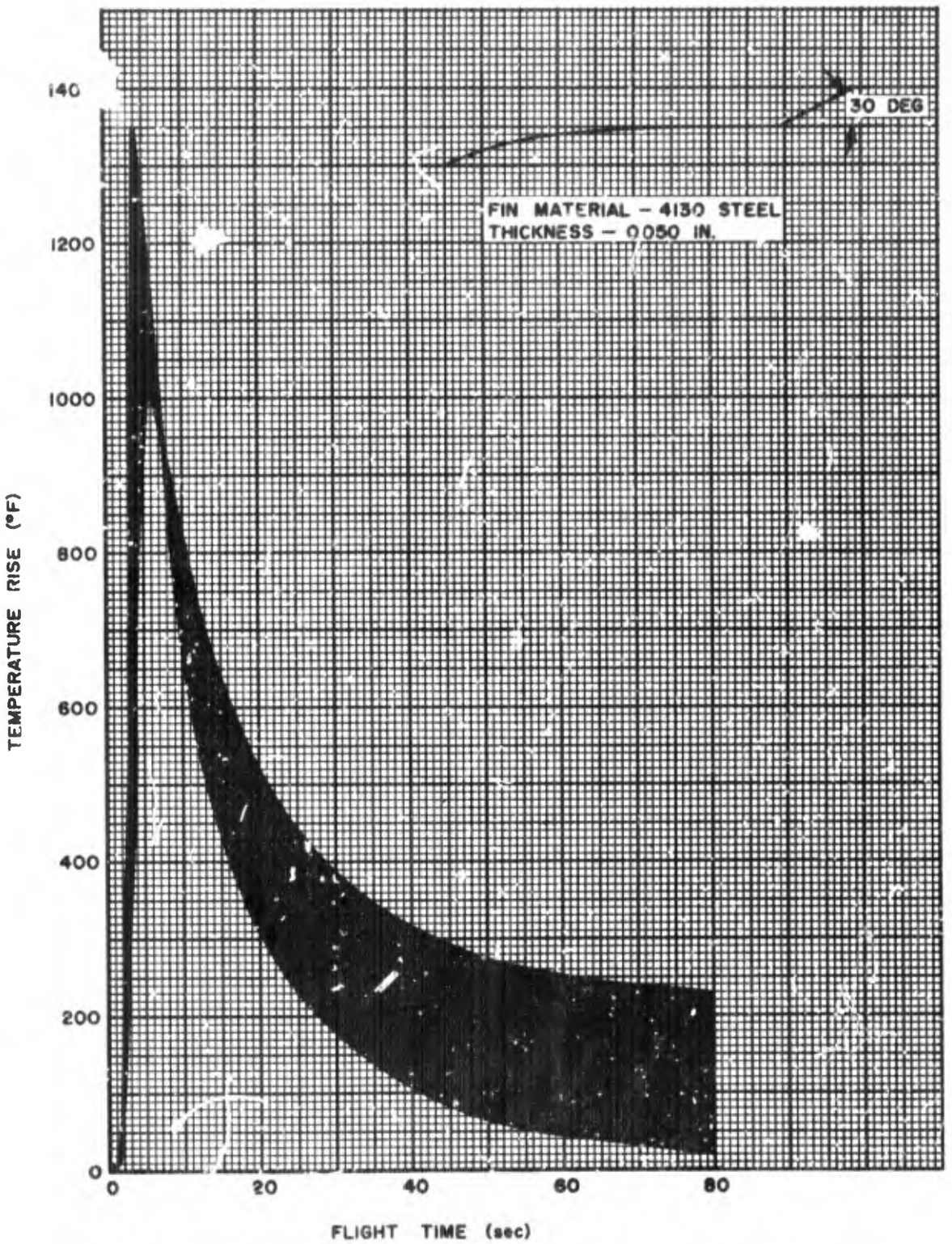

Figure 47. MDSS Rocket Fin Leading Edge Temperature Range

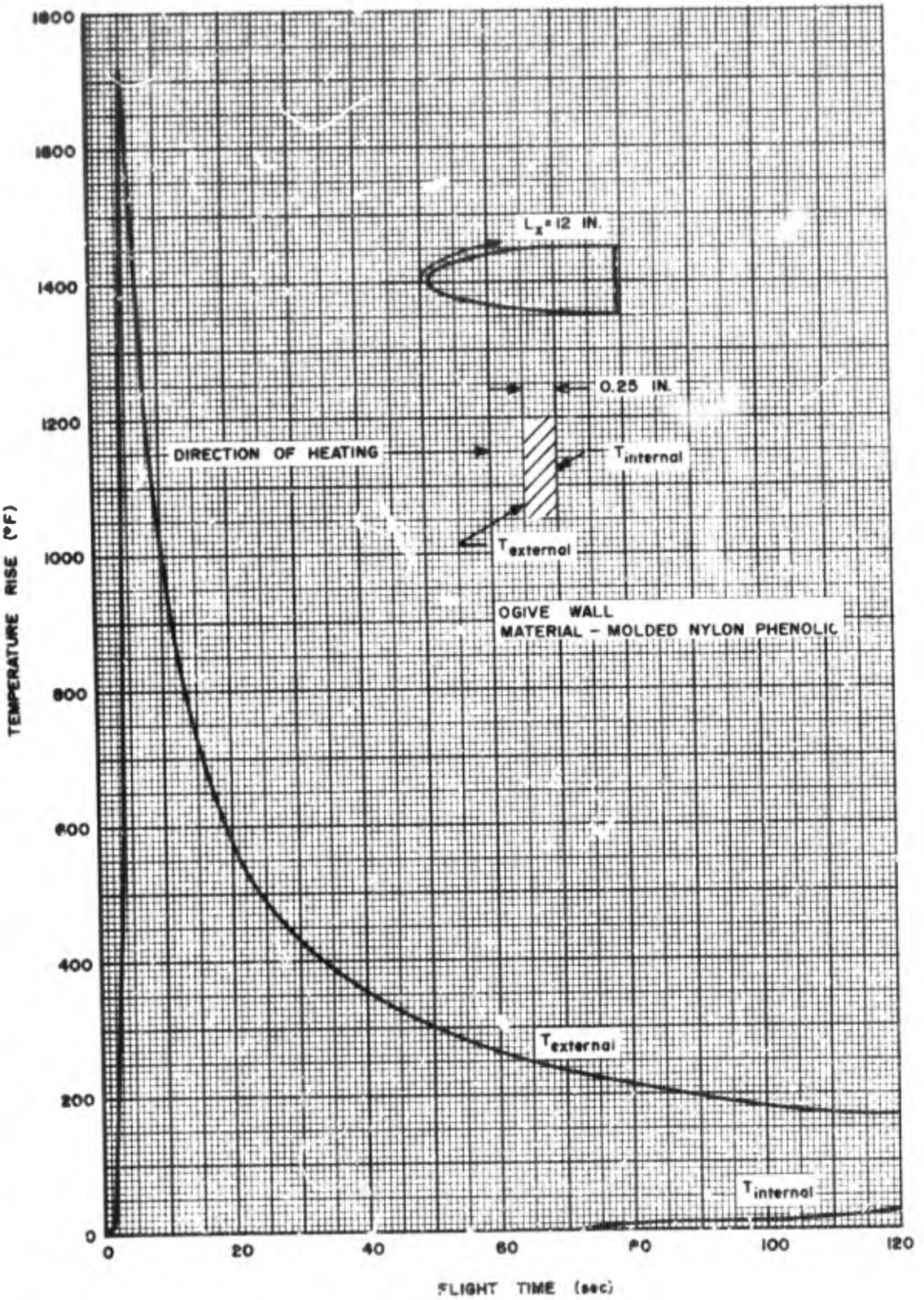

Figure 48. RDT&E Rocket Ogive Wall Temperatures

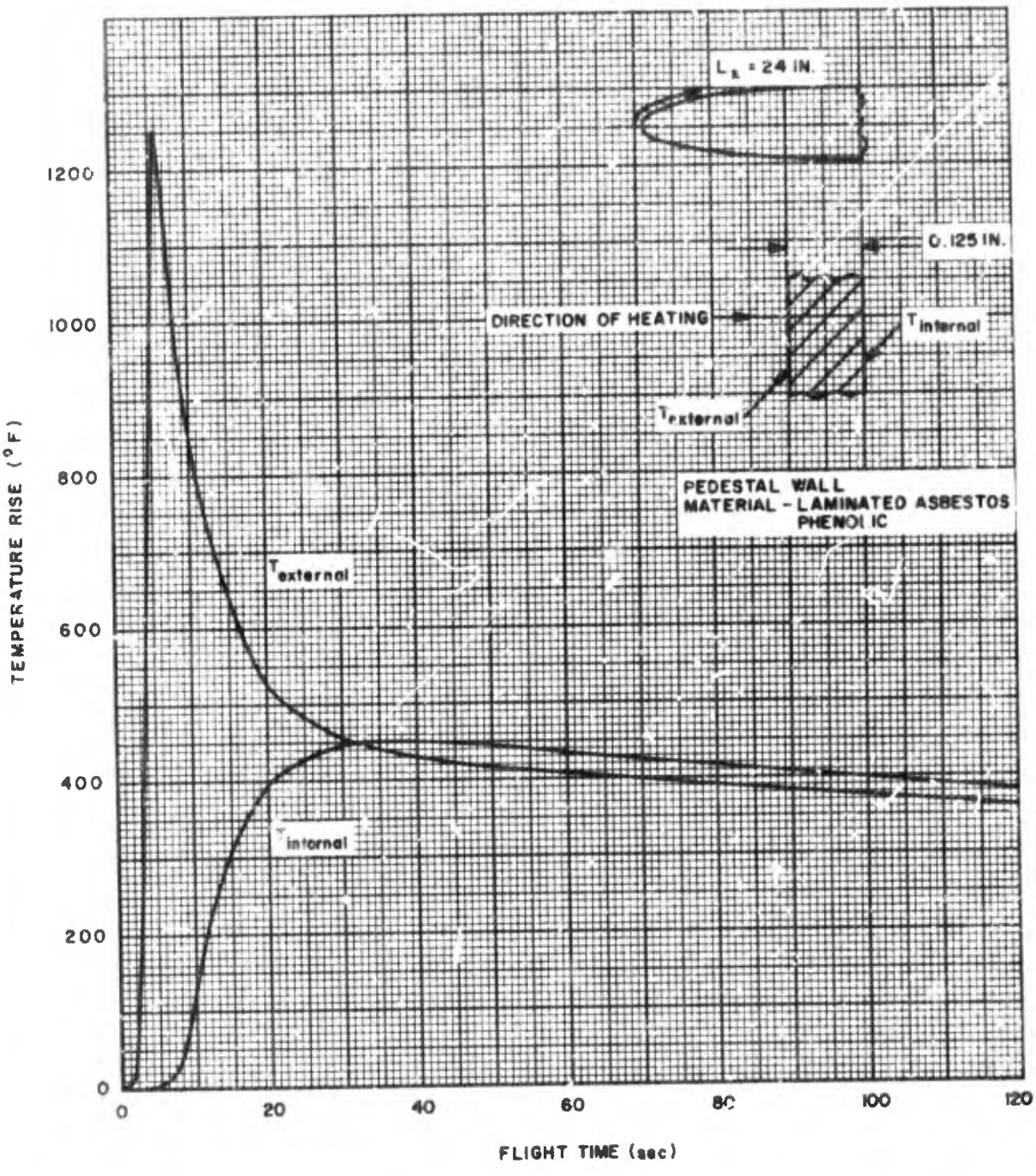

Figure 49. RDT&E Rocket Pedestal Wall Temperatures

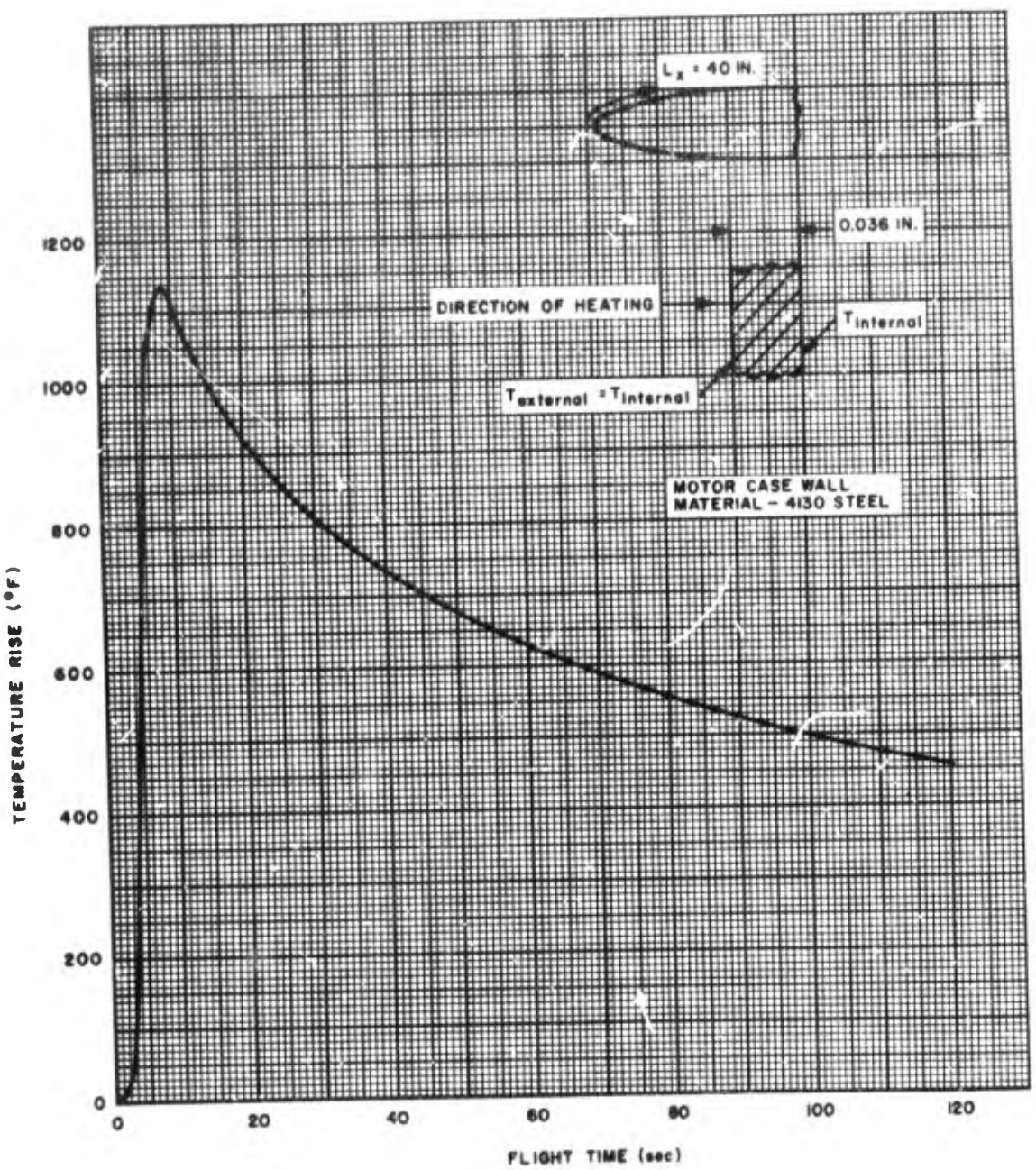

Figure 50. RDT&E Rocket Motor Case Wall Temperatures

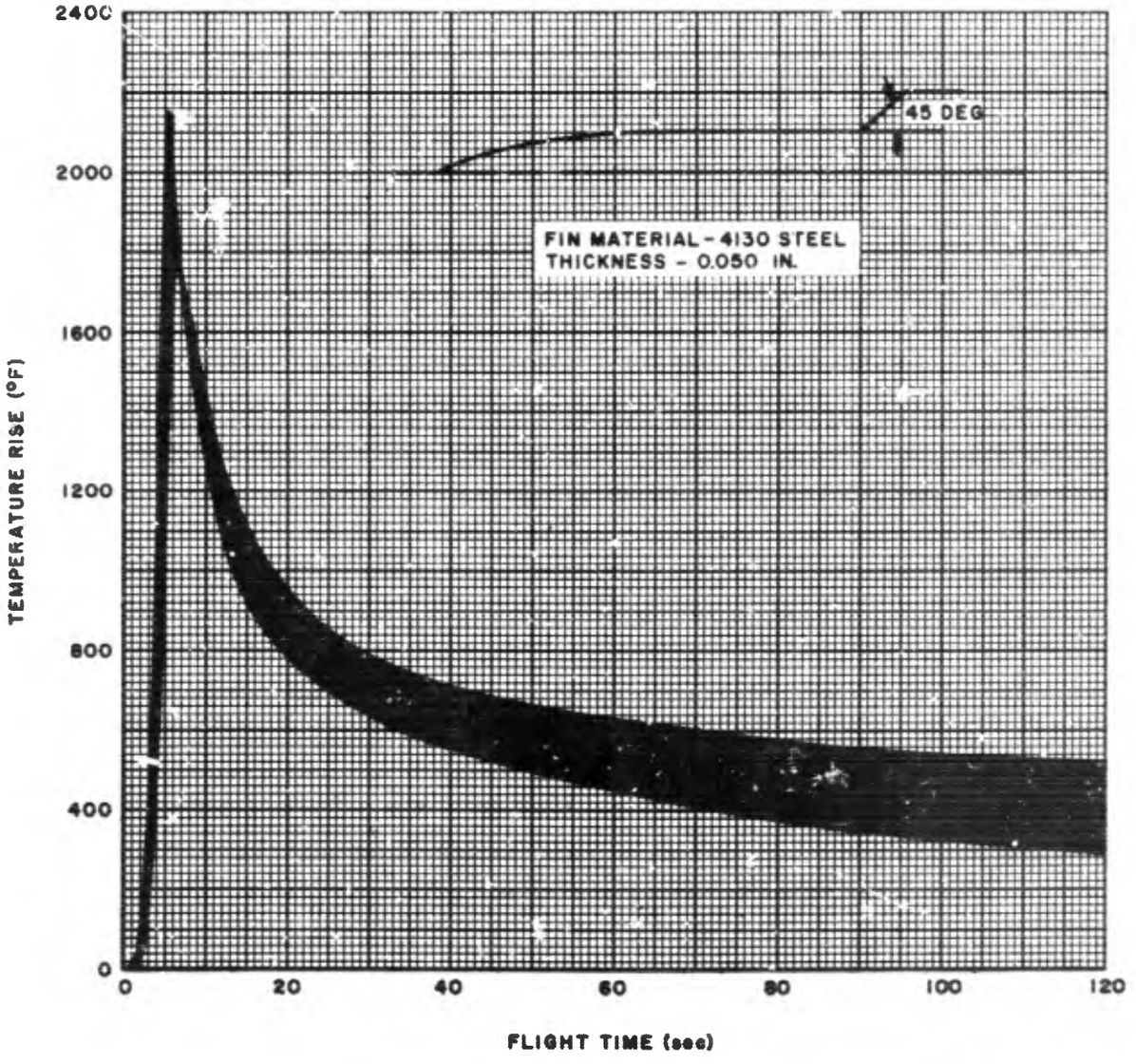

Figure 51. RDT&E Rocket Fin Leading Edge Temperature Range

BLANK PAGE

Appendix C

PERFORMANCE CURVES FOR MDSS AND RDT&E VEHICLES

Figures 52 through 66 represent curves that are the results of the last trajectories run for the MDSS and RDT&E vehicles. Figures 52 through 58 show curves for the MDSS vehicle and Figures 59 through 65 show curves for the RDT&E vehicle performance.

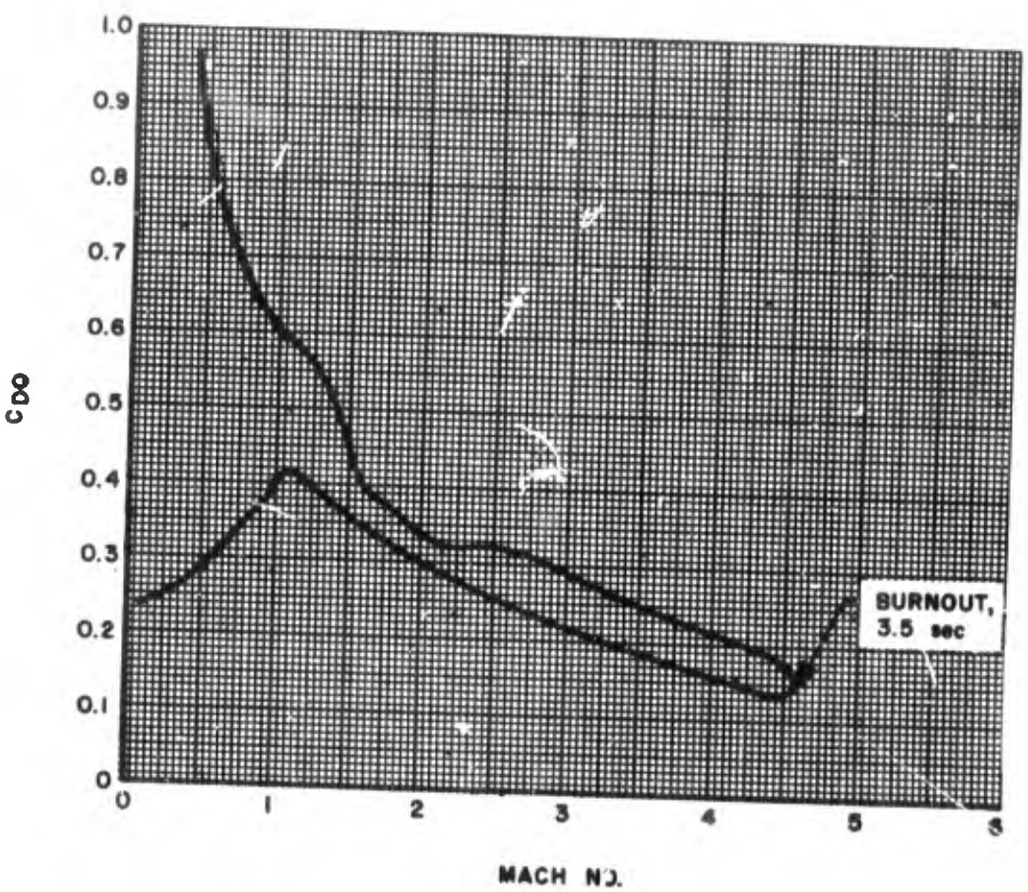

Figure 52. C_{DO} Versus Mach No., MDSS Vehicle

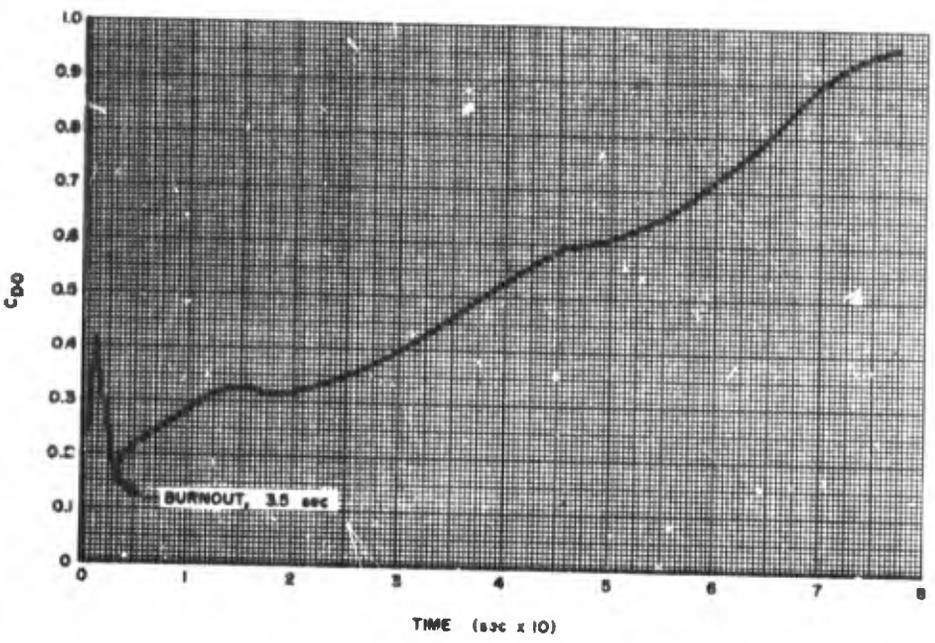

Figure 53. C_{DO} Versus Time, MDSS Vehicle

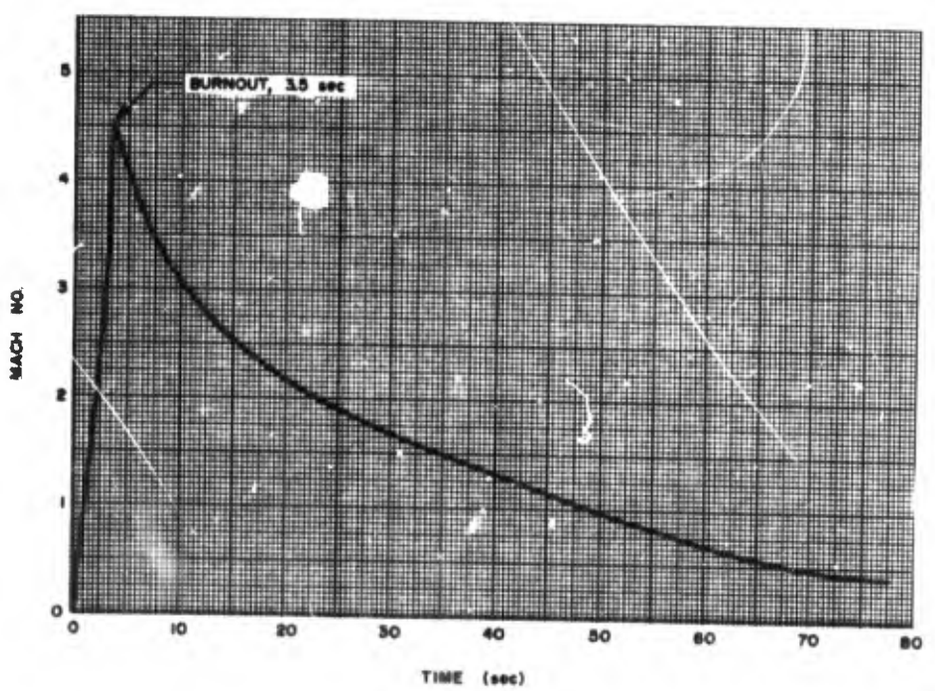

Figure 54. Mach No. Versus Time, MDSS Vehicle

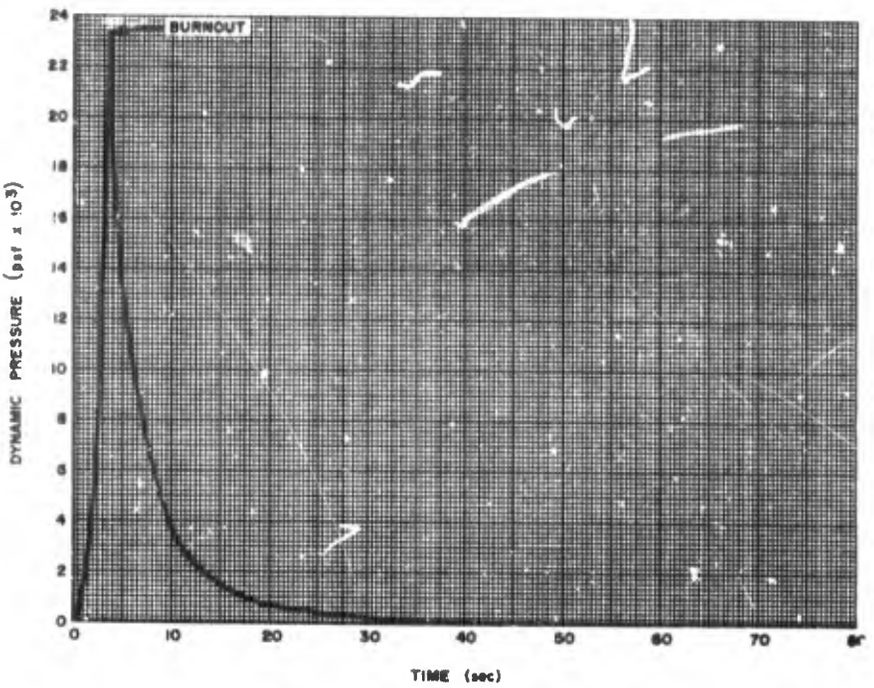

Figure 55. Dynamic Pressure Versus Time, MDSS Vehicle

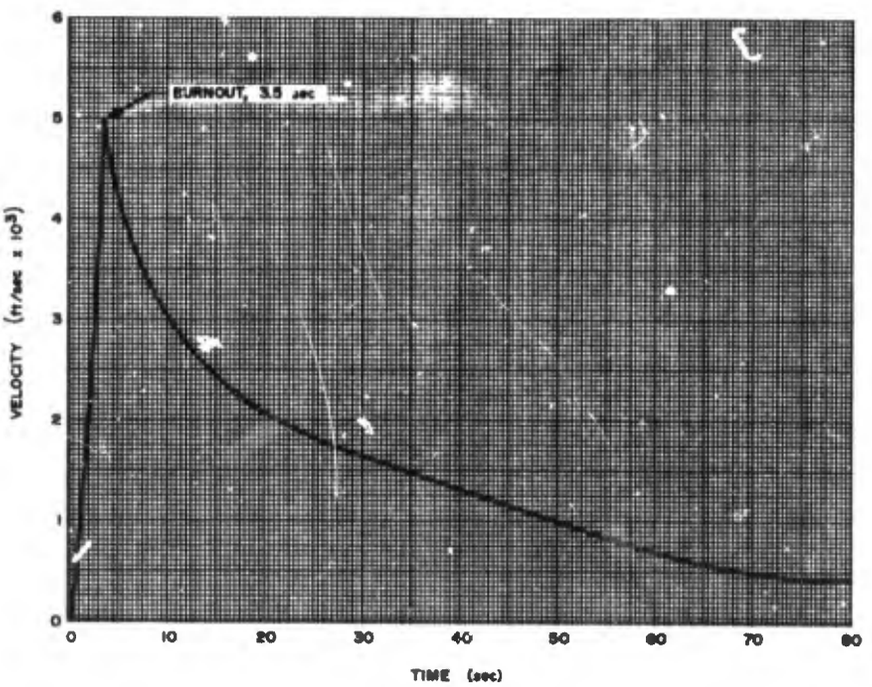

Figure 56. Velocity Versus Time, MDSS Vehicle

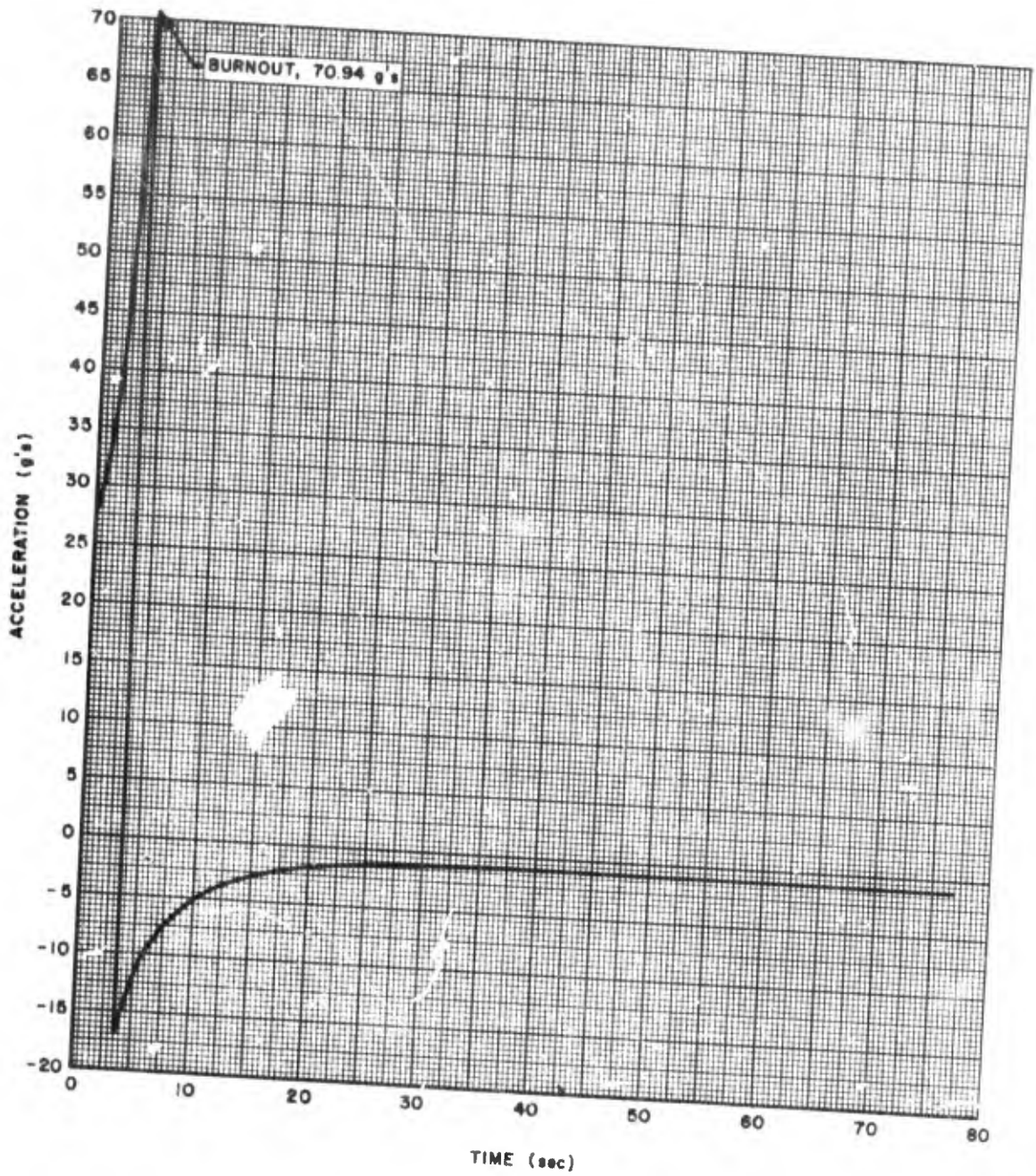

Figure 57. Acceleration Versus Time, MDSS Vehicle

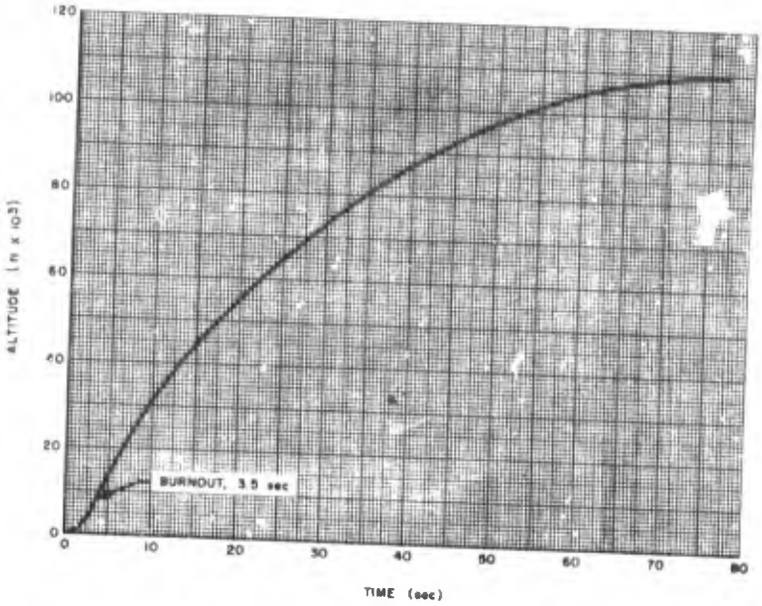

Figure 58. Altitude Versus Time, MDSS Vehicle

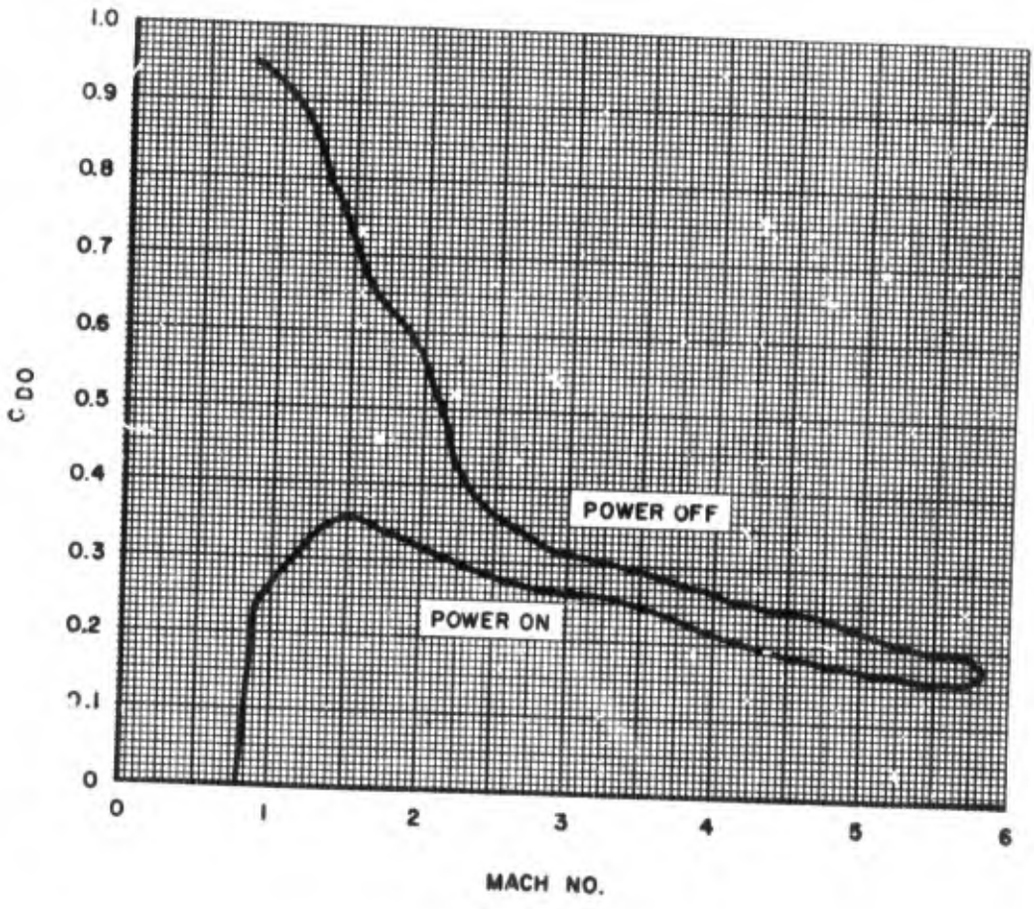

Figure 59. C_{DO} Versus Mach No., RDT&E Vehicle

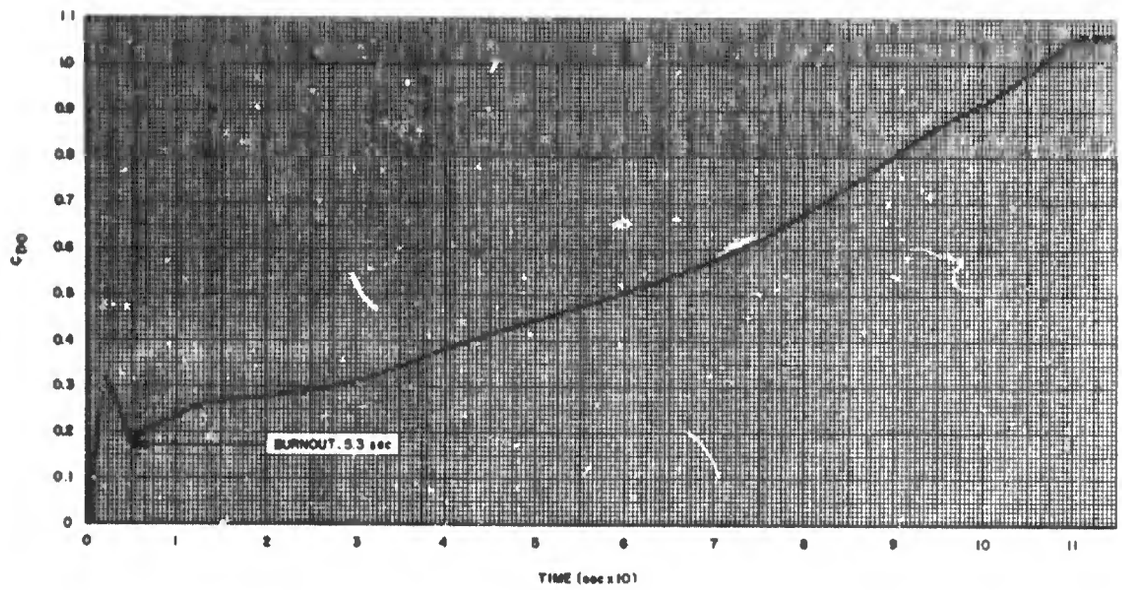

Figure 60. C_{DO} Versus Time, RDT&E Vehicle

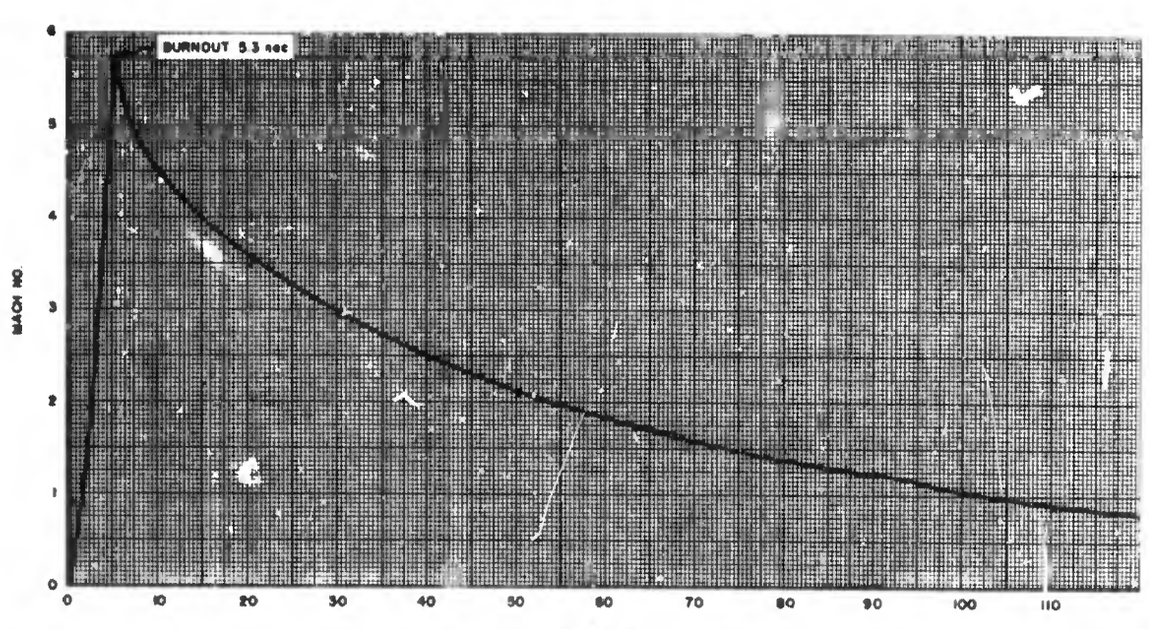

Figure 61. Mach No. Versus Time, RDT&E Vehicle

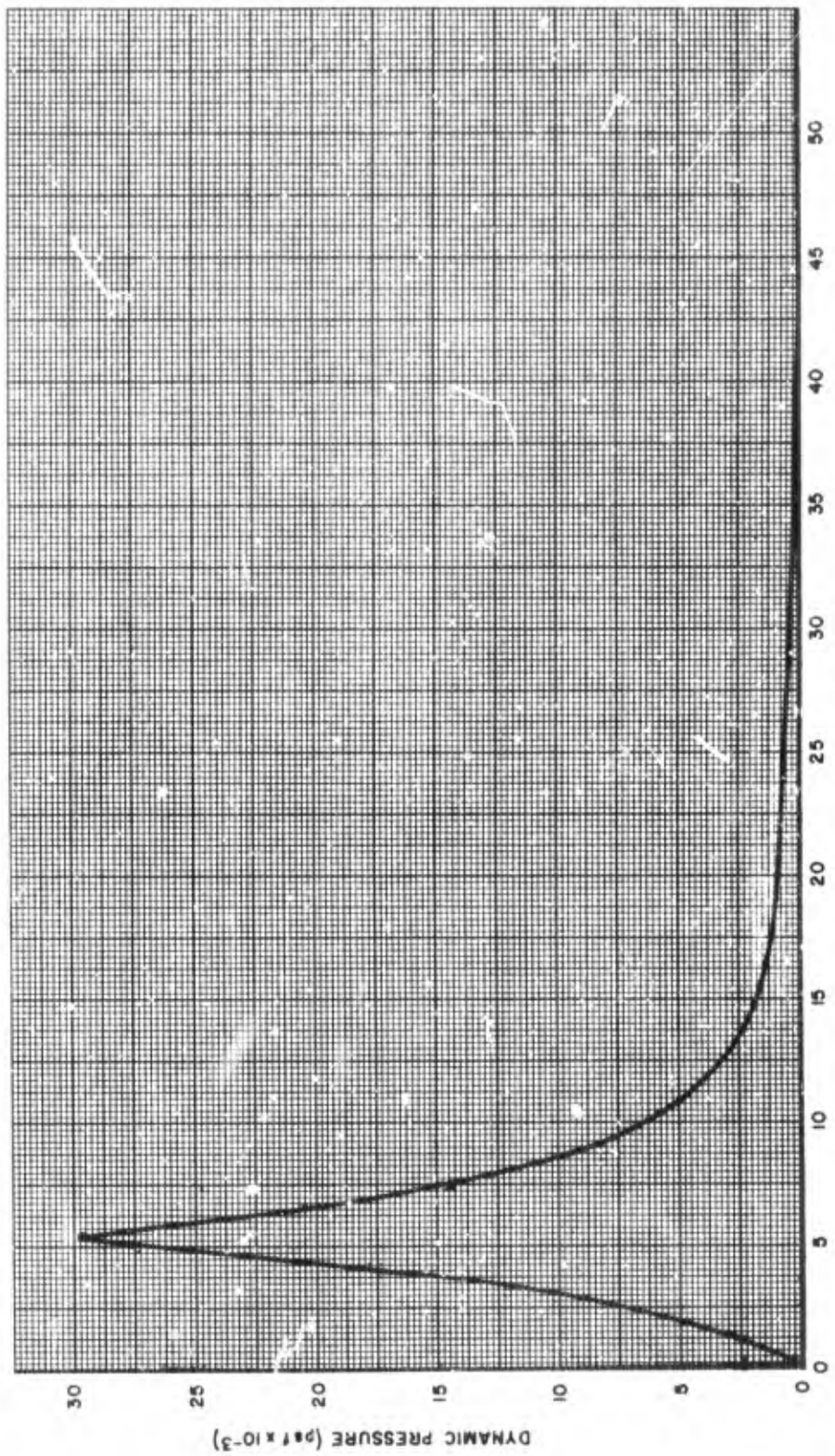

Figure 62. Dynamic Pressure Versus Time, RDT&E Vehicle

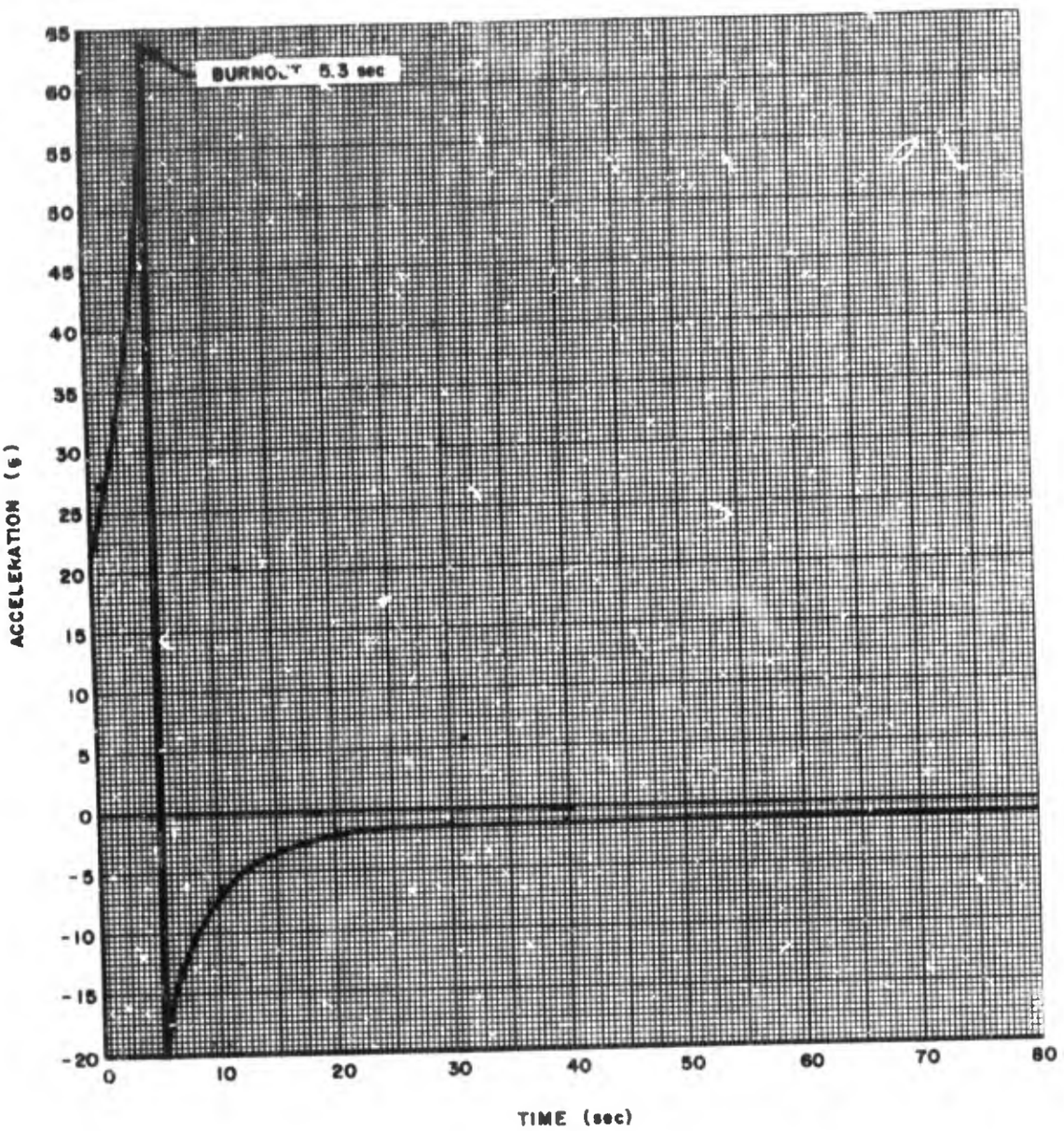

Figure 63. Acceleration Versus Time, RDT&E Vehicle

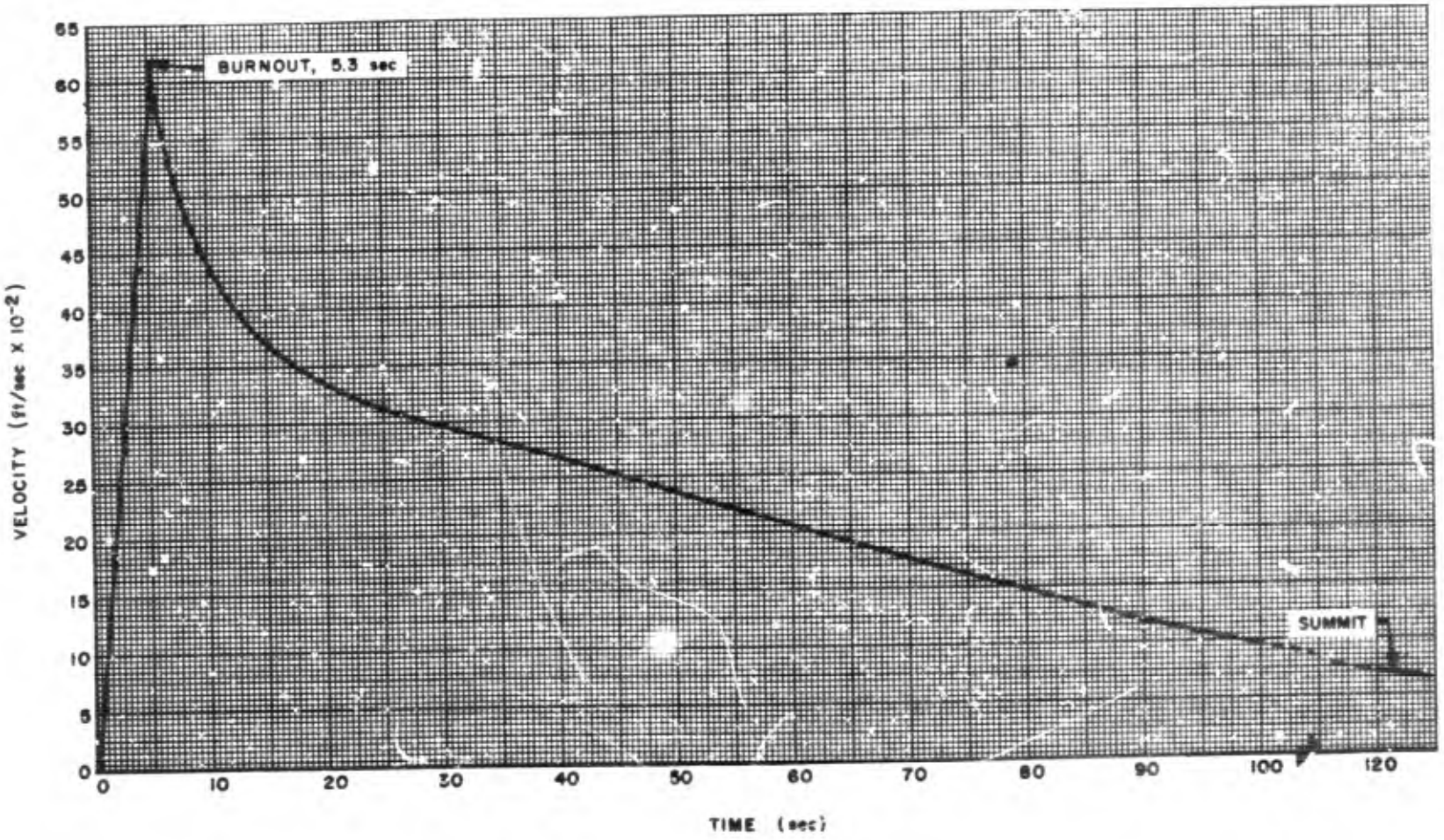

Figure 64. Velocity Versus Time, RDT&E Vehicle

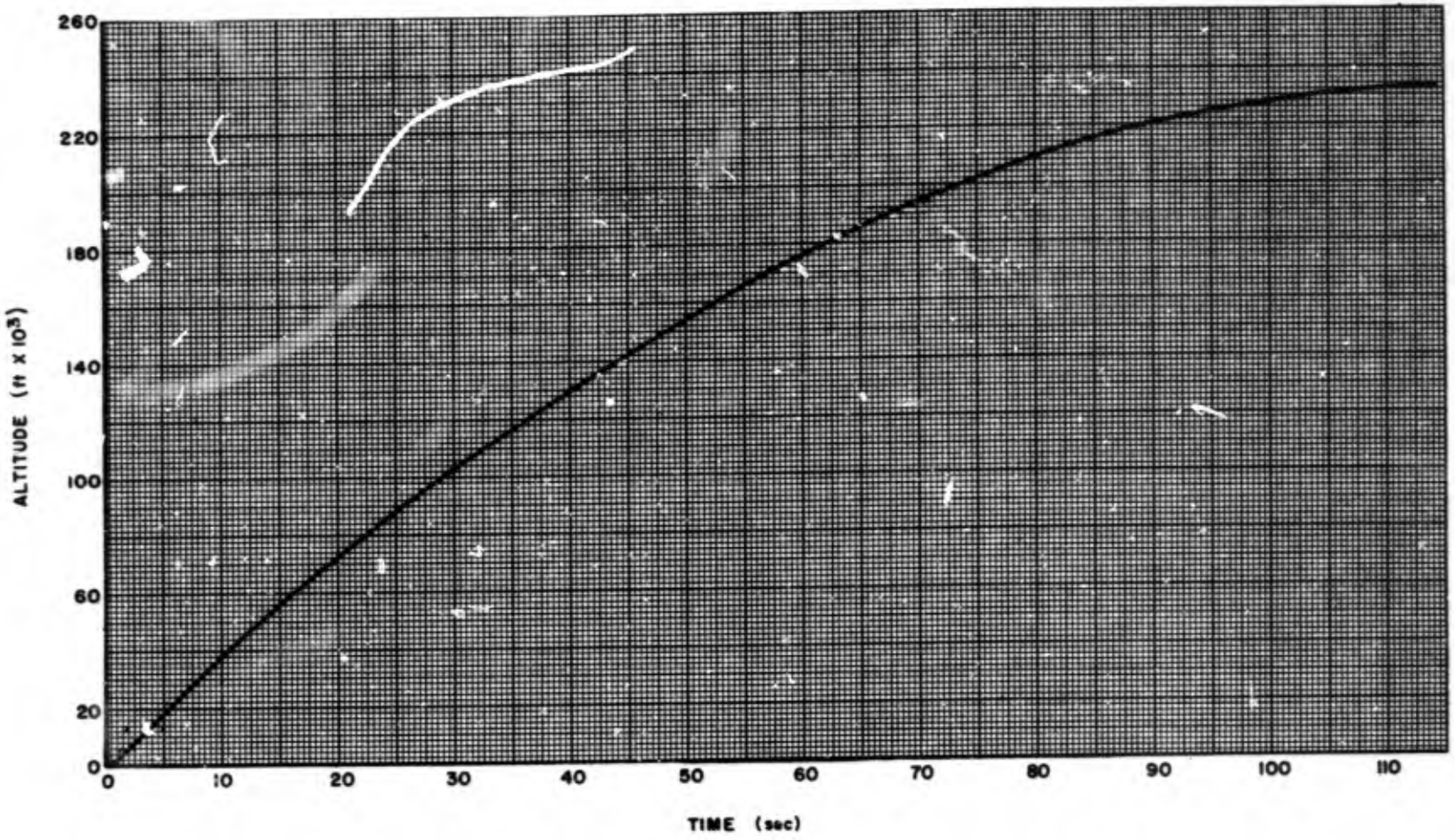

Figure 65. Altitude Versus Time, RDT&E Vehicle

UNCLASSIFIED

Security Classification

DOCUMENT CONTROL DATA - R&D

(Security classification of title, body of abstract and indexing annotation must be entered when the overall report is classified)

1. ORIGINATING ACTIVITY *(Corporate author)*
Structures and Mechanics Laboratory
Research and Development Directorate
U.S. Army Missile Command
Redstone Arsenal, Alabama 35809

2a. REPORT SECURITY CLASSIFICATION
Unclassified

2b. GROUP
N/A

3. REPORT TITLE

METEOROLOGICAL ROCKET PROGRAM FISCAL YEAR REPORT

4. DESCRIPTIVE NOTES *(Type of report and inclusive dates)*
None

5. AUTHOR(S) *(Last name, first name, initial)*
Estes, Glen D.

6. REPORT DATE	7a. TOTAL NO. OF PAGES	7b. NO. OF REFS
27 June 1966	99	None

8a. CONTRACT OR GRANT NO.	9a. ORIGINATOR'S REPORT NUMBER(S)
b. PROJECT NO. (DA) 1S025001D125	RS-TR-66-6
c. AMC Management Structure Code No. 5027.12.46100	9b. OTHER REPORT NO(S) *(Any other numbers that may be assigned this report)* None
d.	

10. AVAILABILITY/LIMITATION NOTICES
This document is subject to special export controls and each transmittal to foreign governments or foreign nationals may be made only with prior approval of this Command, Attn: AMSMI-RS.

11. SUPPLEMENTARY NOTES	12. SPONSORING MILITARY ACTIVITY
None	Same as No. 1

13. ABSTRACT

This report contains results of design, analysis, fabrication, and testing carried out by the Structures and Mechanics Laboratory to advance the design of the Meteorological Data Sounding System and Research Development Test and Evaluation rockets.

A description of each vehicle and results of component test carried out during this phase of the exploratory development program is included.

DD FORM 1 JAN 64 1473

100

UNCLASSIFIED

Security Classification

14. KEY WORDS	LINK A		LINK B		LINK C	
	ROLE	WT	ROLE	WT	ROLE	WT
Meteorological Data Sounding System						
Research Development Test and Evaluation						
FFAR						
Pedestal						
Timer Striker Arm						

INSTRUCTIONS

1. ORIGINATING ACTIVITY: Enter the name and address of the contractor, subcontractor, grantee, Department of Defense activity or other organization *(corporate author)* issuing the report.

2a. REPORT SECURITY CLASSIFICATION: Enter the overall security classification of the report. Indicate whether "Restricted Data" is included. Marking is to be in accordance with appropriate security regulations.

2b. GROUP: Automatic downgrading is specified in DoD Directive 5200.10 and Armed Forces Industrial Manual. Enter the group number. Also, when applicable, show that optional markings have been used for Group 3 and Group 4 as authorized.

3. REPORT TITLE: Enter the complete report title in all capital letters. Titles in all cases should be unclassified. If a meaningful title cannot be selected without classification, show title classification in all capitals in parenthesis immediately following the title.

4. DESCRIPTIVE NOTES: If appropriate, enter the type of report, e.g., interim, progress, summary, annual, or final. Give the inclusive dates when a specific reporting period is covered.

5. AUTHOR(S): Enter the name(s) of author(s) as shown on or in the report. Enter last name, first name, middle initial. If military, show rank and branch of service. The name of the principal author is an absolute minimum requirement.

6. REPORT DATE: Enter the date of the report as day, month, year, or month, year. If more than one date appears on the report, use date of publication.

7a. TOTAL NUMBER OF PAGES: The total page count should follow normal pagination procedures, i.e., enter the number of pages containing information.

7b. NUMBER OF REFERENCES: Enter the total number of references cited in the report.

8a. CONTRACT OR GRANT NUMBER: If appropriate, enter the applicable number of the contract or grant under which the report was written.

8b, 8c, & 8d. PROJECT NUMBER: Enter the appropriate military department identification, such as project number, subproject number, system numbers, task number, etc.

9a. ORIGINATOR'S REPORT NUMBER(S): Enter the official report number by which the document will be identified and controlled by the originating activity. This number must be unique to this report.

9b. OTHER REPORT NUMBER(S): If the report has been assigned any other report numbers *(either by the originator or by the sponsor)*, also enter this number(s).

10. AVAILABILITY/LIMITATION NOTICES: Enter any limitations on further dissemination of the report, other than those imposed by security classification, using standard statements such as:

(1) "Qualified requesters may obtain copies of this report from DDC."

(2) "Foreign announcement and dissemination of this report by DDC is not authorized."

(3) "U. S. Government agencies may obtain copies of this report directly from DDC. Other qualified DDC users shall request through_____."

(4) "U. S. military agencies may obtain copies of this report directly from DDC. Other qualified users shall request through_____."

(5) "All distribution of this report is controlled. Qualified DDC users shall request through_____."

If the report has been furnished to the Office of Technical Services, Department of Commerce, for sale to the public, indicate this fact and enter the price, if known.

11. SUPPLEMENTARY NOTES: Use for additional explanatory notes.

12. SPONSORING MILITARY ACTIVITY: Enter the name of the departmental project office or laboratory sponsoring *(paying for)* the research and development. Include address.

13. ABSTRACT: Enter an abstract giving a brief and factual summary of the document indicative of the report, even though it may also appear elsewhere in the body of the technical report. If additional space is required, a continuation sheet shall be attached.

It is highly desirable that the abstract of classified reports be unclassified. Each paragraph of the abstract shall end with an indication of the military security classification of the information in the paragraph, represented as *(TS)*, *(S)*, *(C)*, or *(U)*.

There is no limitation on the length of the abstract. However, the suggested length is from 150 to 225 words.

14. KEY WORDS: Key words are technically meaningful terms or short phrases that characterize a report and may be used as index entries for cataloging the report. Key words must be selected so that no security classification is required. Identifiers, such as equipment model designation, trade name, military project code name, geographic location, may be used as key words but will be followed by an indication of technical context. The assignment of links, rules, and weights is optional.